Application of Machine Learning To Predict Cyclic Resistance of Silty Sands

MS GEOTECHNICAL ENGINEERING THESIS DISSERTATION

By

Arslan Mushtaq

NUST-2020-MS GEOTECH ENGG 00000330662

Supervisor

Dr. Abbas Haider

NUST Institute of Civil Engineering

School of Civil and Environmental Engineering

National University of Sciences and Technology, Islamabad, Pakistan

2023

This is to certify that thesis titled

Application of Machine Learning To Predict Cyclic Resistance of Silty Sands

Submitted by

ARSLAN MUSHTAQ

Fall 2020 MS-Geotechnical Engineering

00000330662

has been accepted towards the partial fulfilment of the requirements for the award of degree

of

Master of Science in Geotechnical Engineering

Dr. Badee Alshameri

HoD Geotechnical Engineering

NUST Institute of Civil Engineering (NICE)

School of Civil and Environmental Engineering (SCEE)

National University of Sciences and Technology (NUST), Islamabad, Pakistan

Copyright Statement

Plagiarism Certificate (Turnitin Report)

1. I know the meaning of plagiarism and declare that all the work in the document, save for that which is properly acknowledged, is my own. This thesis/dissertation has been submitted to the Turnitin module (or equivalent similarity and originality checking software) and I confirm that my supervisor has seen my report and any concerns revealed by such have been resolved with my supervisor.

2. I have used the NUST Synopsis and Thesis Manual as Author-date-referencing-guide based on the APA convention for citation and referencing. Each significant contribution to and quotation in this dissertation from the work or works of the other people has been attributed and has been cited and referenced.

3. This dissertation is my own work.

4. I have not allowed and will not allow anyone to copy my work with the intention of passing it as his or her own.

Signature_____

Student Name: Arslan Mushtaq

Date: _____

Thesis Acceptance Certificate

It is certified that final copy of MS thesis written by **Mr. Arslan Mushtaq**, Registration No. **00000330662,** of MS Geotechnical Engineering 2020 Batch (NICE), has been vetted by undersigned, found completed in all respects as per NUST Statutes/Regulations, is free of plagiarism, errors, and mistakes and is accepted as partial fulfillment for award of **MS degree in Geotechnical Engineering.**

Signature
(Supervisor): _____
(Dr. Abbas Haider)

Signature
(Head of Department): _____
(Dr. Badee Alshameri)

Signature
(Principal & Dean): _____

Acknowledgment

I would like to express my gratitude to Dr. Abbas Haider, my research advisor, for all the guidance, support, and instruction he provided me throughout my masters studies. I would like to thank the Faculty of NICE at NUST University for providing me with the resources to pursue graduate study. Dr. Badee Alshameri has been incredible mentor, and I'm also grateful to him.

This project would not have been possible without the support of my family and the Almighty, who helped me through all the difficulties. I would also like to thank everyone who has been there for me emotionally and intellectually as I have worked on my coursework.

Thank you all.

Abstract

Machine Learning, an effective tool, is being utilized in geotechnical engineering owing to the amount of data generated in the past. This work utilizes a machine learning based framework to identify a suitable density measure for the cyclic resistance of silty sands and subsequently tests the ability of several ML algorithms in producing the cyclic resistance curve. For this purpose, the published literature is considered a potential source for collecting the results of cyclic triaxial tests conducted at confining pressure of 100KPa on moist-tamped samples of silty sands. The compiled data includes several influencing parameters like the Number of cycles to cause initial liquefaction (N), grain size (D_{50}), coefficient of uniformity (Cu), void ratio, relative density, equivalent void ratio, relative compaction, e_{min}, e_{max}, e_{range}, and fines content. Performing feature selection indicates relative compaction and e_{range} as the most influential parameters. Relative compaction even proved a better parameter than relative density in terms of normalizing the effect of fines on cyclic resistance. On comparing the accuracy of the several models created, Gaussian Process Regression (GPR) emerged as the best-performing algorithm for this problem. The GPR model is then validated on the unseen data. It is noticed that the model predicts the variation of the CSR with the Number of cycles (N) quite satisfactorily but over-predicts with an error up to 25%. This error can be attributed to the combined effect of other minor factors that are not included as input parameters. It can be summarized that relative compaction and e_{range} are capable of predicting the curve with reasonable accuracy.

Table of Contents

List of Figures

List of Tables

Abbreviations and Symbols

Abbreviations

CPT	Cone Penetration Test
CRR	Cyclic Resistance Ratio
CSR	Cyclic Stress Ratio
CSL	Critical state Line
CSSM	Critical State Soil Mechanics
CTx	Cyclic triaxial test
DMT	Flat dilatometer test
SPT	Standard penetration test

Symbols

$(N_1)_{60}$	Normalised SPT blowcount
$(N_1)_{60cs}$	SPT blowcount Normalised for equivalent clean sand
a_{max}	Peak ground acceleration
CRR_{15}	CRR for failure in 15 cycles
$CRR_{7.5}$	CRR normalised to an earthquake magnitude 7.5
CRRss	Cyclic resistance ratio of simple shear test
CRRtx	Cyclic resistance ratio of triaxial test
Dr	Relative density
e	Void ratio
eg	Equivalent intergranular void ratio
e_{min}	Minimum void ratio
e_{max}	Maximum void ratio
qc	Cone resistance
Q_{cn}	Normalised cone resistance
q_{c1N}	Normalised cone resistance
q_{c1Ncs}	Normalised cone resistance for equivalent clean sand
ru	Excess pore water pressure ratio
Vs	Shear wave velocity
ψ	State parameter

Chapter-1

INTRODUCTION

1.1 Background

Liquefaction has received a great amount of attention because of the devastating consequences of this phenomenon. Both laboratory as well as in-situ tests have played an essential role in better understanding the underlying mechanism. In laboratories, liquefaction is commonly studied through various plots like pore-water pressure build-up graphs, stiffness reduction plots, and cyclic resistance curves. These efforts gradually led to the formulation of several numerical constitutive models for the liquefaction assessment of soils. Cyclic resistance curve is one of the important plots which is required to estimate an equivalent number of cycles (N_{eq}), which is the basis for the calculation of the Magnitude scaling factor (MSF) used in simplified procedures. Also, several numerical models demand cyclic resistance curves for calibration purposes. R. W. Boulanger & Ziotopoulou, 2017 stressed using the liquefaction curve as the input parameter for their plasticity soil model (PM4SAND). It usually requires performing a number of cyclic tests to obtain a cyclic curve for a specific soil at specific conditions. Owing to the efforts and limitations involved in laboratory tests, there is a need for an easy solution to this problem. With the advent of machine learning, attempts are being made to address a large number of problems using this technique even in geotechnical engineering. Previously, researchers have used machine learning to generate cyclic curves for clean sands. However, in the real world, sandy soil sometimes contains fines, which can influence the cyclic response of soil to great extent. Presence of fines further complicate the process. Though there exists ambiguity in characterizing the effect of fines on the cyclic curve, overall a negative effect is reported in a majority of previously conducted studies.

1.2 Problem Statement

Commonly, semi-empirical methods developed on in-situ tests (SPT, CPT, DMT) are used to assess the safety of soil against liquefaction. These empirical methods (Idriss & Boulanger, 2008, Boulanger, RW and Idriss, 2014, Marchetti, 2016) only provide information regarding liquefaction susceptibility in terms of factor of safety. To obtain other useful information, laboratory tests are required. Cyclic resistance curve is considered one of impotant plots that can only be obtained by

undergoing extensive laboratory program. If these curves are obtained by any means, numerical constitutive model like PM4Sand can be used to assess the complete behaviour of soil under dynamic load. To eliminate the shortcommings like availability of cyclic apparatus and tedious laboratory procedures, machine learning was employed previously. V. Akhila & Adarsh, 2020; and Young-Su & Byung-Tak, 2006 tried to predict cyclic resistance for clean sands using machine learning. The work on predicting cyclic curves for silty sands using machine learning is very less in number.

1.3 Aims and Objectives

This work is an attempt to study the behavior of soil under cyclic loading and its related influencing parameters, as well as, the application of machine learning algorithms. The aim of the work is to generate a cyclic resistance curve for silty sands by implementing the framework of machine learning. The objectives include the following:

- Compiling the cyclic triaxial test on silty sand samples from published work.
- To assess the ability of different machine learning algorithms in predicting the cyclic curve.
- To obtain the parameters that most describe the behavior of soil under cyclic loading through analyzing the data.

1.4 Scope of Thesis

This work could not provide any solution to resolve the material-specific effect. So, the error in predicting cyclic curve can be quite large or negligible depending upon the type of soil. However, providing the data of soil containing non-plastic fines, cyclic curve can be generated for the same soil at any other fines content quite satisfactorily.

1.5 Thesis Outline

The thesis is organized into five chapters. Chapter-2 discusses the available in-situ procedures for liquefaction assessment at the beginning of the chapter. Afterward, the laboratory methods and the factors that influence the cyclic resistance curves are discussed in detail. This chapter also entails

the basic concept related to machine learning. The procedures of a few of the most popular algorithms are also described towards the end of the chapter.

Chapter-3 details the methodology followed to obtain the desired objectives.

In Chapter-4, results are discussed and presented in the form of plots.

Chapter-5 finally concludes the work by enlisting the valuable results.

And finally, references are listed, and an appendix, which includes the compiled data, is also provided at the end.

Chapter-2

LITERATURE REVIEW

Liquefaction is a phenomenon mostly related to saturated cohesion-less soils. This is associated with the build-up of pore water pressure under the undrained conditions developed by seismic loading. The progressive increase in pore water pressure reduces the mean effective stress until zero causing the soil to lose its strength. This reduction in strength can pose great damage to the structure built on these kinds of soils. Understanding the mechanism of this phenomenon is necessary to deal with the hazards associated with it. There are mainly two kinds of mechanisms: flow liquefaction and cyclic softening. (Robertson & Wride, 1998), delineate the two mechanisms quite exquisitely. According to them, deformations continue to proceed even after the event in the flow liquefaction case while deformations stop in cyclic softening. Cyclic softening gets its name because it can only undergo visible deformation under cyclic loading opposite to flow liquefaction. Flow liquefaction can occur under both static and cyclic loading. Cyclic softening is further subdivided into cyclic mobility and cyclic liquefaction with the difference of stress reversal. Cyclic mobility produces small deformations without any stress reversal unlike cyclic liquefaction.

2.1 Evaluation Methods Based On In-Situ Testing

Liquefaction susceptibility of soil can either be determined from in-situ or laboratory tests. A variety of in-situ procedures are developed and improved over the years. It all started with the semi-empirical framework devised by (Seed & Idriss, 1971), which involved the SPT blow counts correlating the cyclic stress ratio (CSR). Afterwards other in-situ tests like CPTU, DMT and Shear wave were also begin to be utilized in formulation of assessment procedures. The basic notion behind these simplified methods is to calculate factor of safety for liquefaction. Factor of safety, which is the ratio of Cyclic resistance ratio (CRR) to Cyclic stress ratio (CSR), decides whether soil is liquefiable.

$$FS_{liq} = \frac{CRR}{CSR} \qquad (2.1)$$

CRR is obtained using in-situ tests like SPTN, CPTu, shear wave etc. CSR which is a measure of earthquake loading introduced to soil, is obtained through site response analysis. However, a relation is introduced by (Seed & Idriss, 1971) which involves cyclic shear stress and initial effective vertical stress.

$$CSR = \frac{\tau_{avg}}{\sigma'_{vo}} = 0.65\left(\frac{a_{max}}{g}\right) \times \left(\frac{\sigma_{vo}}{\sigma'_{vo}}\right) \times r_d \quad \textbf{(2.2)}$$

Where, a_{max} is the horizontal component of peak ground acceleration, g is the gravitational acceleration, σ'_{vo} is the initial vertical stress and r_d is the stress reduction factor that accounts for the non-rigid response of soil. There are several expressions available in literature for calculating stress reduction factor (r_d), from simplest to complex ones. The fudge factor of 0.65 in the above equation is there to account for the irregularity in earthquake loading. In simple words, 0.65 converts the irregular waves into equivalent uniform cycles.

Once the earthquake loading (CSR) is calculated, the Cyclic resistance ratio (CRR) is the thing that remains in order to calculate the factor of safety against liquefaction. To determine CRR, there are procedures available that will be discussed in following sections. The common thing among all the existing procedures is that they are developed based on historical data and for specific standard conditions. Mostly, standard conditions include Magnitude of 7.5, vertical effective stress of 1 atm, and level grounds. So, in order to use these methods for conditions other than standard ones, adjustment factors are required.

$$CRR = CRR_{7.5} \times MSF \times K_\sigma \times K_\alpha \quad \textbf{(2.3)}$$

MSF is a magnitude scaling factor, K_α is a factor to account for initial stresses, and K_σ is for vertical stress other than 1 atm.

These procedures, despite being the semi-empirical in nature, are preferred by geotechnical engineers owing to various drawbacks of laboratory test. Laboratory test involve difficult procedures for instance, high-quality samples, consumes a lot of money and time, etc.

2.1.1 SPTN-Based Procedures

SPT-based procedure is the first ever semi-empirical method developed by (Seed & Idriss, 1971). After the first procedure, various other formulations that correlate SPTN and CRR are developed by other researchers (Cetin et al., 2004; Idriss & Boulanger, 2008; Youd & Idriss, 2001). These procedures are different from one another in terms of the correction factors they include. However, the common thing among them is $(N_1)_{60}$. The correlations between CRR and SPTN blow counts have suffered adjustments over the years. With the increase in the historical database, $(N_1)_{60}$ gets morphed into equivalent blow counts for clean sand $(N_1)_{60cs}$ to take into account the effect of fines content. (Idriss & Boulanger, 2008) presented the relationship between SPT-N and CRR for silty sands.

$$CRR_{7.5} = \exp\left[\frac{(N_1)_{60cs}}{14.1} + \left(\frac{(N_1)_{60cs}}{126}\right)^2 - \left(\frac{(N_1)_{60cs}}{23.6}\right)^3 - \left(\frac{(N_1)_{60cs}}{25.4}\right)^4 - 2.8\right] \quad \textbf{(2.4)}$$

$$(N_1)_{60cs} = (N_1)_{60} + \Delta(N_1)_{60} \quad \textbf{(2.5)}$$

$$\Delta(N_1)_{60} = \exp\left[\frac{9.7}{FC+0.01} - \left(\frac{15.7}{FC+0.01}\right)^2 + 1.63\right] \quad \textbf{(2.6)}$$

$$(N_1)_{60} = C_N C_D C_R C_E C_S N \quad \textbf{(2.7)}$$

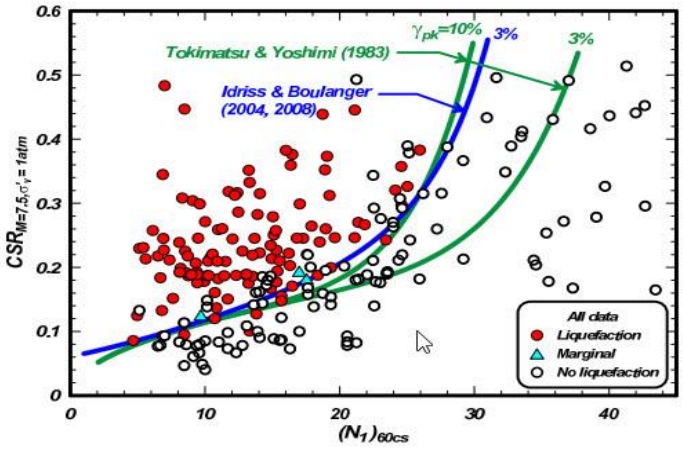

Fig 2-1 Liquefaction Susceptibility Based on SPTN

(I. Boulanger, 2010)

2.1.2 CPT-Based Procedures

Given the limitation of SPT test in providing continuous profiling of site, CPT test started to gain popularity. One of the benefits of CPT is that it provides continuous soil profiling unlike SPT. With the increase in usage of CPT, researchers also started to relate CPT parameters with the CRR (Boulanger, RW and Idriss, 2014; Moss et al., 2006; Robertson, 2009). The procedures presented by different researchers differ a lot in terms of formulations and approach used. For instance, (Robertson & Wride, 1998) use soil behavior type index while (Boulanger, RW and Idriss, 2014) use different approach. Similar to CRR vs SPTN, Idriss and Boulanger 2014 also presented relationship between CRR vs tip resistance (qc) based on the historical data as shown in Fig.2-2. The procedure presented by (Boulanger, RW and Idriss, 2014) is described below:

$$CRR_{7.5} = \exp\left[\frac{q_{c1Ncs}}{113} + \left(\frac{q_{c1Ncs}}{1000}\right)^2 - \left(\frac{q_{c1Ncs}}{140}\right)^3 - \left(\frac{q_{c1Ncs}}{137}\right)^4 - 2.8\right] \quad (2.8)$$

$$q_{c1Ncs} = (q_{c1Ncs}) + \Delta(q_{c1Ncs}) \quad (2.9)$$

$$\Delta(q_{c1Ncs}) = \left(11.9 + \frac{q_{c1Ncs}}{14.6}\right) \exp\left[1.63 - \frac{9.7}{FC+0.01} - \left(\frac{15.7}{FC+0.01}\right)^2\right] \quad (2.10)$$

$$q_{c1Ncs} = C_N \frac{q_t}{p_a} \quad (2.11)$$

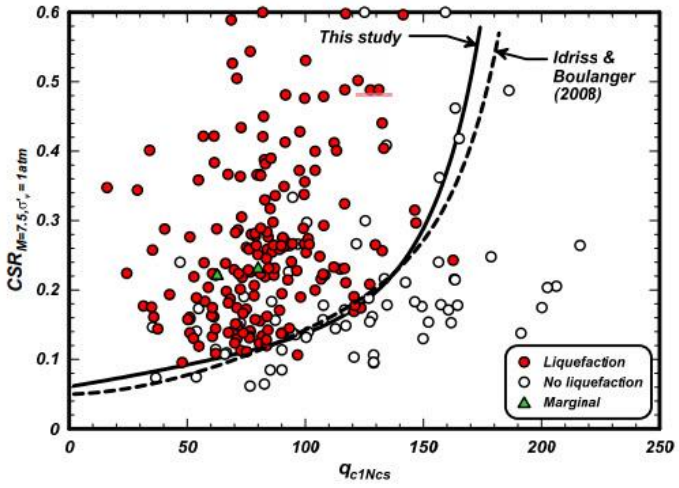

Fig 2-2 Liquefaction Susceptibility Based on CPT
(Boulanger, RW and Idriss, 2014)

The procedure of **Robertson and Wride 1998** involves following equations. Few of those equations got updated in 2009 by Robertson.

$$CRR_{7.5} = 93 \left[\frac{Q_{tncs}}{1000} \right]^3 + 0.08 \qquad \text{If } 50 < Q_{tncs} < 160 \tag{2.12}$$

$$CRR_{7.5} = 0.833 \left[\frac{Q_{tncs}}{1000} \right] + 0.05 \qquad \text{If } 50 > Q_{tncs} \tag{2.13}$$

$$Q_{tncs} = K_c \times Q_{tn} \tag{2.14}$$

If $I_c < 1.64$ K=1 else:

$$K_c = -0.403I_c^4 + 5.581I_c^3 - 21.63I_c^2 + 33.75I_c - 17.88 \tag{2.15}$$

$$I_c = [\, (3.47 - \log(Q_{tn}))^2 + (\log F_r + 1.22)^2 \,]^{0.5} \tag{2.16}$$

$$Q_{tn} = \left(\frac{q_c - \sigma_{vo}}{p_a} \right) \times \left(\frac{p_a}{\sigma_{vo}} \right)^n \tag{2.17}$$

$$F_r = \left(\frac{f_s}{q_c - \sigma_{vo}} \right) \times 100 \tag{2.18}$$

$$n = 0.381 \times I_c + 0.05 \times \left(\frac{\sigma_{vo}}{p_a} \right) - 0.15 \tag{2.19}$$

2.1.3 DMT-Based Procedures

Flat plate dilatometer test is used to measure in-situ strength and other properties of soil. As it is sensitive to stress history, cementation and pre-straining, this test also started to gain attention for liquefaction evaluation. There exist a relation between one of its parameter K_D and CRR. (Marchetti, 2016) presented a CRR relation which is developed by incorporating the Q_{cn} and K_D relation into the CRR relation of (Idriss & Boulanger, 2006). The evaluation of liquefaction from DMT is not as popular as SPTN or CPT.

$$CRR_{7.5} = \exp\left[\frac{Q_{cn}}{540} + \left(\frac{Q_{cn}}{67}\right)^2 - \left(\frac{Q_{cn}}{80}\right)^3 - \left(\frac{Q_{cn}}{114}\right)^4 - 3\right] \quad (2.20)$$

$$Q_{cn} = 25K_D \quad (2.21)$$

2.1.4 Shear Wave Velocity Based Procedures

The reason behind using the small strain parameter for evaluating the large strain phenomenon is that shear wave gets influenced by the same factors as the liquefaction. The conventional in-situ tests like SPTN and CPT are accurate to describe the plastic phenomenon, still many researchers feel the urge to relate the shear wave with CRR. With the improvements in in-situ shear wave methods, the use of shear wave in assessing liquefaction potential has been increased. The drawback of using shear wave is similar to SPT that is it cannot detect the thin layers. However, the use of shear wave is favorable in situations where soils are hard enough to get penetrated by SPT or CPT. The commonly used procedures based on shear wave to assess liquefaction potential is that of (Andrus et al., 2004) and (Kayen et al., 2013). **Andrus & Stokoe 2004** formulations are presented in following equations.

$$CRR = \left[0.022\left(\frac{K_{a1}V_{s1}}{1000}\right)^2 + 2.8\left(\frac{1}{V_{s1*} - K_{a1}V_{S1}}\right) - \frac{1}{V_{s1}^*}\right] \times K_{a2} \quad (2.22)$$

$$V_{S1} = V_s \times \left(\frac{P_a}{\sigma'_{vo}}\right)^{0.25} \quad (2.23)$$

$$V_{s1}* = 215 \text{ m/s} \qquad FC < 5\% \quad (2.24)$$

$$V_{s1}* = 215 - 0.5(FC - 5) \qquad 5\% < FC < 35\% \quad (2.25)$$

$$V_{s1}* = 200 \text{ m/s} \qquad FC > 35\% \quad (2.26)$$

Kayen et al 2013 presented a probabilistic nature of the framework. Following are the equations from **Kayen et al 2013**.

$$CRR = \exp\left[\frac{1}{1.946}\{-(0.0073V_{s1})^{2.8011} - 2.6168\ln M_w - 0.0099\ln \sigma_{vo}' + 0.0028FC - 0.4809\Phi^{-1}(PL)\}\right] \quad \textbf{(2.27)}$$

$$PL = \Phi\left[\frac{1}{0.4809}\{(0.0073V_{s1})^{2.8011} - 1.946\ln CSR - 2.6168\ln M_w - 0.0099\ln \sigma_{vo}' + 0.0028FC\}\right] \quad \textbf{(2.28)}$$

Ahmadi & Akbari Paydar, 2014, through experimental work proved Andrus & Stokoe method as a conservative method and furthered that accurate assessment of liquefaction require formulation of soil-specific CRR-V_{s1} relation through experiments.

2.2 Laboratory Based Evaluation Methods

Laboratory tests have remained central in geotechnical engineering to understand the complex behavior of soils under controlled conditions. Notwithstanding the fact that these tests are cost-inefficient, time-consuming, and tedious to perform, the major advancements from empirical equations to constitutive models were made based on these laboratory results. In liquefaction studies, these laboratory tests proved valuable in understanding the effect of various influencing parameters. There are a number of methods exist for liquefaction assessment: stress-based, strain-based, energy approach, critical state method and shear wave velocity.

The most commonly used equipment for this purpose are cyclic triaxial test and cyclic simple shear test. However, the other instruments like hollow cylinder, torsional shear, shaking table and ring shear test are also being used for liquefaction studies. Though it is not possible to imitate the exact field conditions in the laboratory. But for reliable results it is essential to carry out the tests under conditions close enough to field ones including both in-situ state and seismic loading. The in-situ conditions include effective stress, density, deposition of soil, and water conditions while seismic loading include mainly the intensity and propagation of shear wave. The mechanism of different equipment impose different loading conditions, so the results from one equipment might be different from the ones obtained using another equipment. It is considered that shear waves propagate upward during the seismic event and cyclic simple shear is the equipment that mimics these loading conditions quite accurately.

The core differences between cyclic triaxial and cyclic simple shear are that of loading direction and stress rotation. Cyclic triaxial test operates on deviatoric loading opposite to cyclic simple as well as field stress conditions. Despite the ill representation of seismic loading conditions, triaxial setup is more regularly used in laboratories because of its common availability. (Jefferies et al., 2015) presented the actual loading imposed on soil in field, as shown in fig 2-3.

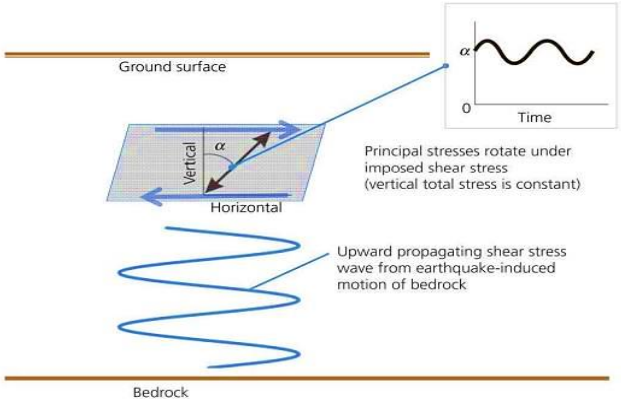

Fig-2-3 Actual Loading Imposed on Soil in Field
(Jefferies et al., 2015)

Besides the proper field representation, identification of liquefaction state is also important for consistency in results. There are mainly two criteria for identification of failure state: i. pore water pressure ii. Strain/deformation criteria. The widely used criteria is pore-water pressure ratio (r_u) which is a ratio of change in pore pressure to initial confining pressure. In triaxial condition, $r_u = \Delta u / \sigma_{3c}'$ while in simple shear it is $r_u = \Delta u / \sigma_{vo}'$. According to this criteria, soil is considered to be liquefied when r_u reaches a value of one. But this pore pressure generation is dependent mainly on compaction and type of soil. It means that loose soils undergo large deformation when $r_u=1$ unlike dense soils. In liquefaction, the increase in pore-pressure is accompanied by the accumulation of strain (El et al., 2016). So, it is recommended to use this criterion together with the strain criteria. Strain criteria defines liquefaction as a state when the soil reaches certain level of strain. This strain level varies from 2 to 10% (Wu et al., 2004), but most commonly its value is 5% D.A axial strain in triaxial condition as recommended by (Ishihara, 1993) and 7% D.A shear strain in simple shear setting (Onder Cetin & Tolga Bilge, 2012; Vaid & Sivathayalan, 1996). The relationship between double amplitude (D.A) axial strain and D.A shear strain in terms of poisons ratio is presented by (Kokusho, 2017) as $\varepsilon_{D.A} = \gamma_{D.A}/(1+ v)$. For undrained conditions, poisons ratio is 0.5 so, $\gamma_{D.A}= 1.5 \times \varepsilon_{DA}$.

2.2.1 Stress-Based Method

Stress based method include the factor of safety, which determined by dividing the resistance of soil by the stress applied. The resistance of soil is commonly obtained through laboratory cyclic tests.

Cyclic Resistance Curves

The results of the laboratory tests are interpreted in form of graphs. The plots like pore-pressure generation, strain accumulation, cyclic resistance curves and modulus reduction are considered important in studying the soil behavior under cyclic loading. Cyclic curves are plots between the cyclic stress ratio and the number of cycles till failure. CSR is the cyclic stress ratio which is a shear stress normalized by initial vertical effective stress in cyclic simple conditions. While it is ratio of shear stress to initial effective confining pressure. Initial liquefaction is considered as a failure state which is determined by either r_u or strain criteria. Depending upon different definition of failure, different cyclic curves are obtained as is visible in fig 2-4.

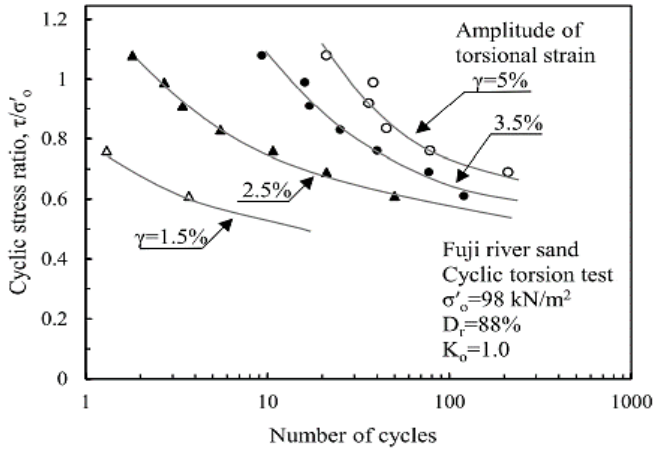

Fig 2-4 Cyclic Curves for Different Strain Levels
(adapted from Ishihara, 1985)

Cyclic resistance curves are obtained through performing number of tests on samples with same initial conditions (density and confining pressure) at different CSR. It is observed from the fig that CSR changes inversely with the number of cycles. The following equation is widely used to describe the relation between CRR and number of cycles:

$$CRR = aN^{-b} \quad \textbf{(2.29)}$$

Where a and b are fitting parameters, which are different for different sands. The parameter 'b' defines the slope of the curve which commonly ranges from 0.08 to 0.4. (Kishida & Tsai, 2014) used the value of 0.34 for this parameter for all the sands in calculating N_{eq}.

2.2.2 Energy Method

Just like stress method, the basic principal of energy method involves comparing the seismic demand with soil capacity to resist it. The energy based methods came to use because of two main reasons. These methods, unlike stress method, quantify earthquakes in terms of energy which is quite simple. The other benefit is that they incorporate the effect of both stress and strain methods. When a soil is subjected to dynamic loading, part of this energy is dissipated into the soil. The energy dissipated into the soil can be determined through the hysteresis loop formed in a stress-strain space (Fig 2-5). In cyclic triaxial test, dissipated energy is calculated from the deviatoric stress-strain hysteresis loop (Eq- 2.30), while for simple shear stress-strain loop (Eq-2.31). A typical hysteresis loop is shown in Fig 2-5.

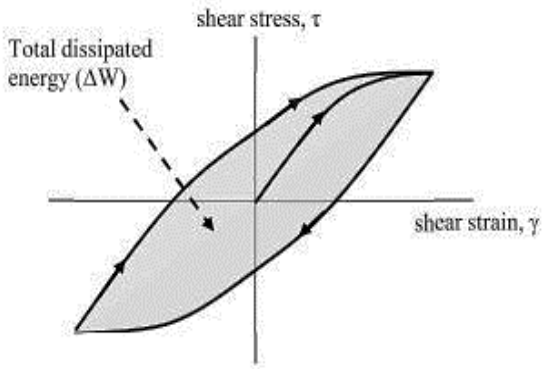

Fig 2-5 Shear stress-strain Plot
(Green & Mitchell, 2001)

$$\Delta W = \frac{1}{2}\sum_{i=1}^{n-1}(\sigma_{d,i+1} + \sigma_{d,i})(\varepsilon_{a,i+1} - \varepsilon_{a,i}) \quad \textbf{(2.30)}$$

$$\Delta W = \frac{1}{2}\sum_{i=1}^{n-1}(\tau_{i+1} + \tau_i)(\gamma_{i+1} - \gamma_i) \quad \textbf{(2.31)}$$

It is observed from previous studies that energy per unit volume required to cause liquefaction increases with the increase in density. (Baziar et al., 2011) developed an equation to determine capacity energy as a function of relative density confining pressure, coefficient of uniformity (cu), mean grain size (D_{50}) and fines content.

2.2.3 Laboratory Shear Wave Methods

The potential advantages of shear wave velocity urged researchers to relate it with the large strain phenomenon. Besides the method based on in-situ shear wave, many researchers have correlated laboratory shear wave with the cyclic resistance. Most prominent work is that of (Y.-G. Zhou & Chen, 2007) who proposed a relation between CRR and shear wave velocity. (Ahmadi & Akbari Paydar, 2014) also developed CRR-Vs1 relation for different soils and concluded that relation is soil-specific which is not applicable to all soils. Shear wave can also be used to assess the quality of the sample by comparing the in-situ shear wave with the shear wave measured in laboratory. Even shear wave can account for the fabric effect. The results of the tests performed by (Wang et al., 2006) proved that a reconstituted sample prepared at the same initial shear wave velocity as of undisturbed sample can represent the in-situ cyclic strength.

2.2.4 Critical State Soil Mechanics

Since the conception of critical state soil mechanics coined by (Roscoe et al., 1958), this framework has been employed to describe number of mechanical properties of the soil. After its success in static conditions, researchers started to use it in cyclic scenarios. Variety of parameters based on CSSM have been introduced from which state parameter (ψ), proposed by (Jefferies & Been, 2006), has proved its worth (Qadimi & Mohammadi, 2014). It is observed in many studies that this state parameter not only normalizes the effect of density and confining pressure but also that of fines content on cyclic resistance (Hsiao & Phan, 2016; Mohammadi & Qadimi, 2015; A. Papadopoulou & Tika, 2008; Wei & Yang, 2019a). Fig 2-6 shows the relationship between CRR and (ψ) for Anzali sand, which shows a indirect relation between them.

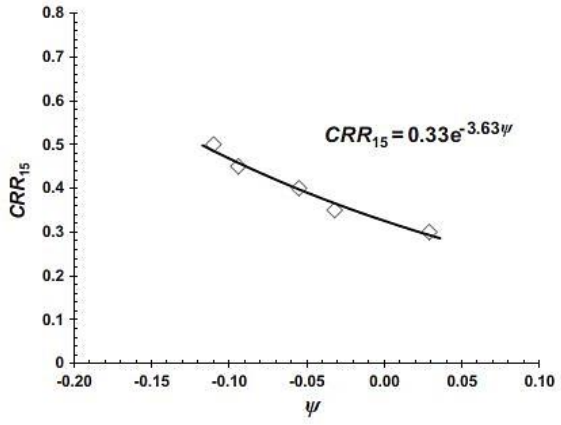

Fig 2-6 CRR- ψ Plot for Anzali Sand
(Mohammadi & Qadimi, 2015)

Though a unique relation can be drawn between CRR and state parameter (ψ), but the scatter in the data shows that this parameter cannot capture the effect of other factors like fabric of soil. The problem with the critical state approach is that the accurate determination of Critical state line is not possible. Many attempts have been made to determine the in-situ state parameter (ψ) as well. But determining this parameter from in-situ test (CPT) is not as easy as it may looks. Apart from difficulties involved in calculations, it is considered a better method than SPTN or CPTU based procedures since no adjustments are required in this method unlike SPTN or CPT methods.

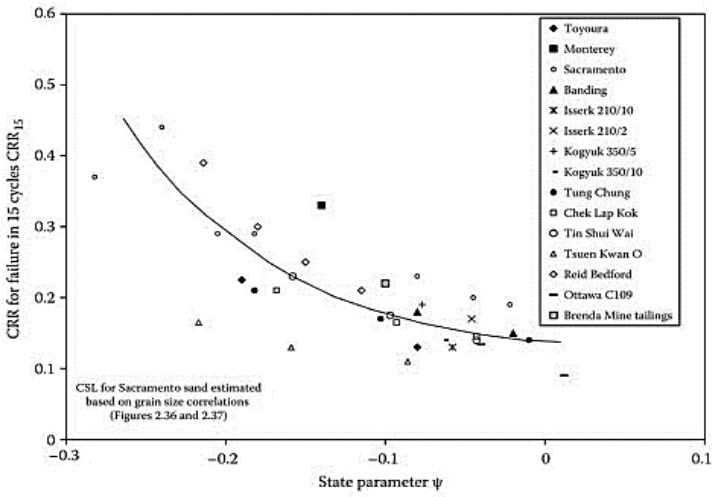

Fig 2-7 Relationship between CRR and State Parameter
(Jefferies et al., 2015)

After all the efforts made in carrying out laboratory studies, various robust constitutive models are being used today. These models directly or indirectly include the critical state concept in their formation. The disadvantages associated with the numerical analysis is large number of parameters to be calibrated through laboratory tests. Also, just like other methods they work within certain accuracy.

2.3 Factors Influencing Cyclic Resistance

The behavior of soil subjected to dynamic loading is influenced by several factors which include state conditions, soil properties and loading characteristics. The impact of these factors on the phenomenon has been understood individually in many previous studies. The factors are broadly categorized as:

i. **State conditions**: density, confining stress and initial stresses.
ii. **Soil properties**: gradation, grain size, soil type and shape of grain, and fabric of the soil.
iii. **Loading properties**: frequency, loading conditions, intensity, and loading pattern.

2.3.1 State Conditions

State conditions include relative density, confining pressure, initial stresses and fabric of the soil. There are different measures to define the compactness of soil, for instance, relative density, dry density, void ratio and inter-granular void ratio (in case of silty sands). Relative density is a measure that reflects on the degree of compactness of soil with respect to the maximum density a particular soil can achieve. It is observed that with the increase in density, soil tendency to liquefy decreases (Mandokhail et al., 2017). It is because the dense soil tends to dilate which prevents building of positive pore water pressure during cyclic load. CRR can also be related with the void ratio, but relation is soil specific as shown by (Ahmadi & Akbari Paydar, 2014) who used the data for different clean sands. The great amount of studies on silty sands show that CRR curve for same sand with fines content plummets to lower position than clean sand. From these results it can be said that fines content changes the type of soil. But because of the trend that exist in soil with increasing fines content, a wide range of studies devoted to normalize the effect of fines. Further discussion on fines content effect will be discussed in next section.

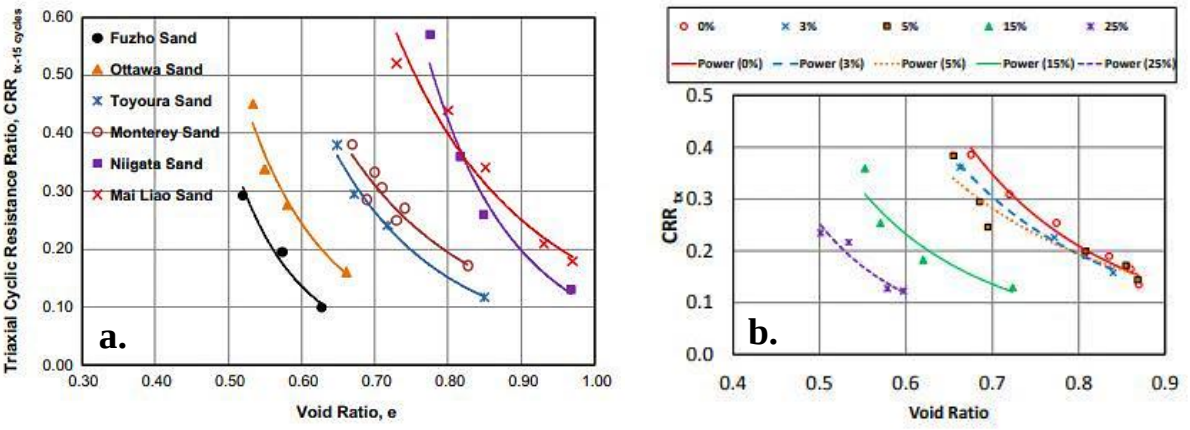

Fig 2-8 Relationship between CRR and Void ratio **(a)** Clean sands (Ahmadi & Akbari Paydar, 2014) **(b)** Silty sand (Akbari-Paydar & Ahmadi, 2015)

In contrast to relative density, confining pressure has adverse effect on the liquefaction strength of soil. The capacity of soil to resist liquefaction decreases with increasing confining pressure. But the effect of confining pressure is more prominent in dense soils and its effect for loose sands is nearly negligible (Vaid & Sivathayalan, 1996). (Mandokhail et al., 2017) collected cyclic resistance data for several clean sands from the literature published previously and confirmed that sand type, relative density, confining pressure, type of test and sample preparation method influence the liquefaction resistance.

One of the most influential factor which is not easy to simulate in laboratories is fabric of the soil. This immeasurable factor can lead to inconsistent results for the same soil upon loss of fabric. 'Fabric' is a one word that incorporates different phenomenon like aging of soil, deposition of soil and cementation present in soil. Separate studies have conducted on these fabric related factors with all confirming their great impact on cyclic resistance. Fabric is the reason for preferring undisturbed samples over the reconstituted ones. But because of the effort required in achieving high quality undisturbed samples, engineers are left with no other option but reconstituted samples. In laboratories, samples are prepared with different techniques mostly, moist tamping, water sedimentation and air pluviation. The Cyclic resistance curves for samples prepared using different techniques differ a lot. This difference is attributed to the different fabric formed using different techniques. Though it is difficult to reproduce the same fabric in the laboratory but through different sampling technique the effect of fabric can be understood. It is observed in previous studies that moist tamped samples yield more strength to liquefaction than others.

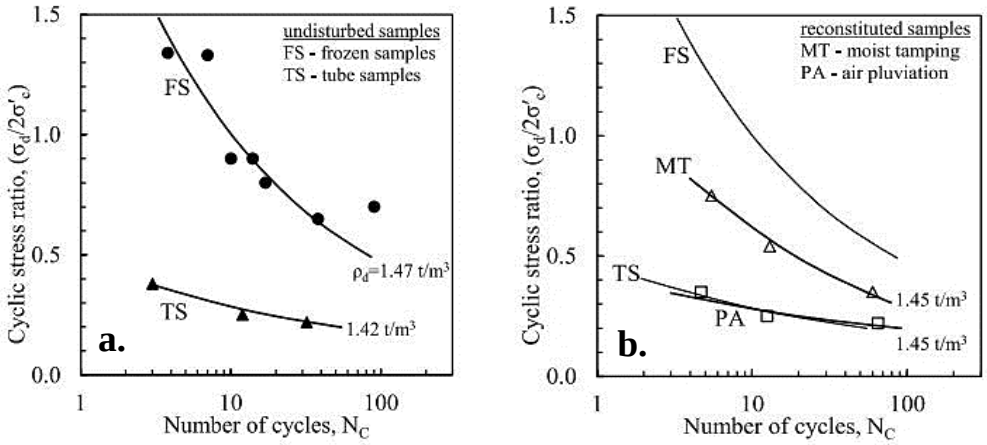

Fig 2-9 Sampling Effect **(a)** Undisturbed samples **(b)** Reconstituted samples (after Yoshimi et al 1984)

There exists a clear distinction between the field and laboratory results. Literature shows that SPT-N and CPT based methods predict positive effect of fines on cyclic strength contrary to the laboratory results (Taylor et al., 2015). (Kokusho et al., 2012) attributed this contradiction to cementation of soil. Though Fabric that exists in field cannot be reproduced in laboratory, different sampling methods in laboratory somehow elaborate on deposition effect. Despite its poor representation of the deposition in field, moist tamping is preferred over other sampling techniques in case of silty-sands to avoid segregation of the fines. Likewise other fabric related factors like layering effect and ageing have been studied previously (Amini & Qi, 2000; Cappellaro, 2019).

2.3.2 Soil Properties

The impact of factors related to the soil like particle size, particle shape, gradation, and fines content on liquefaction has been reported previously.

The percentage of particles with size smaller than 0.075 mm are referred to as fines content. Fines content can be plastic or non-plastic in nature depending upon the mineralogy. With the revelation that silty sands can also liquefy, many researchers directed their focus to this topic. It is observed that plastic fines decreases the cyclic resistance of soil, but the interaction of non-plastic fines is bit complicated. This is a reason that a good amount of attention has been paid to understand the effect of non-plastic fines on liquefaction strength. For better understanding, a lot of studies have been conducted on homogeneous samples with systematic increase of fines content. The results presented by one researcher does not support the results of the other researchers. Some reported an

increase of strength with the fines others concluded with opposite results. With the further clearance on the behavior of the silty sands, researchers seem to agree on the same concept. They believe that interaction of fines content with the coarser particles is something that defines the behavior of soil at macro level. In the process, terms like inter-granular void ratio and threshold fines content came into existence. It is noticed in many works that there is a change of trend after a certain amount of fines content regarded as threshold fines content. Threshold fines content is a boundary between sand-dominated structure and silt-dominated structure. Theoretically, in a sand-dominated structure, silts either stay in voids formed by coarser sands or they take part in load carrying mechanism keeping the sand as a major contributor. Fig 2-10 presented by (Thevanayagam et al., 2002) explains the mechanism quite well. Once the threshold fines content is past, the sand-dominated structure shifts to silt-dominated. The range for threshold fines content range between 25 and 40 for majority of soils. However, it is not even a unique value for same soil (Baziar & Sharafi, 2011; A. . Papadopoulou, 2008) .

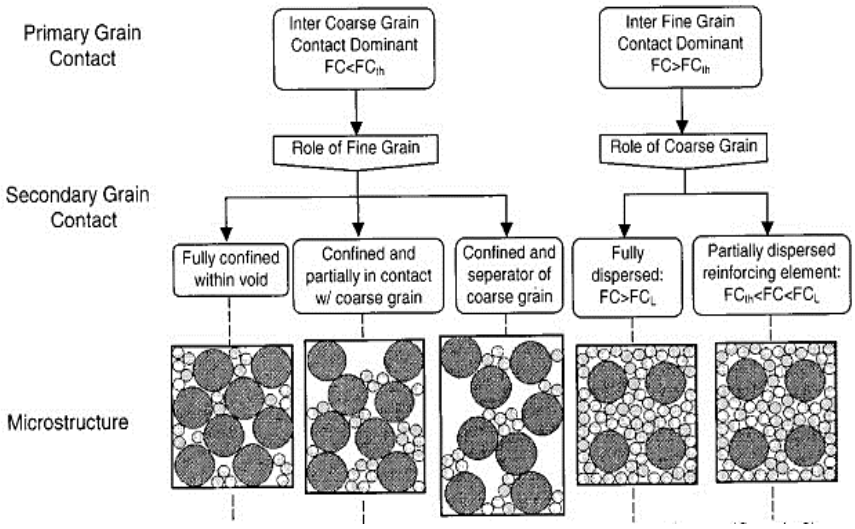

Fig 2-10 Sand-Silt Interaction schematic diagram
(Thevanayagam et al., 2002)

Majority of previous work reports the negative effect of fines content upto threshold fines content. To account the fines effect inter-granular void ratio, which is then morphed into equivalent void ratio, is introduced. Following equation is introduced for equivalent void ratio.

$$e^{*} = \frac{e + (1-b)f_c}{1-(1-b)f_c} \quad \textbf{(2.32)}$$

The parameter 'b', which determines the amount of fines involved in taking load, is not an easy parameter to determine. It usually requires back calculation. However, (Goudarzy et al., 2017) presented the following equation.

$$b = [1 - \exp\left(-\frac{a\left(\frac{f_c}{f_{thres}}\right)^{n_b}}{k}\right)]\left(\frac{rf_c}{f_{thres}}\right)^r \quad \textbf{(2.33)}$$

where, fc = fines content, r= d_{50}/ D_{10} , D_{10} = size of sand at 10% passing, d_{50} = size of silt at 50% passing, f_{thres}= threshold fines content , K= 1- $r^{0.25}$. f_{thres} can be determined by the following equation by (Rahman et al., 2008). Nb and a are the fitting parameters whose values are suggested as 1 and 0.3 by Laskari et al 2014. (Goudarzy et al., 2016) also observed that the values of these parameters vary with the soil and suggested their values to be optimized for maximum R2.

$$F_{thres} = 0.40 \times \left(\frac{1}{1+ \exp\left(0.5 - 0.13 \cdot \left(\frac{1}{r}\right)\right)} + r \right) \quad \textbf{(2.34)}$$

Besides the amount of fines, shape of the grains is another factor on which this interaction related behavior highly depends on (J. Yang & Luo, 2015; J. Yang & Wei, 2012). For clean sands, only shape of the sands matters while in silty sands both the shape of fines and sand cause behavioral change.

2.3.3 Loading Characteristics

As stated earlier, different test equipment impose different stress conditions to soil specimen. These stresses are also different from the conditions experienced by the soil in field. Cyclic simple shear conditions are not same but closer to field conditions. But triaxial setup is most commonly used because of its availability. It is observed that the results from cyclic triaxial test differ from those obtained through cyclic simple shear. Mostly, the CRR from Triaxial test is always higher than simple shear test (Nong et al., 2021; Sadrekarimi, 2016). The curves presented by (Mandokhail et al., 2017) using the data of (Peacock & Seed, 1968) shows that curves from triaxial testings lie above but with lesser in curvature than those of cyclic simple shear (Fig 2-11) .

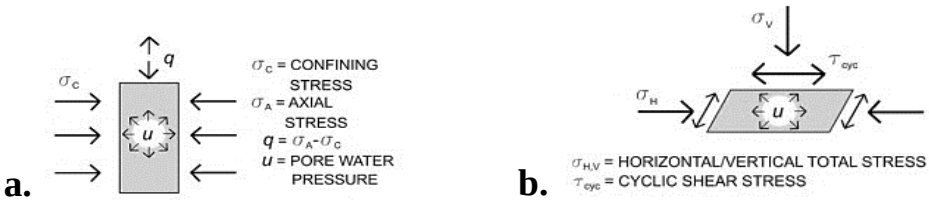

Fig 2-11 Stress Conditions **(a)** Cyclic Triaxial Setting **(b)** cyclic simple shear test (Cappellaro, 2019)

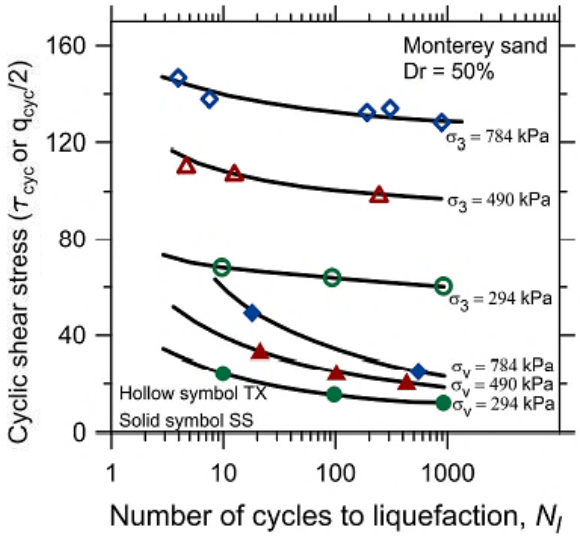

Fig 2-12 Cyclic Curves for Different Tests (Mandokhail et al., 2017)

This difference, which results in dissimilarity between the values of CSS and CTX, is attributed to anisotropic conditions (k_o=1) of cyclic simple shear test. If K=1 CRRtx is equal to CRRss. However, for $K_o \neq 1$ condition, conversion factors are available inliterature to convert the CRRtx to CRRss, but actual function is more complex which depends on many factors than simply on K_o (Misko-2017, Vaid and Sivathayalan 1996). Later studies used c_r which is a ratio between CRR_{ss} and CRR_{tx}, and reported the dependence of this factor on density and confining pressure. Various studies have been devoted to find relation between CRR from triaxial test and CRR from simple shear test. Most commonly used conversion factor, which is mainly a function of k_o, is that of Ishihara et al 1985.

$$CRR_{ss} = \left(\frac{1+2(k_o)_{ss}}{3}\right) CRR_{tx} \quad \textbf{(2.35)}$$

2.4 Introduction to Machine Learning

Machine learning is a data driven technique which enables computers to learn from data. An algorithm that could understand the patterns and make relation from data is necessary in order to perform this task. This second half of this chapter introduces the fundamental concepts of machine learning along with the challenges and steps involved in the creation of machine learning model. The procedures of a few of the most popular algorithms are also described towards the end of this chapter. Most of the concepts presented in this chapter are taken directly from a famous book written by (Géron, n.d.).

2.4.1 Machine Learning Classification

Depending upon the amount and type of supervision required during training, machine learning can be of four types: Supervised, semi-supervised, unsupervised and reinforcement learning. Each kind differs from other in terms of data, algorithms, purpose and mechanism.

In **supervised learning**, training data which is used to feed an algorithm includes labels (desired solutions/output).In simple words, algorithm develops a relation between input and output variables present in data and creates a predicting model. The supervised learning has two cases: classification and regression. Fig 2-13 shows the difference between the two. Classification is used when the desired solution is to classify the data based on input variables while regression deals with numeric value. For instance, identification of the spam mails is a classification problem while predicting price of a house is a regression. Most common algorithms for supervised learning are: K-Nearest Neighbors (KNN), Linear regression, logistic regression, Decision trees, Support vector machines (SVM) and neural networks. The details on different algorithms will be presented later in this chapter.

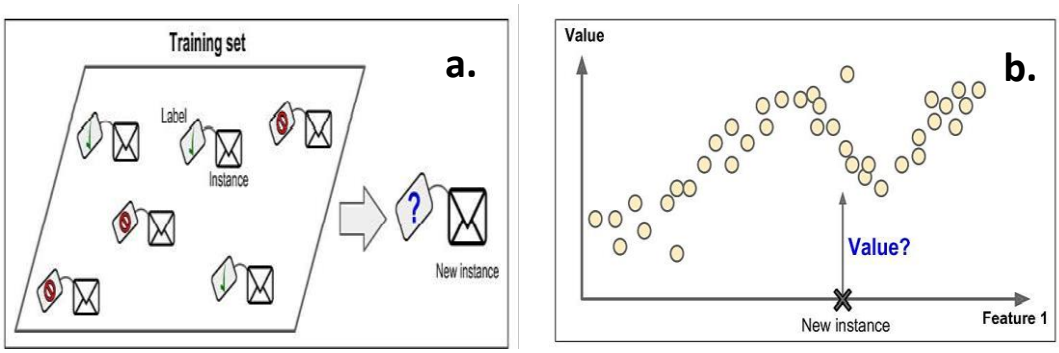

Fig 2-13 Supervised Learning **(a)** Classification **(b)** Regression (Géron, n.d.)

Unsupervised learning does not include any output variables in data. This kind of learning is used for clustering, visualization and dimensionality reduction, and anomaly detection. Clustering algorithm finds connections on its own and makes groups of similar data. For instance, algorithm makes groups of persons based on their reading interest as shown in fig 2-14 (a). Likewise, unsupervised learning is also useful in detecting unusual activity like credit card suspicious transaction. Anything that is different from the routine would be detected as 'anomaly' by the algorithm, just as shown in fig 2-14 (b). The common algorithms for clustering include K-means, DBscan and Hierarchical Cluster Analysis (HCA). The algorithms like Principal Component Analysis (PCA) and One-class SVM are used for dimensionality reduction and anomaly detection respectively.

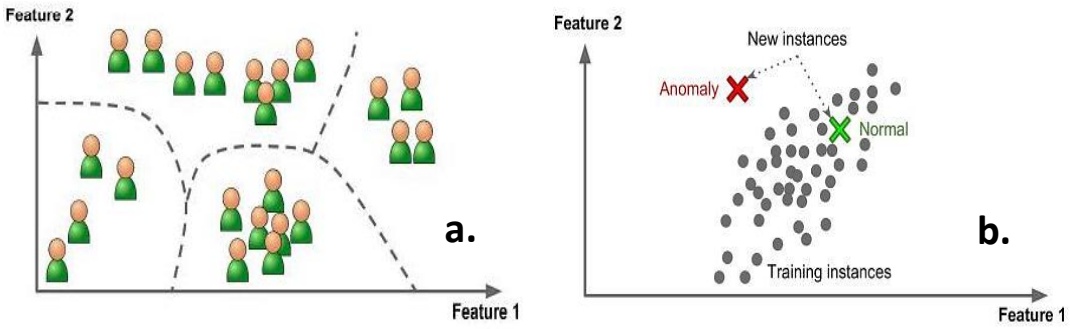

Fig 2-14 Unsupervised Learning **(a)** Clustering **(b)** Anomaly Detection (Géron, n.d.)

Semi supervised learning involves both supervised and unsupervised systems. In this learning, little amount of data is labelled while the remaining data is unlabeled. Perfect example to this is identification of a person in a group like google photos. Once a new photo is uploaded it recognizes the person and all you need is to label that person. This is how semi supervised learning works (fig 2-15).

Reinforcement learning is entirely different from the other learning systems. System learns by observing the environment and performing some sort of action. And the system gets rewarded every time it makes right decision and system learns this way. Training a robot is a good example for this kind of learning.

Based on criterion that whether a system can learn incrementally, machine learning can be of two types: Batch learning and Online learning. Batch learning is not capable of learning incrementally. First system is trained on all the available data and then it is launched without learning anymore. If the pattern in data changes then training is again required on new data unlike online learning. Online learning can learn incrementally and hence, great for the system that deals with continuous data (like stocks).

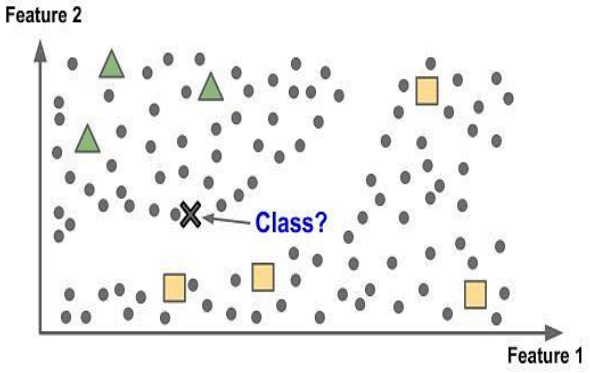

Fig 2-15 Semi-Supervised learning (Géron, n.d.)

2.4.2 Challenges Involved In Machine Learning

Notwithstanding the fact that machine learning is a revolutionary technique, it also faces challenges along the way. The most common problems it deals with are either data-specific or algorithm-related.

1. Issues associated with Data

The issues related to data include quantity as well as quality of the data. It is observed by (Banko & Brill, 2001) that on fairly large data, different algorithms perform quite similar. They suggested that instead of spending time and money on building more algorithms, quantity of data should be ensured. However, in everyday life where we mostly deal with medium sized data, choice on algorithm cannot be ignored (Halevy et al., 2009).

Sometimes, model performs poor not because of quantity but quality of data. For quality data, data must include all the relevant features with less noise in it. For instance, in predicting the price of a house, the possible input features could be location, size of the house, facilities available etc.

However, considering gender as an input to predict the price might not be accurate. Feature engineering can help ensuring quality of data by removing outliers, dealing with missing values, finding most related features and performing other processes.

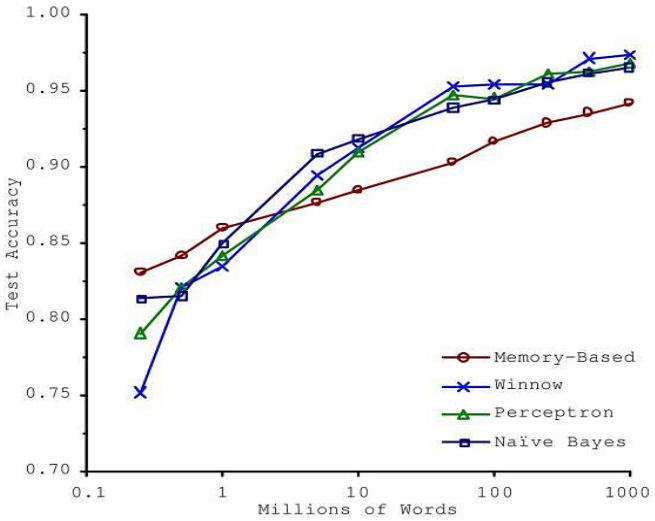

Fig 2-16 Performance of Algorithms for Large Data
(Banko & Brill, 2001)

2. Issues Related to Algorithm

The issue that arise because of algorithm include overfitting and under-fitting. When the model happens to preform exceptional on training data but poor on unseen data it is referred as overfitting. Overfitting is usually associated with the degree of complexity of an algorithm relative to the quantity and noise in data. For instance, a complex algorithm like deep neural network can detect subtle patterns if the data is too noisy and quantity is too small. Under-fitting is quite opposite to overfitting. It happens when algorithm is too simple to understand underlying patterns. The ideal case of model is when it performs better on both training as well as testing data sets.

These challenges can be resolved by using feature engineering to improve data quality, regularization in case of overfitting and use of complex algorithm with more parameters in under-fitting situation.

2.4.3 Feature Engineering

Feature engineering involves a variety of operations to deal with any inconsistency present in data. Most common operations include: handling of missing data, Handling of categorical data, Removal of outliers, feature selection and Transformation of data.

i. Handling of Missing Data:

The raw data can have a lot of missing values in it. To deal with those missing values so that they don't affect the training process there are two options. Either to delete those missing data altogether or to fill the missing ones with appropriate values. Sometimes, removing the missing datasets can result in loss of data in large amount. So it is preferred sometimes to use mean, median or mode to fill the missing value.

ii. Categorical Data:

Computer is not designed to understand the categorical or string data. So it becomes a necessity to convert any string present in dataset to numeric values like in form of binary numbers. In doing so, technique like hot encoding is most commonly employed.

iii. Cleaning and Transformation of data:

The major source of inconsistency in data arise from outliers or noise. So, a fair amount of attention should be given in removing them during pre-processing stage. There are techniques like 3-standard deviation and inter-quartile range method to identify the outliers. To visualize the outliers, 'boxplot' is commonly used for this purpose.

Transformation of the data is also a feature engineering operation which brings all the features to a same scale. Transformation reduces the computational effort and makes things easier for an algorithm to understand the patterns.

2.4.4 Feature Selection

The last but the most important process is finding out features that highly relate to the output. Using irrelevant features can not only lead to dubious results but also be a cause of 'curse of dimensionality'. It is also important to ensure that the input parameters are independent of each

other else issues relating to multi-collinearity arise. Multi-collinearity does not affect accuracy much but it changes the coefficients and P-values (Michael H. Kutner, Christopher J. Nachtsheim, John Neter, 2013). The techniques for feature selection are categorized into three groups: Filter methods, Wrapper methods and embedded method (Tadist et al., 2019).

Filter methods: Filter methods do not involve any model. These are the simplest methods that just focus on the features themselves. Pearson correlation, spearman correlation, chi-squared, ANOVA are a few of them.

Wrapper Methods: These methods check the accuracy of the model by adding or removing the feature to assess the impact of that feature on the output. Recursive feature elimination and sequential feature selection (forward selection, backward selection, floating forward and backward selection) are the most popular wrapper methods. The most efficient both in respect to computation and accuracy is forward selection method (Bemister-Buffington et al., 2020).

The underlying procedure of Forward feature selection is worth to describe here. In first loop, it creates models for every input parameter and select a parameter that gives the best accuracy among all other parameters. In second loop, more models are formed using two parameters but every combination include best parameter from previous loop. The combination of two parameters which gives the best accuracy is selected for 3rd loop. This can be better understood from the fig 2-17 presented here.

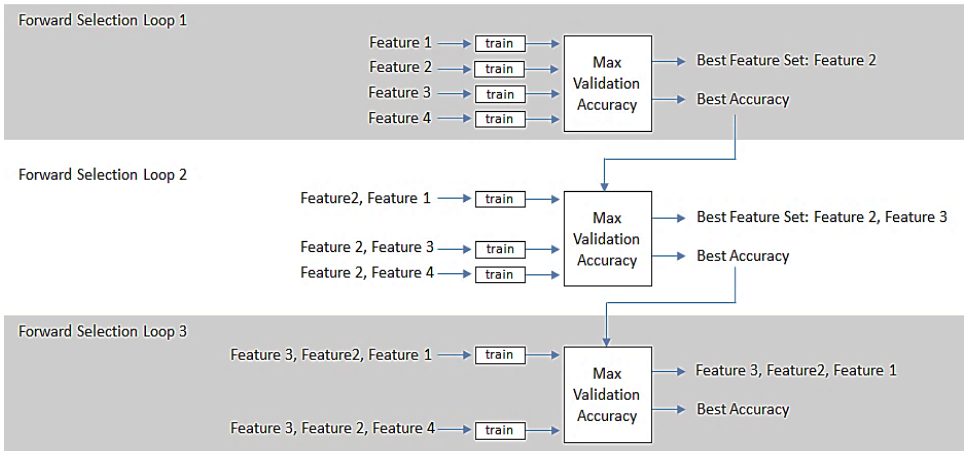

Fig 2-17 Sequential Forward Feature Selection (Mathworks)

Embedded methods: These methods are embedded in the models. Once the model is created, model automatically perceive the most influencing features. Unlike wrapper methods, there is no need to iterate the model for the number of times the features. L-1 regularization, Random-forest and decision trees are a few of them.

2.4.5 Optimization And Regularization

The purpose of both regularization and optimization is same which is to make model more efficient. Optimization is searching for the best set of parameters that can reduce errors and increase the accuracy of the model. While regularization is to improve the ability of the model on testing data by restraining few of the model parameters during training phase. So, optimization and regularization are performed in training phase having slightly different purpose. There are several optimization techniques are available that help in searching the best hyper-parameters. Gridsearch, Randomsearch and Bayesian optimization are the popular ones. In this section, a bit more information on Bayesian optimization technique will be shared.

Bayesian Optimization

Owing to the limitations present in Gridsearch and Randomsearch, Bayesian optimization technique is preferred over them. This technique builds a surrogate model of the objective function since surrogate model is much easier than the objective function. At the start, this surrogate performs poor but after several iterations, the surrogate approaches the true objective function. Based on the assumption that if surrogate performs well with a specific combination of hyper-parameters then the real model will also yield good performance with the same set of hyper-parameters. This way the best combination of hyper-parameters is identified. So, the generic steps for Bayesian technique involves:

1. Building a surrogate model
2. Finding the best parameters for surrogate model
3. Apply the hyper-parameters to the true objective function
4. Update the surrogate model with new results
5. Repeat the process till model stops to improve.

2.4.6 Evaluation Measures

A model is evaluated using an appropriate performance matrix. To assess a regression model, Root mean squared error (RMSE), Mean absolute error (MAE) and R-squared (R2) are commonly used performance measures. For problems related to classification, performance measures based on confusion matrix like accuracy, precision, recall and F-score are more common. Confusion matrix counts the number of accurate predictions (True Positive (TP), True Negative (TN)) and number of inaccurate values (False Positive (FP), False Negative (FN)). Based on confusion matrix precision, recall or accuracy can be measured.

$$\text{Precision} = \frac{\text{TP}}{\text{TP+FP}} \tag{2.36}$$

$$\text{Recall} = \frac{\text{TP}}{\text{TP+FN}} \tag{2.37}$$

$$\text{Accuracy} = \frac{\text{TP+TN}}{\text{Total Numbers}} \tag{2.38}$$

Root mean squared Error (RMSE) and Mean absolute error (MAE) both are the ways to measure error between the target values and the predicted ones. They measure the distance between the predicted vectors and target vectors in order to get errors. RMSE uses Euclidean distance while MAE works on Manhattan distance. The lesser the errors the more accurate is the model. RMSE is more sensitive to outliers that is why it is recommended to use MAE if outliers exist in data. The formulation of RMSE and MAE are presented in below equations. These error estimators are also referred as cost functions and are useful in building a model with minimum error.

$$\text{RMSE (X, h)} = \sqrt{\frac{1}{m}\sum_{i=1}^{m}(\text{h}(\text{x}^{\text{i}}) - y^{i})^2} \tag{2.39}$$

$$\text{MAE (X, h)} = \frac{1}{m}\sum_{i=1}^{m}\left|\text{h}\left(\text{x}^{\text{i}}\right) - y^{i}\right| \tag{2.40}$$

Where, m = number of instances, x^i = i^{th} instance's feature vector, h = operation function, $h(x^i)$ = prediction on i^{th} instance's feature vector, y^i = target value of i^{th} instance

2.5 Machine Learning Algorithms

Tasks related to machine learning can be performed without even knowing much about the algorithm. But having an understanding of how an algorithm works can help a lot on deciding a right algorithm for a problem in hand. It will also help in debugging the errors in case they occur. The most common supervised learning algorithms will be discussed here in this section. As mentioned earlier, supervised learning can be used for classification and regression purposes. Some of the algorithms are used for only one problem while others can be used for both cases.

2.5.1 Linear Regression

Linear regression is the simplest algorithm exist in machine learning, suitable for linear data. Linear model uses weighted sum of input features plus a bias term (θ_o) as shown in equation. Model uses mean squared error (MSE) as a cost function to minimize the error. Most common way of reducing this cost function is gradient descent.

$$y = \theta_o + \theta_1 x_1 + \theta_2 x_2 + \theta_3 x_3 + \ldots\ldots + \theta_n x_n \quad \textbf{(2.41)}$$

where, y = predicted value, n is a number of input features, θ_i = weight of the i^{th} feature, θ_o = bias term

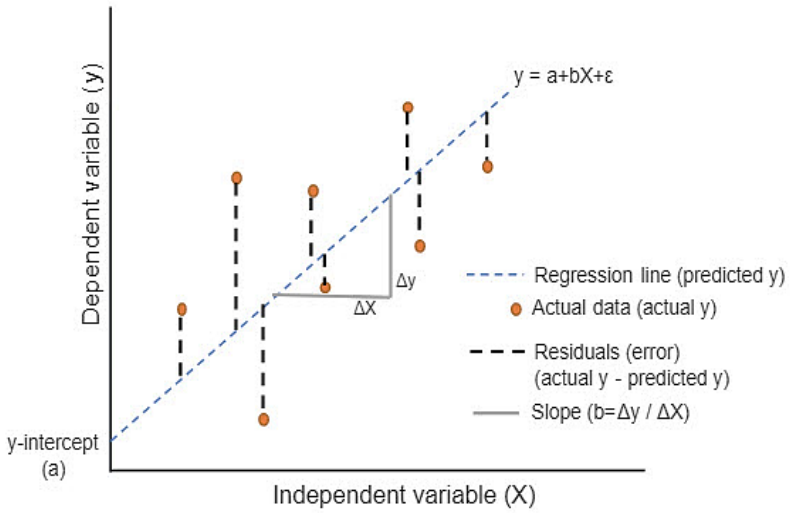

Fig 2-18 Linear Regression Fitting on data

Gradient descent helps in getting an optimal solution by finding the best weights for each feature. The basic idea is to tweak the weights iteratively in order to reduce the cost function. It is not only used in linear regression but in every algorithm where weights are used as basis, for instance, ANN. An important parameter associated with gradient descent is "learning rate" which decides the size of step in reaching the minimum loss. Learning steps should neither be too small to increase computational effort nor too large to miss the global minimum. Sometimes depending upon cost function, there are chances that gradient descent will stuck in local minima instead of reaching global minimum. The cost function used in linear regression never faces such problem of local minima. There are different methods of gradient descent based on time required to find minimum error. Batch gradient, mini-batch gradient, and stochastic gradient are common methods, with batch gradient being the slowest and stochastic gradient being the fastest one.

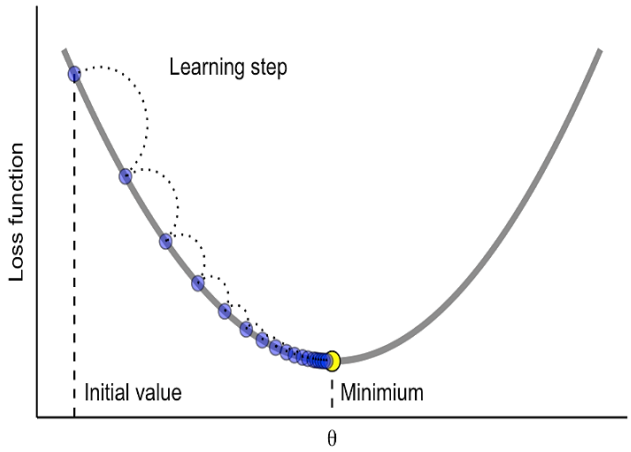

Fig 2-19 Gradient Descent (Boehmke & Greenwell, 2019)

Linear regression can be used to fit the non-linear data by adding the powers of feature as new features and then training the model on these extended features. This model is then referred as **polynomial regression**. But with the increase in degree the chances are that the model will start overfitting the data. To cater this overfitting problem, weights are usually constrained by different methods. Ridge regression, Lasso regression and elastic nets are common methods to improve generalizability in linear regression.

2.5.2 Logistic Regression

This algorithm classifies an instance by estimating probability that instance belongs to a particular class. If the probability is greater than 0.5 it belongs to that class otherwise it relates to other class. This model is the simplest and is used only for classification problems.

2.5.3 Decision Trees

Decision trees, used for both regression and classification problems, are capable of fitting data on complex data. Decision trees start with the root node and continue to split in children nodes till leave nodes are obtained. Leave nodes are considered to be pure nodes that are unable to split further. The important terms commonly used in decision trees are shown in Fig 2-20. Algorithm identifies the leave nodes based on purity matrix. The most commonly used purity matrices are gini and entropy in classification problem. In case of regression, MSE or MAE is used as a purity matrix. Algorithm tries to split the training data in a way that reduces the impurity in classification or MSE in regression.

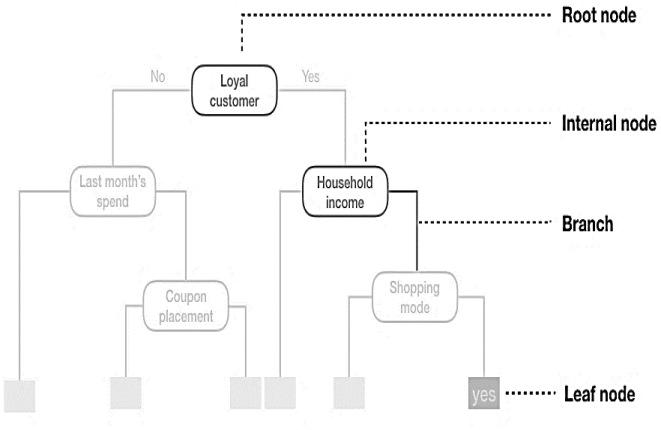

Fig 2-20 Terminologies used in Decision Trees
(Boehmke & Greenwell, 2019)

One of the advantages of decision trees is that they do not require feature scaling or centering. But, they overfit the data if left unconstrained. The reason is that these are non-parametric algorithms unlike linear regression which have predetermined number of parameters. The non-parametric algorithm does not make a lot of assumptions prior to training and adapt itself to the training data.

So, regularization is necessary to avoid overfitting, which includes either pre-pruning or post-pruning. Another drawback of decision trees is that they are sensitive to rotation of data as well as small variation in data. Random forest is an ensemble technique that can deal with the instability of decision trees.

2.5.4 Ensemble Techniques

Sometimes instead of relying on an individual predictor, predictions from a group of predictors are aggregated to get better results. A group of predictors may or may not include same algorithm. Ensemble techniques always enhances the performance even if the individual predictors are weak learners. This hypothesis of "always improves the performance" is true only if the predictors are perfectly independent. Independent predictors make uncorrelated errors which is not possible if trained on the same data or using same algorithm. To make it possible, either different algorithms are used on same data or same algorithm is trained on random subsets of data. There are four ensemble techniques which include voting and aggregating, Bagging and pasting, Boosting, and Stacking, with bagging as a most common used technique. Voting and aggregating uses same training data for different algorithms, then the predictions of algorithms are aggregated. Aggregation is simply a mode for classification and mean for a regression problem.

Bagging and pasting trains the same algorithm on random subsets of the training data. The only difference between bagging and pasting is that of sampling replacement. Bagging allows the instances to be sampled multiple times for the same predictor unlike in pasting. It is observed that bagging, also referred as bootstrap aggregating, performs better than pasting. The popular and powerful algorithm based on decision trees trained using bagging method is Random Forests. As it is mentioned earlier that decision trees are unstable and overfit more often. The solution to this problem lies in ensemble technique like Random Forests. Random forests has almost same hyper-parameters as that of decision trees. These hyper-parameters can be regularized to get the optimized results. An added benefit to random forests is that they make it easy to measure the relative importance of each feature, hence, helpful in feature selection process. The downside of random forests is that it is a black-box model which means that the mechanism involved in getting prediction cannot be interpreted unlike decision trees.

Another popular ensemble technique is **Boosting**. The basic process involved in boosting is the training of predictors by sequential improvement of the previous model. Because of its sequential

training, this technique uses more time as compared to bagging method (parallel training). There are many boosting algortihms exist, of which Adaboost and Gradient boosting are the most popular ones. Adaboost pays more attention to the training instances that the previous predictor under-predicted. Those underpredicted instances are then given more weightage when model is trained for the second time. The weights are updated again for training for the third time and so on. The mechanism of the Gradient boosting is similar to Adaboost but gradient boosting works with residual errors instead of weights. XGboost is nothing but the optimized version of gradient boosting. If the model overfits it can be regularized either by reducing number of estimators or regularizing the base predictor, which is applicable to both bagging and boosting technique. However, in case of boosting another regularization technique called "Shrinkage", which involves reducing learning rate, can be used as well.

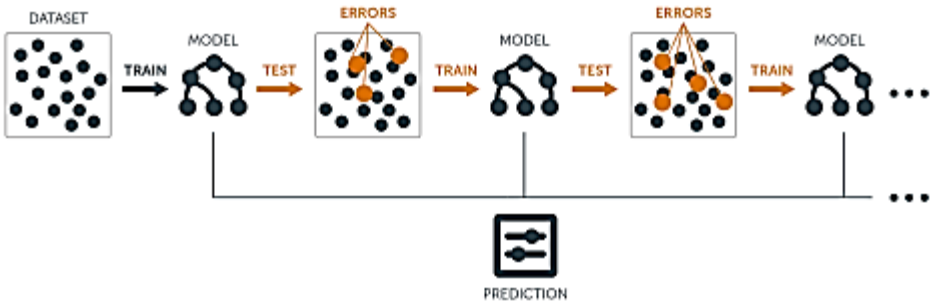

Fig 2-21 Steps involved in Boosting method
(Boehmke & Greenwell, 2019)

Stacking is the last ensemble technique which is quite different from other methods in a sense that instead of using trivial functions to aggregate the predictions of different predictors, it uses a model to perform this task. The working of this method is simple. First, the data is divided into two, half of which is used to train the models while other half is used to get predictions. The predictions obtained are used as an input for a final model, also called blender, which makes the final prediction. It is also possible to train several layers of blender with different algorithm in each layer. This method is not so common in use.

2.5.5 Multivariate Adaptive Regression Splines

Multivariate adaptive regression splines (MARS) is a more convenient approach to capture the

non-linear pattern in data than polynomial regression. Firstly, it is a non-parametric algorithm, unlike polynomial regression which means there is no need to predefine parameters. Secondly, it never becomes a reason for multicollinearity which arises because of additional features in case of polynomial regression. It performs piecewise linear regression and forms knots (kinks) where data changes its trend. Algorithm continues to find knots producing potentially non-linear prediction equation. The process involved in MARS can be explained in Fig.2-22.

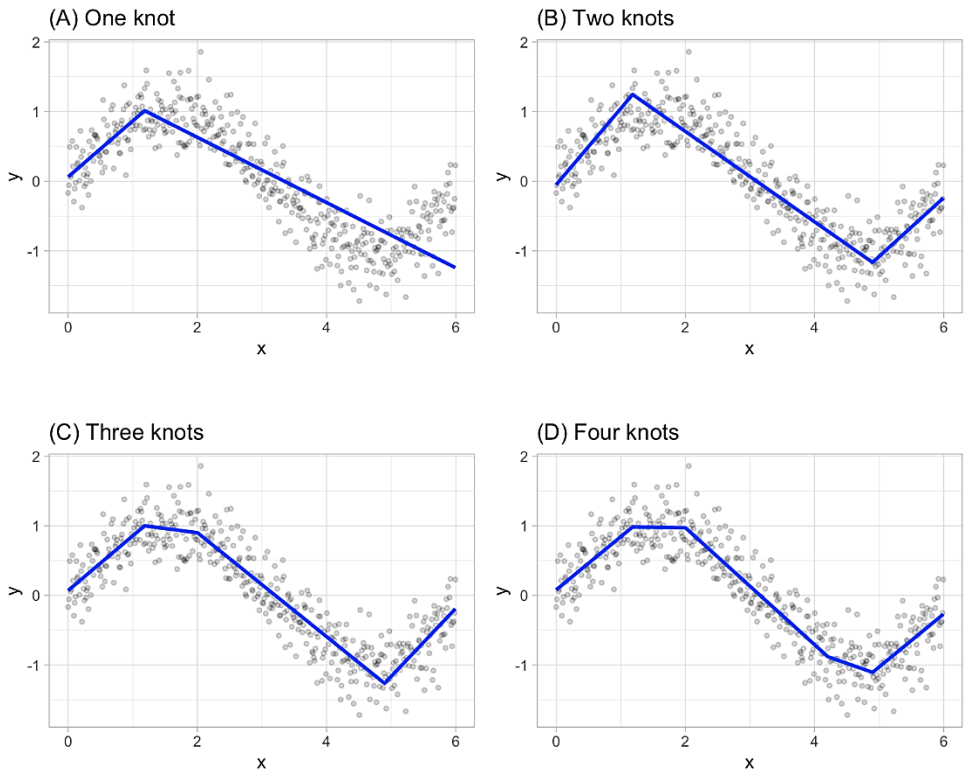

Fig 2-22 Fitting of the data by MARS **(a)** One Knot **(b)** Two Knots **(c)** Three Knots **(d)** Four Knots (Boehmke & Greenwell, 2019)

Too many knots can reduce the generalizability of the model. So, once all the knots are identified it is important to drop the less important knots. This process of reducing knots is called pruning. Two most important parameters for this algorithm to be tuned are degree of interactions and maximum number or terms retained in final model. The bright side of this model is that it includes feature selection mechanism which automatically include or exclude a feature by assessing its impact on the error. Besides, this algorithm does not require feature scaling. The only disadvantage associated with this model is that it trains slow because it scans each value to identify cutpoints (knots).Now that we have studied few models, Fig 2-23 presents how a different algorithm fits the data differently.

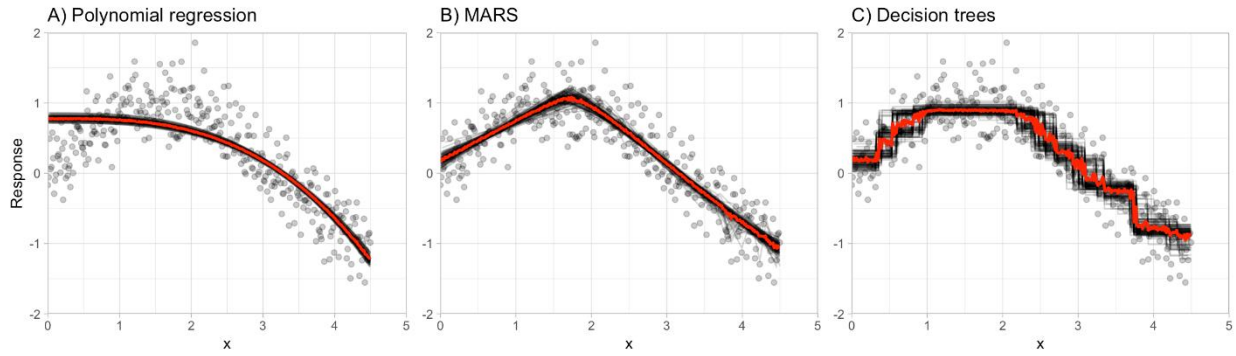

Fig 2-23 Fitting Comparison of Different Algorithms **(a)** Polynomial Regression **(b)** MARS **(c)** Decision Trees (Boehmke & Greenwell, 2019)

2.5.6 Support Vector Machine

Like Decision trees, Support vector machine is a versatile machine learning model which can be used for both regression and classification problems. It is also used for outliers detection. SVM is more popular for classification of medium to small sized data. SVM can be performed on both linear and non-linear data. In case of linear SVM, the two different classes are separated linearly while non-linear is useful for complex data. Fig 2-24 presents a comparison between linear and non-linear SVM fitting to data. Just like polynomial regression, non-linear SVM adds new features and then fit the linear SVM model on those additional features. This method of adding new features is quite interesting unless the degrees are too high. In high degrees, adding new features increases computational effort. The solution to this problem is a kernel trick. Kernel trick make it possible to get the same results as if the new features are added without adding them in actual. Most commonly used kernels are linear, polynomial, Gaussian RBF, and sigmoid.

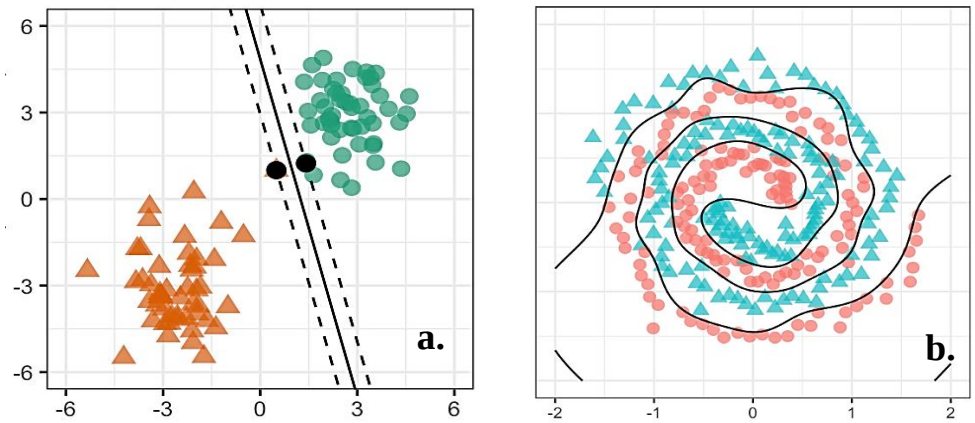

Fig 2-24 Support Vector Machine Boudaries **(a)** Linear SVM **(b)** Non-Linear SVM (Boehmke & Greenwell, 2019)

2.5.7 Artificial Neural Network

The working mechanism of artificial neural networks is different than the other available machine learning algorithms. They train themselves by passing the information through connection between the neurons imitating the biological neural system. One of the simplest neural network is perceptron which contains one input layer and one output layer with no hidden layer in between them. Each neuron, also referred as linear threshold unit (LTU), in input layer is connected to all the inputs. A neuron outputs the result after applying activation function to the weighted sum of all the inputs connected to that neuron. The architecture of a single neuron comprise of an operator and an activation function as shown in fig 2-25. An operator usually adjusts the weights while activation function brings non-linearity. Earliest activation function used in linear threshold unit (LTU) was step function. But step function does not work well with gradient descent because of no slope. So, to deal with this limitation, a variety of activation functions have been proposed over the years. Logistic function, hyperbolic tangent function, Relu, leaky relu and sigmoid are few of the prominent ones. These activation functions are used depending upon the situation and the expected range of output. For instance, hyperbolic tangent function restricts the output function between -1 to 1 while logistic function ranges between 0 and 1.

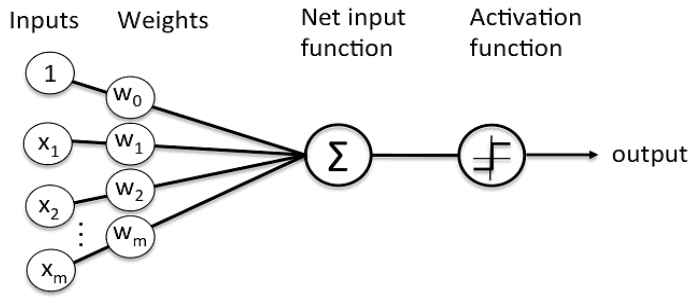

Fig 2-25 Architecture of single Neuron
(Boehmke & Greenwell, 2019)

Given the limitation of simple perceptron that it is incapable of understanding complex patterns, **multilayer perceptron (MLP)** came into existence. MLP, which is a stack of perceptrons, comprised of input, output and hidden layers. MLP gets trained in two passes; forward pass and backward pass. This training process is referred as Backpropagation neural network. A small batch of instances is passed to input layers, which then pass the information to first hidden layer. Hidden layer's connection weights are initialized randomly to prevent training from failure. The neurons

present in that first hidden layer process the information and transfers the output to next layer till it reaches the output layer. This transfer of information from input layer to output layer with hidden layers in between is called forward pass. Once the prediction is made, the process is performed in reverse direction to compute the errors made during learning. This is referred as backward pass. After the successful computation of errors last step is to tweak the weights associated with each input. To accomplish this task algorithm performs gradient descent step to reduce the error. The loss function usually used in regression is either MSE or MAE while in classification problem cross-entropy is more common.

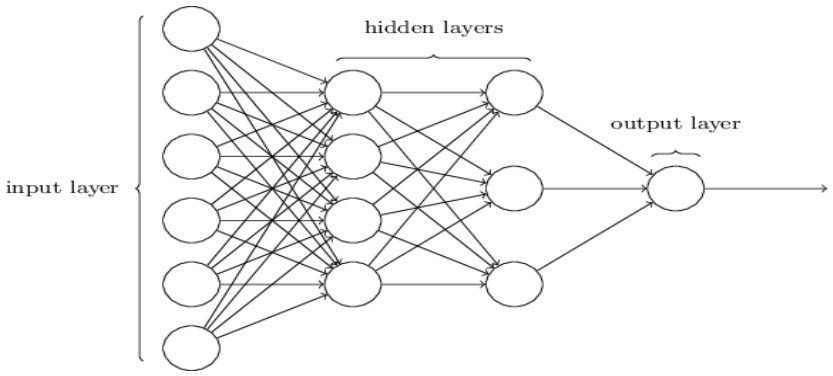

Fig 2-26 MultiLayer Perceptron /Deep Network

Problems associated with deep neural network

Deep neural network faces a few problems. Vanishing/exploding gradient problem is one of the common issues faced by deep neural network which commonly arises because of an inappropriate activation function. When there are too many layers in between input and output layers, the weights become smaller and smaller as the training progress leaving gradient descent to never converge to an optimal solution. This is referred as vanishing of gradient descent. If the weights grow bigger and bigger this situation is called exploding of gradient. The solution to this issue is found in careful selection of activation function- an activation function that can prevent saturation. By far Relu and leaky Relu are considered reliable. The other parameter which needs to be selected with a bit more attention is optimizer. In order to speed up convergence it is suggested to try optimizer other than gradient descent- the simplest optimizer- else algorithm can stuck into local minima as sown in fig 2-27. Adagrad and RMSprop are other available options for optimizers.

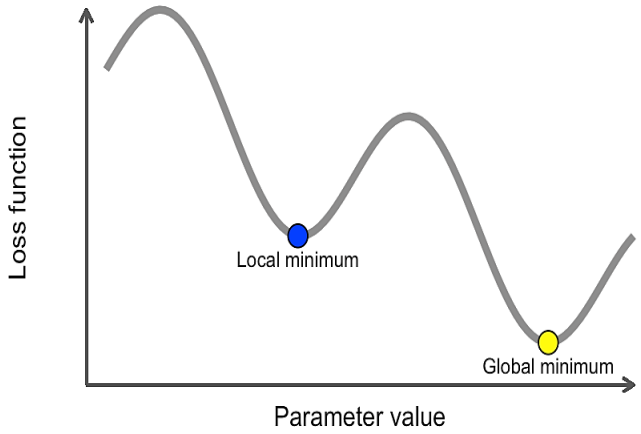

Fig 2-27 Vanishing Gradient Descent (Boehmke & Greenwell, 2019)

ANN Optimization

ANN has a range of parameters to tweak if an optimized model is desired. For instance, number of neurons in a layer, number of layers, type of activation function for each layer, weight initialization and many more. Gridsearch can be used to decide on the optimum number of layers and number of neurons. In most cases model with one or two hidden layers works exceptional but for more complex data demands more layers. Easy solution to find the optimum number of layers is to start with a single layer and continue to increase until it starts overfitting. A model with large number of hidden layers are also called deep neural networks. As far number of neurons are concerned, neurons in input and output layers will depend upon the dimension of inputs and output. For hidden layers it is observed that decent amount of neurons in a layer does the job. Many suggest ignoring optimization for number of neurons and layers, use regularization (l_1 & l_2, early stopping, dropout) instead on the model with enough number of neurons and layers. Likewise there are loads of hyper parameters to be tuned like learning rate, optimizer, activation function, batch size etc. There are a few rules available on each important hyper-parameters for optimal results. For instance, optimal learning rate should be half the maximum learning rate, and batch size should neither be too small nor too big usually in between 10 to 32.

Chapter-3

METHODOLOGY

Machine learning has emerged as an effective tool to deal with complicated problems in many fields. Given the amount of data generated in the past, researchers have started utilizing this technique even in geotechnical engineering. Machine learning has proved so efficient tool that a lot of ML-based constitutive model exist in geotechnical engineering today (P. Zhang et al., 2021). Previously, many papers have been published that employed machine learning techniques for liquefaction assessment. Literature on machine learning specific to liquefaction exist in a huge number. Some used field data SPTN, CPTu and Shear wave (Ardakani & Kohestani, 2015; Goh, 1996; Jiang et al., 2018; Pham, 2021; Y. Zhang et al., 2021; Zhao et al., 2021; J. Zhou et al., 2019) while others used laboratory data to predict the cyclic curves (V. Akhila & Adarsh, 2020; Sharafi & Jalili, 2014; Young-Su & Byung-Tak, 2006) in their relevant works. This work is also devoted to implement machine learning algorithms to predict cyclic resistance curves for silty sands. Machine learning involves a few general steps, shown in fig 3-1, which are followed in this work to accomplish the desired objectives.

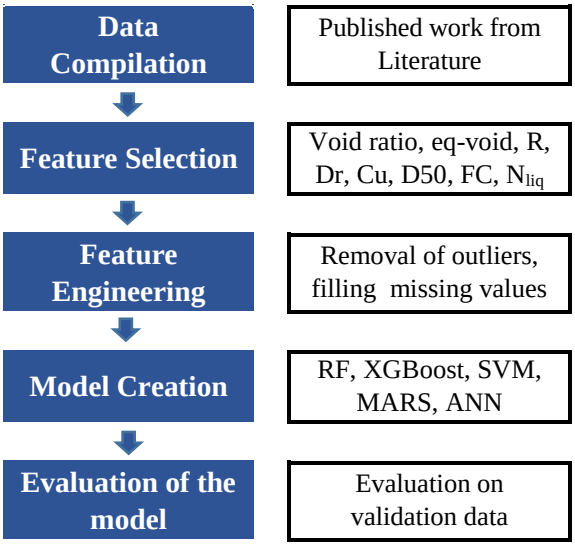

Fig 3-1 Steps Involved in machine learning

The methodology, tools used for machine learning models, and the results obtained will be the center of discussion in this chapter. Matlab is used as a tool for model creation while python is

used for data analyzation and visualization purposes. Python has a range of libraries that make the work much easier.

3.1 Data Compilation

The problem in hand depends on many factors as has been discussed in chapter 2. Some of them are easy to measure (like relative density, confining pressure), some are immeasurable (like fabric effect) while few of them are not available (like shape parameters). The possible and reliable source for the required data collection can be previously published work. Depending upon the quantity of available data, few of the factors are constrained and only the most influential factors are taken as inputs. The data gathered and compiled from the published literature (Askari et al., 2011; Belkhatir et al., 2011; Green & Mitchell, 2001; Kokusho et al., 2012; Oka et al., 2018; Rangaswamy et al., 2010) that include the results of only cyclic triaxial test on silty sands.

The data points are screened out for same confining pressure of 100 KPa, FC=0 to 40% and similar sampling method (moist tamping) to rule out the effect of various factors. By screening the data and using only one test method, confining pressure, fabric effect and stress condition are kept constant. Initially at data collection stage, following variable inputs are included: Number of cycles to cause liquefaction **(N)**, Coefficient of uniformity **(Cu)**, Grain size for 50% passing of sand **(D_{50})**, Fines Content **(FC),** minimum void ratio (e_{min}), maximum void ratio (e_{max}) and void ratio (e). The desired target variable, cyclic stress ratio **(CSR),** is also included in data. After assessment of the data, few input parameters are calculated based on void ratio which are relative density, relative compaction and equivalent void ratio. The equivalent inter-granular void ratio is calculated using the equations presented in chapter-2. The number of cycles required to cause initial liquefaction (which include both Ru =1 and axial strain D.A=5%) is selected as a failure criteria in this study. Table-1 provides necessary information on the data collected from literatur

Table-3-1 Information on Compiled Data from Literature

Sr.	Host Sand	D_{50} (mm)	d_{50} (mm)	Fines Content (%)	Relative Density	Test	Failure Criteria	Data Points	Reference	Data Split
1	Monterey Sand	0.46	0.03	0,5,10,15,25,35	10 - 98	CTX-MT	Ru =1 or 5% D.A strain	54	(Green & Mitchell, 2001)	
2	Yatesville Sand	0.17	0.03	0 – 37	-44 - 78	CTX-MT	Ru =1 or 5% D.A strain	97	(Green & Mitchell, 2001)	
3	Christchurch Sand (FBM)	0.168	0.02	1,10,20,30	5 - 81	CTX-MT	Ru =1 or 5% D.A strain	55	(Cubrinovski & Rees, 2010)	
4	Christchurch Sand (PSM-1)	0.208	0.018	0,10,20	5 - 44	CTX-MT	Ru =1 or 5% D.A strain	14	(Cubrinovski & Rees, 2010)	
5	Christchurch Sand (PSM-2)	0.175	0.018	0,10,25	14 - 70	CTX-MT	Ru =1 or 5% D.A strain	14	(Cubrinovski & Rees, 2010)	
6	Firozkooh Silty sand	0.25	0.017	0,15,30	15,30,60	CTX-MT	Ru =1 or 5% D.A strain	31	(Askari et al., 2011)	
7	Chlef Sand	0.68	0.05	0,5,10	12,45,50,60	CTX-MT	Ru =1	12	(Belkhatir et al., 2011)	
8	Futtsu Sand	0.18	0.06	0,5,10,20,30	30-76	CTX-MT	5% D.A strain	39	(Kokusho et al., 2012)	Training Data
9	M31 sand	0.3	0.0225	0,5,15,25,35	7-90	CTX-MT	5% D.A strain	53	(A. . Papadopoulou, 2008; A. I. Papadopoulou & Tika, 2021)	
10	Ahmedabad Sand	0.39	0.038	0,5,10,15,20,25	16-63	CTX-MT	Ru =1	23	(Sitharam et al., 2013)	
11	Toyoura Sand	0.19	0.08	10,20	3-55	CTX-MT	Ru =1	18	(Wei & Yang, 2019)	
12	Anzali Sand	0.28	-	0	3-55	CTX-MT	Ru =1	12	(Mohammadi & Qadimi, 2015)	
13	Cherthala Sand	0.28	0.09	0,10,30	50	CTX-MT	Ru =1 or 3-6% D.A strain	9	(M. Akhila et al., 2019)	
14	Hokksund sand	0.44	0.035	0,5,10,15,20,30	25-35	CTX-MT	Ru =1	24	(S. Yang et al., 2004)	
15	Mai Liao silty sand	0.13	0.03	0,15	32-82	CTX-MT	5% D.A strain	28	(Huang et al., 2004)	
16	Silica Sand No.6	0.159	0.017	0,20,30	41-52	CTX-MT	5% D.A strain	13	(Enomoto, 2019)	
17	Dhuvaran Silty Sand	0.112	0.085	0,15,30	23,43	CTX-MT	Ru =1 or 5% D.A strain	12	(Rangaswamy et al., 2010)	
18	Ottawa Sand	0.67	-	30	40	CTX-MT	Ru =1	3	(Amini & Qi, 2000)	Validation Data
19	F-75 Sand	0.3	0.02	0,5,15,30	12-81	CTX-MT	Ru =1	15	(Oka et al., 2018)	
20	Mai Liao silty sand	0.13	0.03	30	65	CTX-MT	5% D.A strain	4	(Huang et al., 2004)	
21	Monterey Sand	0.46	0.03	20	60	CTX-MT	Ru =1 or 5% D.A strain	4	(Green & Mitchell, 2001)	

***CTX**= Cyclic Triaxial test, **MT**= Moist tamping, D_{50} = 50% passing of sand, d_{50}= 50% passing of fines*

Chapter-4

RESULTS AND DISCUSSIONS

4.1 Feature Selection

In this step, three methods are used to decide on the most influencing factors. First one is spearman heatmap which falls under the category of filter methods. The heatmap for our compiled data is presented in Fig-4-1. It is observed from the heatmap that the most related parameters are relative compaction, relative density, equivalent void ratio and void ratio. All of these highly related parameters define the compactness of soil. This confirms the importance of compactness in studying liquefaction of soil. It is suggested not to use both the factors that have strong relation between them. So, only one of them (relative compaction, relative density, equivalent void ratio and void ratio) is used. Looking at the heatmap, the best parameters should be: Relative compaction, erange, D_{50} and Log N. Though Log N is showing lesser relation with the output, still it is added because CRR curve cannot be produced if Log N is not included. The decision on input parameters will be finalized after using other selection methods.

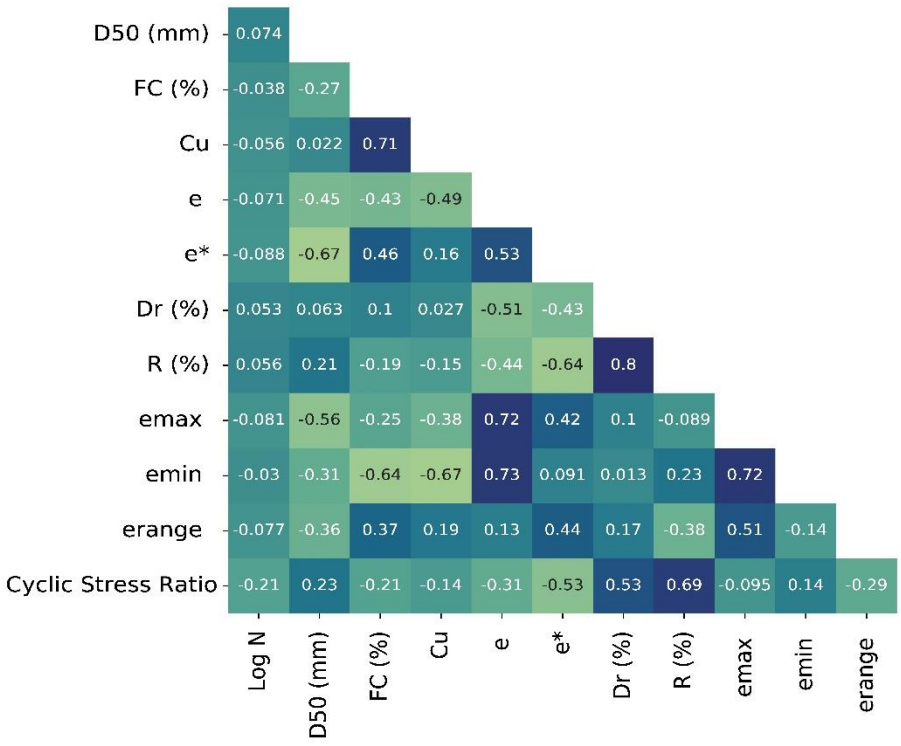

Fig 4-1 Spearman Correlation Heatmap

The second method that we employed to assess the importance of feature is embedded method. The model used to calculate the importance is Random Forest. It is evident from Fig-4-2 that relative compaction stays at first position and D_{50} at second. So, based on this method we consider relative compaction, D_{50} and Log N as important input parameters to define our problem.

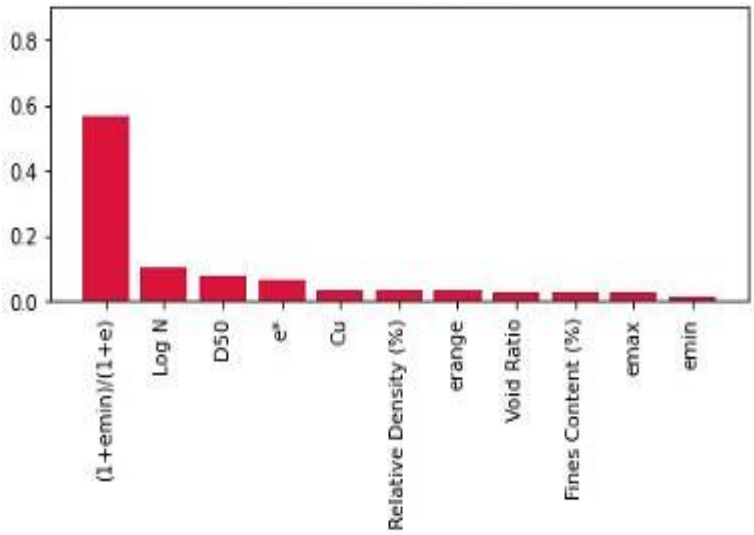

Fig 4-2 Feature Importance based on Random Forest Model

The third and the last method used for feature selection is Forward sequential method. This method lies under the category of wrapper method and considered as the most reliable one. Working of this method is already discussed in chapter-2. However, the results obtained from this method are shared in Fig-4-3. It is evident from Fig-4-3 that relative compaction, erange and log N are the top three influencing parameters.

```
pd.DataFrame.from_dict(sfs1.get_metric_dict()).T
```

	feature_idx	cv_scores	avg_score	feature_names	ci_bound	std_dev	std_err
1	(9,)	[0.22195948221780903, 0.590237787130027, 0.159...	0.369003	((1+emin)/(1+e),)	0.208257	0.162031	0.081016
2	(7, 9)	[0.5302086320916855, 0.6097943289467741, 0.473...	0.582673	(erange, (1+emin)/(1+e))	0.094356	0.073412	0.036706
3	(7, 8, 9)	[0.5248375096881948, 0.6593658057570251, 0.579...	0.640212	(erange, Log N, (1+emin)/(1+e))	0.101429	0.078915	0.039457
4	(4, 7, 8, 9)	[0.6561370772205228, 0.7320354435556876, 0.681...	0.713737	(Cu, erange, Log N, (1+emin)/(1+e))	0.06125	0.047655	0.023827

Fig 4-3 Forward Sequential Method

The significance of relative compaction over other density measures can be assessed from the plot presented in Fig-4-4. The graph contains the CRR values for several soils with fines content. It is noted from the plot that there is well defined relation of CRR with relative compaction. The comparison is made with other density measures in Fig-4-4. It turns out that relative compaction presents better relation than others. Though the scatter in data for relative compaction is lesser than that in case of relative density but this parameter is still not capable to account for material specific effect. However, it is seen that relative compaction can normalize the effect of fines upto some extent. Fig-4-6 presents the plot between CSR for N=15 and density measures for F-75 sand with fines content. Of all the measures, relative compaction proved to be better than others in normalizing the effect of fines.

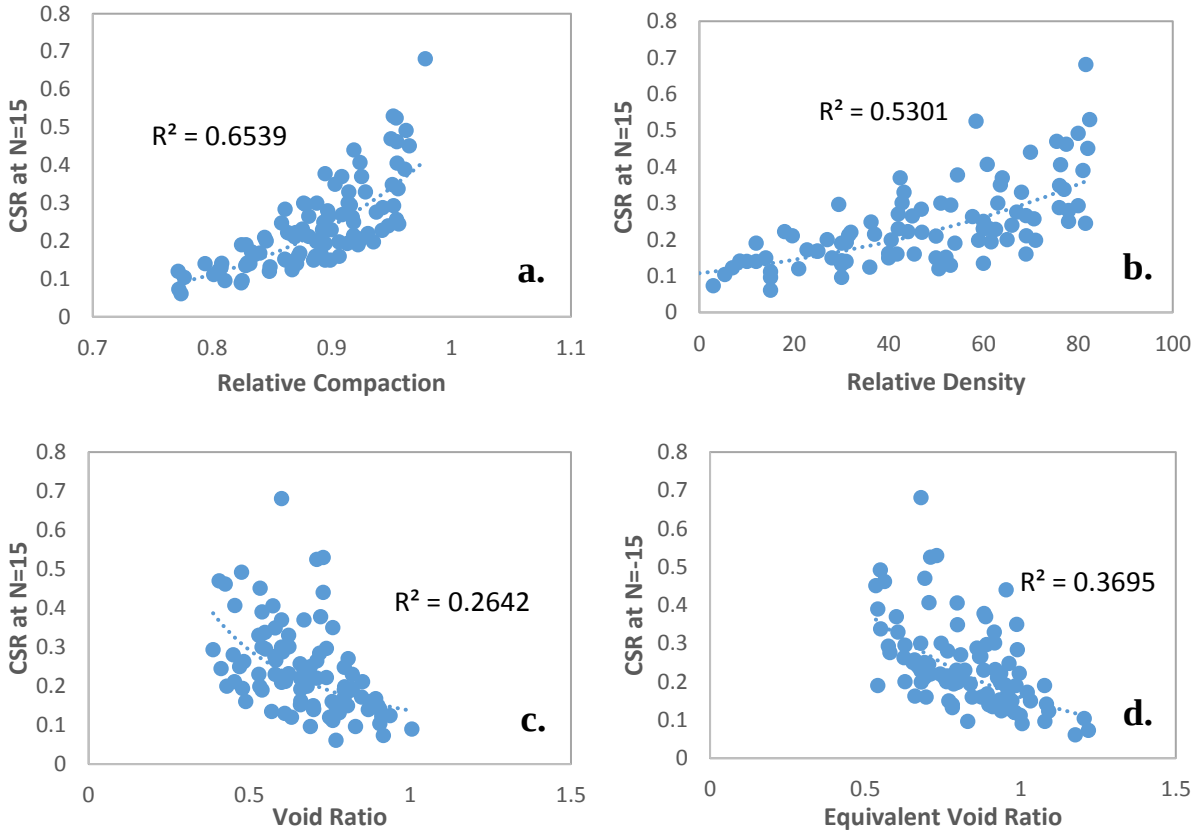

Fig 4-4 Comparison of Density measures **(a)** Relative Compaction **(b)** Relative Density **(c)** Void Ratio **(d)** Equivalent Void Ratio

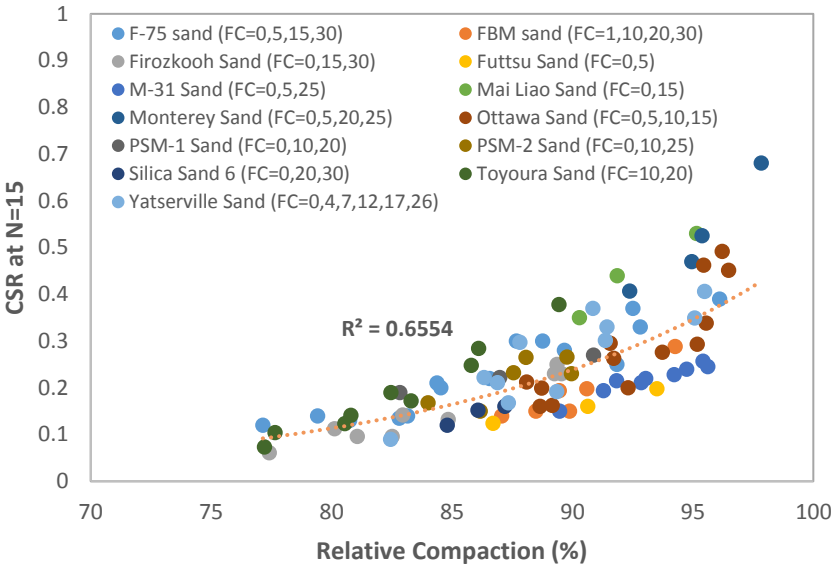

Fig 4-5 Cyclic Resistance v/s Relative Compaction

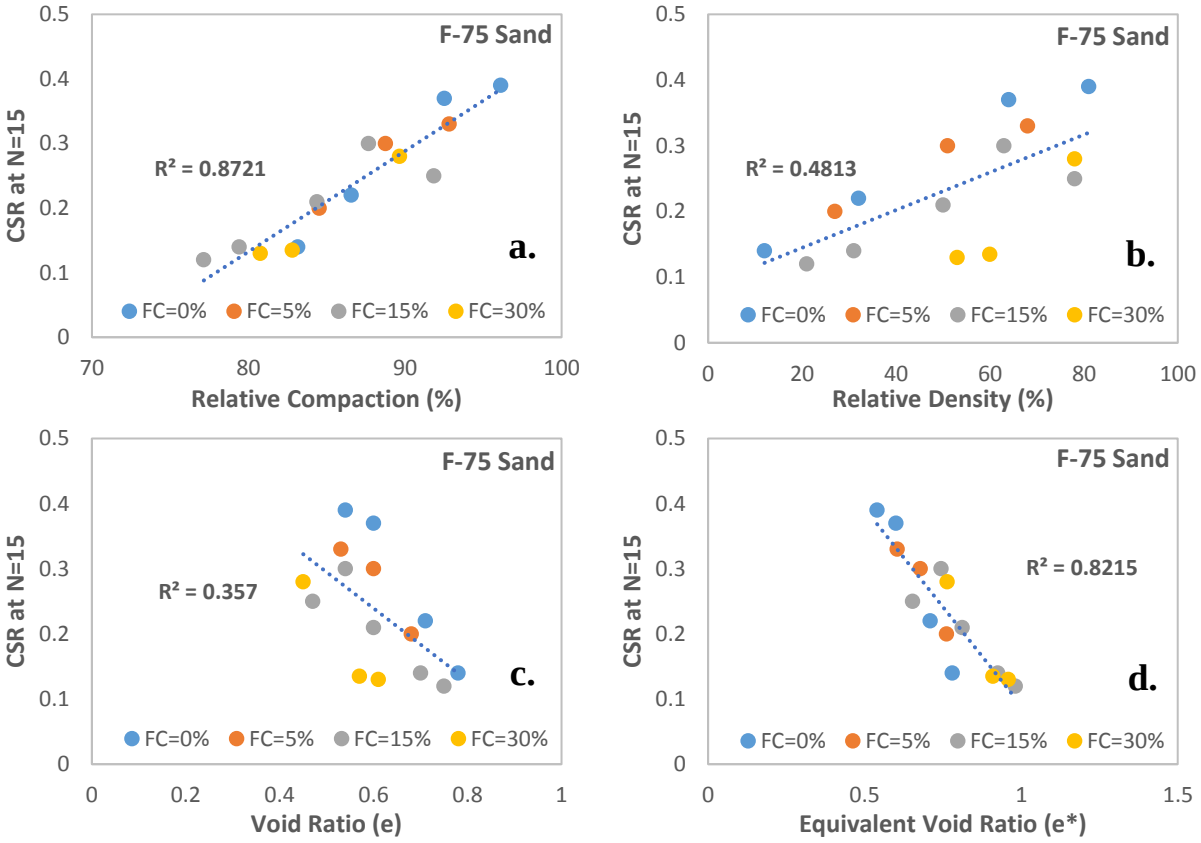

Fig 4-6 CR-Curves for F-75 sand **(a)** Relative Compaction **(b)** Relative Density **(c)** Void Ratio **(d)** Equivalent Void Ratio

4.2 Feature Engineering

Feature engineering deals with the pre-processing of the data, as mentioned earlier, which is essential for good results. It includes removal of outliers, handling of missing data, standardization and transformation and handling of categorical data. In this work, removal of outliers, and transformation of the data are performed. The plots like histogram and boxplot are useful in data visualization. Histogram plots help identifying the quality of data through distribution while Box Plots are helpful to decide on the outliers. Libraries in python can help performing these tasks. Histograms in Fig-4-7 show the variance in the data for the selected variables. Histogram for Number of cycles (N) was showing skewness this is the reason for using Log N instead of N. Also the distribution for fines content is not impressive. So using this parameter as input might not yield good results. Instead using a parameter that can account for fines is advisable. In our case, relative compaction proved to be a good measure for fines affect. The distribution of other parameters used as input seems satisfactory.

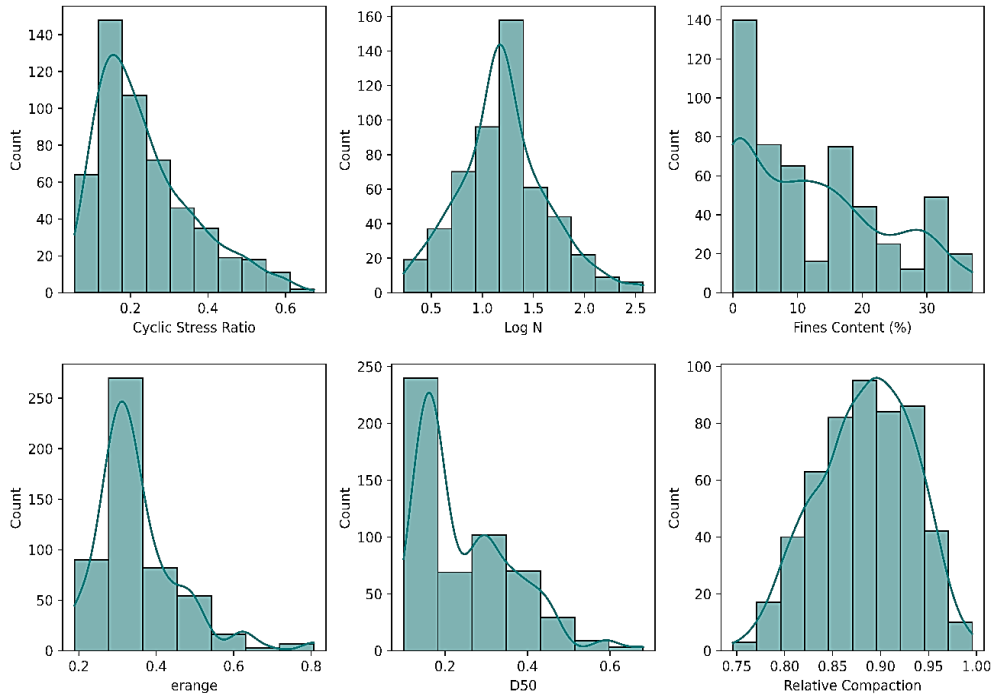

Fig 4-7 Histogram Plots for input Features and output variable

The extreme values or outliers are removed from the respective variable column by using boxplots.

4.3 Model Creation

After pre-processing of data, the data is fed to an algorithm that could find the relation and make predictions based on data. The collected data, reduced to 530 after cleaning process, is used for training of the model. Instead of dividing the data into training and testing data sets, complete data is used for training purpose. Cross-validation is used to assess both the quality of data and accuracy of the model. Bayesian optimizer is used for creating optimized models in Matlab. The optimized hyper-parameters for combination of Relative compaction, erange and Log N are shown in Table 4-1 for each model created.

Table 4-1 Tuned Hyper-parameters for Models

Sr.	Algorithm	Tuned Hyper-parameters
1	Gaussian Process Regression (GPR)	Basis Function: constant Kernel function: Non-isotropic Rational Isotropic Kernel Scale: 0.19 Sigma: 0.087 Standardize: True
2	Ensemble (Bagging)	Minimum leaf Size: 8 No. of learners: 30
3	Ensemble (Boosting)	Minimum Leaf Size: 8 No. of Learners: 30
4	Artificial Neural Network (ANN)	Number of fully connected layers: 3 Activation Function: Relu Lambda: 0 Neurons: 10 in each layer
5	Support Vector Machine (SVM)	Kernel function: Linear Kernel Scale: 1 Box Constraint: 0.116 Epsilon: 0.0116

The accuracy of the models are assessed based on several parameters R2, RMSE and MAE. It is advisable to always create more than one model and use the one with highest accuracy among all. It was observed that Gaussian process regression outperformed other algorithms used for the

given problem. How well Gaussian process regression is trained can be seen in Fig-4-8. There are few points which deviate a lot from the actual value. These points indicate that a small portion of data is not consistent with the rest of data. This inconsistency can reduce the accuracy of the model which certainly it did. It is easy to assess the quality of data but it is really hard to locate the portion of inconsistent data. The results of the models are tabulated in Table-4-2.

Table 4-2 Performance of Models

Sr.	Accuracy Measure	GPR	RF	Ensemble (Boosting)	ANN	SVM
1	R-Squared	0.87	0.81	0.78	0.72	0.65
2	Root Mean Square Error	0.049	0.057	0.059	0.063	0.081
3	Mean Absolute Error	0.033	0.041	0.047	0.054	0.06

***GPR**= Gaussian Process Regression, **RF**= Random Forest, **ANN**= Artificial Neural Network, **SVM**= Support Vector Machine*

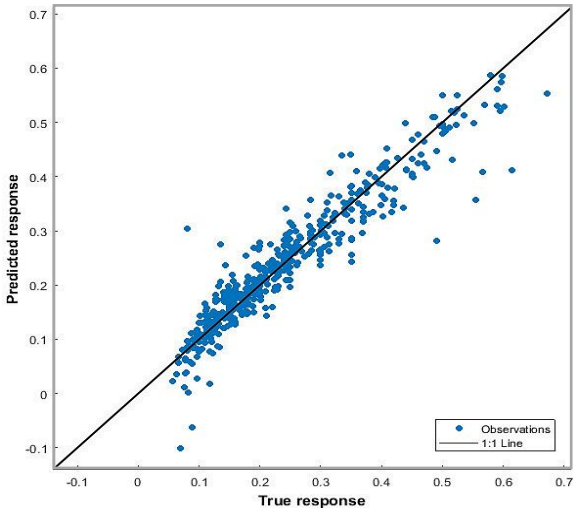

Fig 4-8 Training Process of GPR Model

Beside these above mentioned machine learning models, two response surface analysis based models are also created to estimate Cyclic resistance ratio (CSR at N=15). Total of 96 data points for 15 number of cycles from the total of 530 datasets are taken out to create RSA-based models.

The surface predicts the CRR using two input parameters. It was observed that relative compaction and D_{50} give maximum possible accuracy for a given model. Fig-4-9 is a surface and contours created by a polynomial regression model having a degree of polynomial of 3. It was observed that increasing the degree of polynomial from 2 to 3 increased the R2 from 0.66 to 0.73.

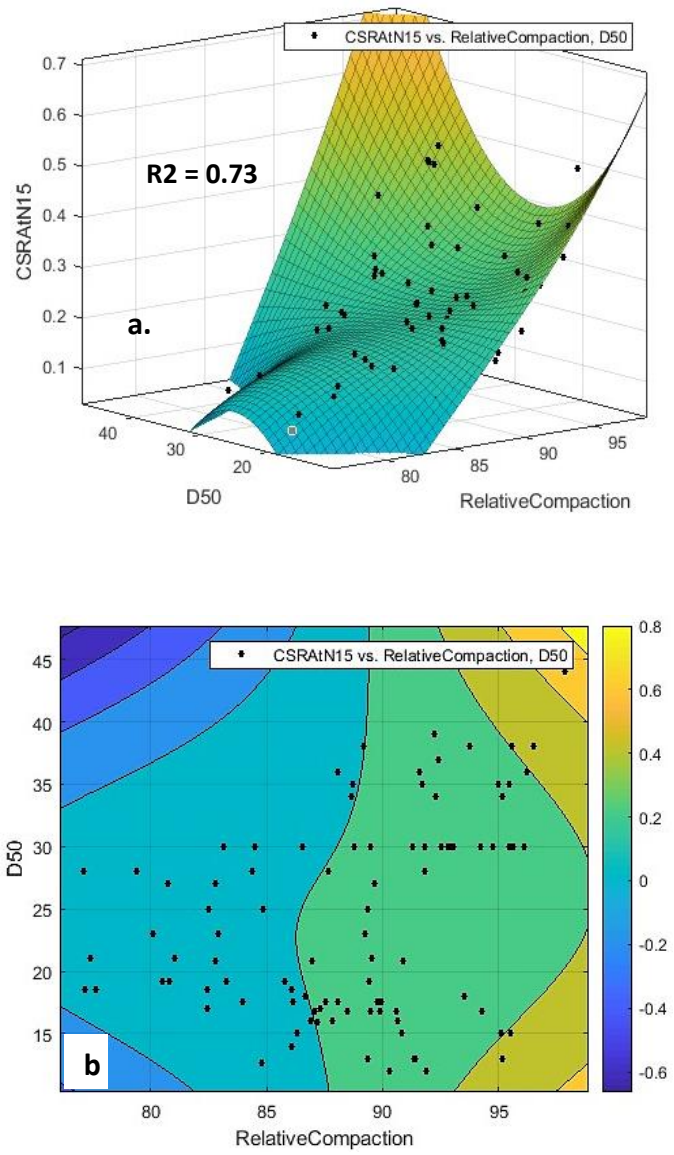

Fig 4-9 a) 3-D Surface generated by Polynomial regression model **b)** 2D nomogram

Likewise, Fig-4-10 shows the 3d-surface and nomogram obtained by using MARS algorithm. The max_terms = 750 and max_degree = 3 are the optimal hyper-parameters for MARS model. It is noted that R2 value for MARS (0.77) is slightly greater than that of polynomial regression

model. This is because MARS model is a non-parametric model which decides the surface on its own unlike polynomial regression.

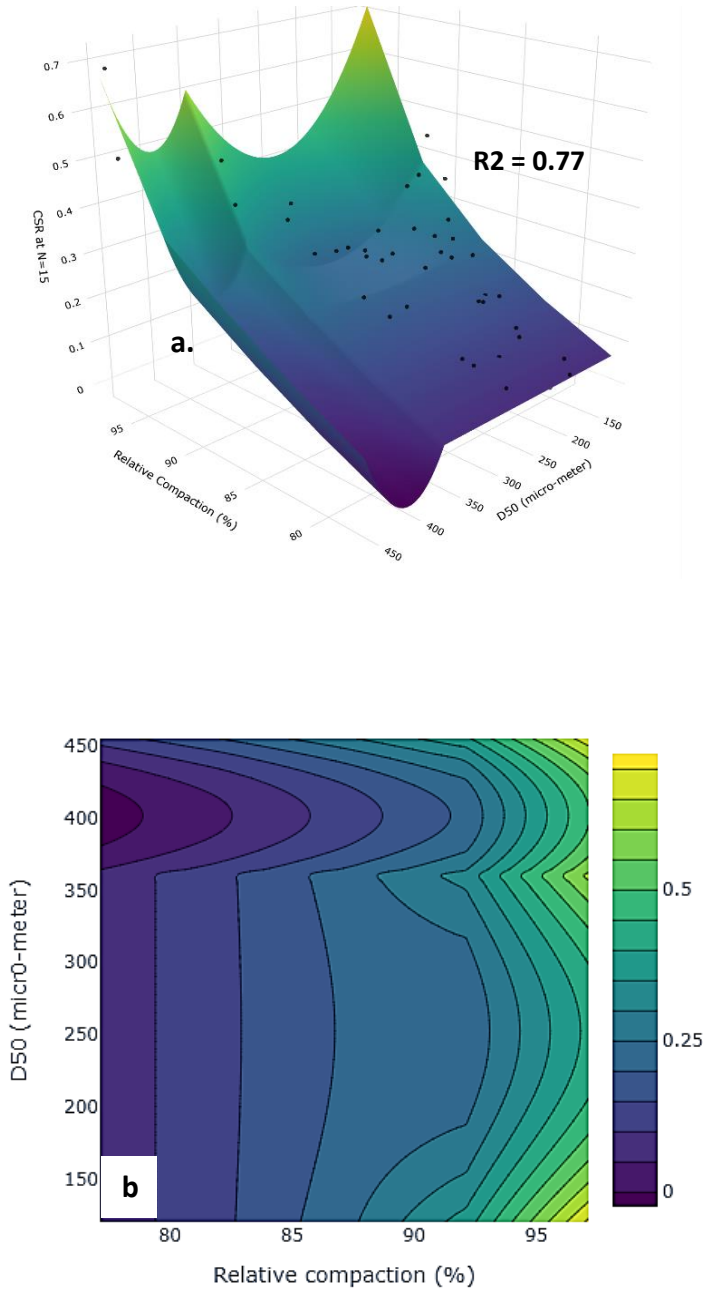

Fig 4-10 a) 3-D Surface plot by MARS **b)** 2D contour plots

4.4 Evaluation And Validation

Once the model is created it is then tested and validated on the unseen data. For that purpose, the data of (M. Akhila et al., 2019; Amini & Qi, 2000; Wei & Yang, 2019b) are utilized for evaluating the performance of GPR model in predicting the cyclic curve. For the evaluation of the response surface based models data sets of Lalita 2018 are used. Although the details of these data is provided in Table-3-1, complete data sets are provided at the end of this chapter. Fig-4-11 to Fig-4-13, the predicted curve and the curve obtained through testing can be compared.

It is observed that the predicted curve follows the similar trend as of the actual curve, but it over-predicts.

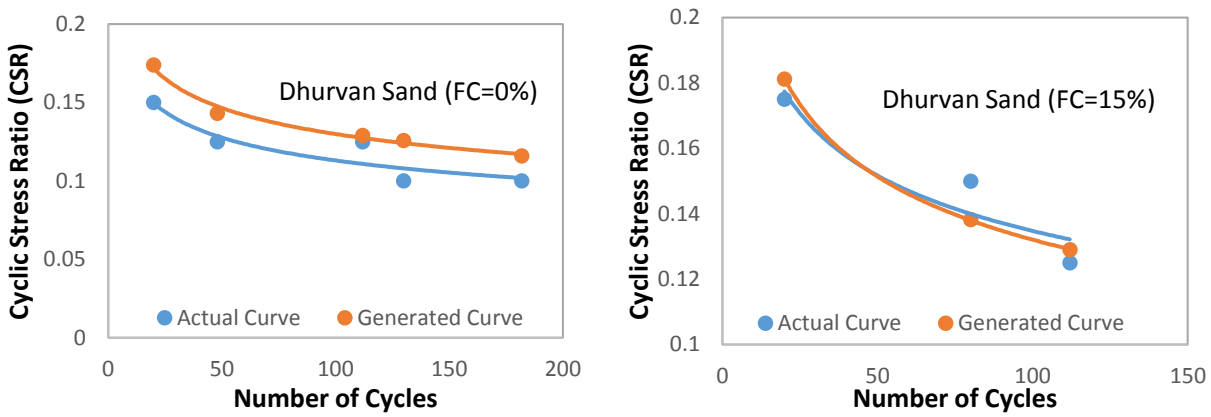

Fig 4-11 Actual vs Predicted curve for Dhuvaran Sand

The error between the actual and the predicted curves ranges between 10% to 50%. For 15% fines, the error is next to nothing, which indicates that the parameters that are used for creating models are efficient but not sufficient. However, the error in case of 30%, which is around 50%, suggests that one parameter that could take into account the minor effects of other parameters should be added to improve on the results. The error could also be attributed to the small inconsistency present in training data as was observed during training phase and the uncertainties in the testing methods for minimum and maximum void ratio reported by many researchers (Rees

2010, Askari 2011). The results of Ottawa sand does not show any big error but there is slight change of curve due to more over prediction of CSR for low no. of cycles.

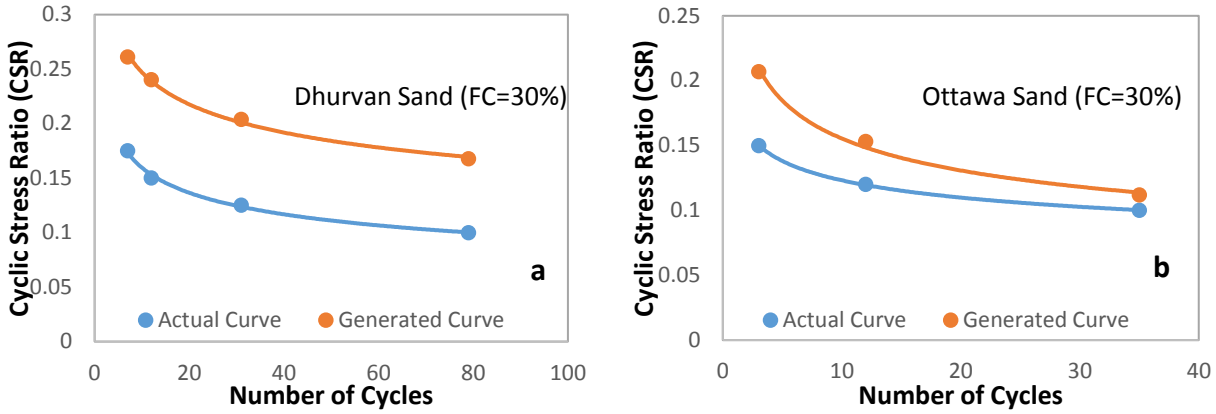

Fig 4-12 Actual vs Predicted curve for **a)** Dhurvan Sand (30% FC) **b)** Ottawa Sand (30% Fines)

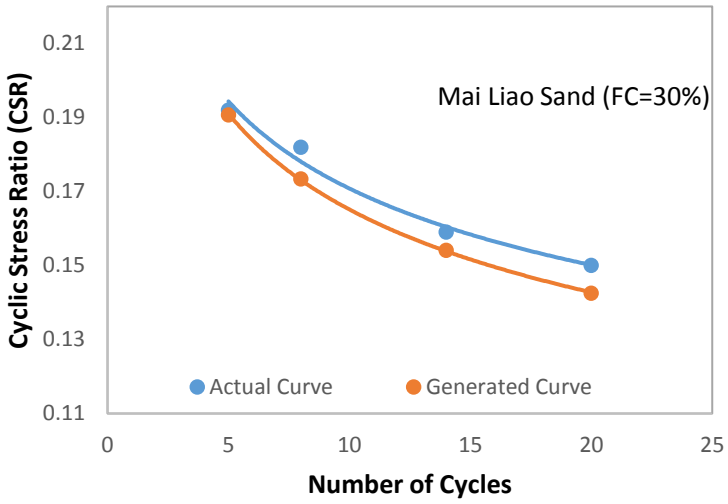

Fig 4-13 Actual v/s Predicted curve for Mai Liao soil

Further, one more curve was generated for the soil that was part of training process but those points for curve was not included in training data. Fig-4-13 is a proof that if soil data is added in training data for one condition then model can predict the curve on other condition quite accurately. This also confirms that the error we seen in previous validations is because of soil specific effect. So, one parameter that can take into account the effect of material effect can reduce the error. It was mentioned earlier that relative compaction can somehow take into account the effect of fines. To put this notion to test, model is validated on soil, which was part of training

data set, for different fines content which were unseen for the model. Fig 4-14 is a proof of the fact that model can predict for other fines content with least error.

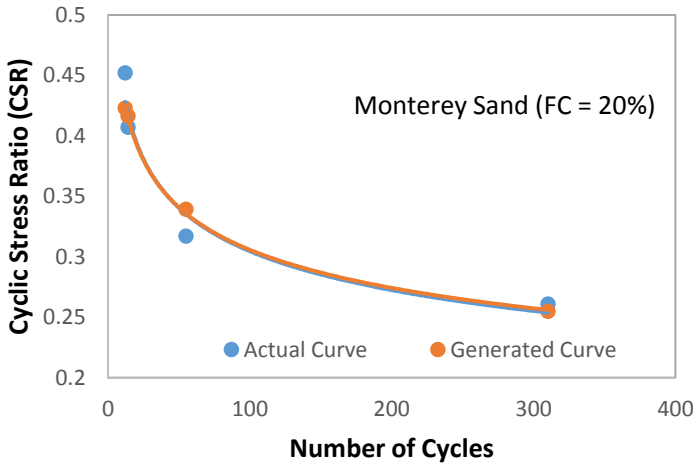

Fig 4-14 Validation for Fines content

Fig-4-15 presents the error in prediction made by RSA-based models. As it was suggested by the R2 value, the error made by these models is quite large. It is noted from the fig 4-15 that Mars predicted better with no value greater than 30% unlike Polynomial regression model, in which case around two values even exceeded 50%. Both the cases are mostly under-predicting the CRR value for the soil used for validation purpose.

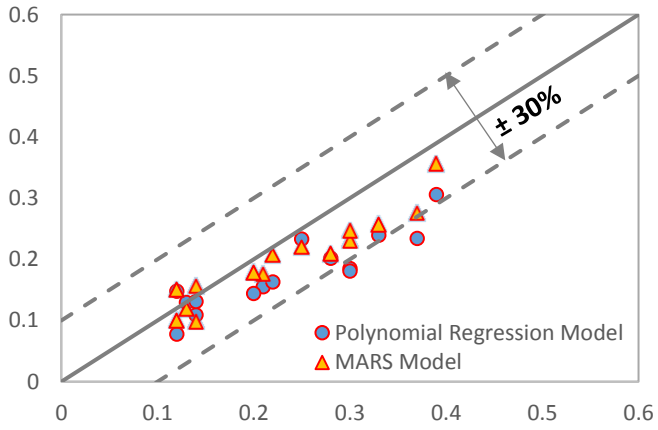

Fig 4-15 observed vs predicted for RSA-Based Models

Table-4-3 Validation Data set for Cyclic Resistance Curve (used for GPR Model)

Sand Type	Fines Content (%)	Void Ratio	Relative Density (%)	D50	Cu	emax	emin	erange	Relative Compaction	Cyclic Stress Ratio	Cycles to Initial Liq'n	Ref.
Dhuvaran sand	0	0.903	23.8	0.112	1.54	0.98	0.68	0.30	88.02	0.150	20	(Rangaswamy et al., 2010)
Dhuvaran sand	0	0.903	23.8	0.112	1.54	0.98	0.68	0.30	88.02	0.125	48	
Dhuvaran sand	0	0.903	23.8	0.112	1.54	0.98	0.68	0.30	88.02	0.100	130	
Dhuvaran sand	0	0.903	23.8	0.112	1.54	0.98	0.68	0.30	88.02	0.088	174	
Dhuvaran sand	15	0.829	42.6	0.1	1.64	0.97	0.65	0.32	89.94	0.175	20	
Dhuvaran sand	15	0.829	42.6	0.1	1.64	0.97	0.65	0.32	89.94	0.150	80	
Dhuvaran sand	15	0.829	42.6	0.1	1.64	0.97	0.65	0.32	89.94	0.125	112	
Dhuvaran sand	15	0.829	42.6	0.1	1.64	0.97	0.65	0.32	89.94	0.100	182	
Dhuvaran sand	30	0.842	43.9	0.09	2.13	1.02	0.62	0.40	87.95	0.175	7	
Dhuvaran sand	30	0.842	43.9	0.09	2.13	1.02	0.62	0.40	87.95	0.150	12	
Dhuvaran sand	30	0.842	43.9	0.09	2.13	1.02	0.62	0.40	87.95	0.125	31	
Dhuvaran sand	30	0.842	43.9	0.09	2.13	1.02	0.62	0.40	87.95	0.100	79	
Ottawa Sand	30	0.7238	34	0.65	93.00	0.87	0.44	0.43	83.54	0.150	3	(Amini & Qi, 2000)
Ottawa Sand	30	0.7238	34	0.65	93.00	0.87	0.44	0.43	83.54	0.120	12	
Ottawa Sand	30	0.7238	34	0.65	93.00	0.87	0.44	0.43	83.54	0.100	35	
Mai Liao Silty Sand	30	0.810	65	0.11	3.70	1.21	0.59	0.62	88.01	0.159	14	(Huang et al., 2004)
Mai Liao Silty Sand	30	0.810	65	0.11	3.70	1.21	0.59	0.62	88.01	0.150	20	
Mai Liao Silty Sand	30	0.810	65	0.11	3.70	1.21	0.59	0.62	88.01	0.182	8	
Mai Liao Silty Sand	30	0.810	65	0.11	3.7	1.213	0.593	0.62	88.01	0.192	5	
Monterey Sand	20	0.456	60.4	0.37	17	0.627	0.344	0.283	92.30	0.452	12.1	(Green & Mitchell, 2001)
Monterey Sand	20	0.455	60.8	0.37	17	0.627	0.344	0.283	92.38	0.261	310.2	
Monterey Sand	20	0.455	60.8	0.37	17	0.627	0.344	0.283	92.38	0.407	14.1	
Monterey Sand	20	0.454	61.1	0.37	17	0.627	0.344	0.283	92.43	0.317	55	

Table-4-4 Validation Data set for Cyclic Resistance Ratio (used for RSA-Based Models)

Sand Type	Fines Content (%)	Void Ratio	Relative Density (%)	D50	Cu	emax	emin	erange	Relative Compaction	Cyclic Resistance Ratio	Cycles to Initial Liq'n	Ref.
F-75	0	0.54	81	0.30	2.1	0.82	0.48	0.34	96.10	0.39	15	(Oka et al., 2018)
F-75	0	0.60	64	0.30	2.1	0.82	0.48	0.34	92.50	0.37	15	
F-75	0	0.78	12	0.30	2.1	0.82	0.48	0.34	83.15	0.14	15	
F-75	0	0.71	32	0.30	2.1	0.82	0.48	0.34	86.55	0.22	15	
F-75	5	0.60	51	0.30	2.0	0.78	0.42	0.36	88.75	0.3	15	
F-75	5	0.68	27	0.30	2.0	0.78	0.42	0.36	84.52	0.2	15	
F-75	5	0.53	68	0.30	2.0	0.78	0.42	0.36	92.81	0.33	15	
F-75	15	0.60	50	0.28	7.5	0.85	0.35	0.5	84.38	0.21	15	
F-75	15	0.54	63	0.28	7.5	0.85	0.35	0.5	87.66	0.3	15	
F-75	15	0.70	31	0.28	7.5	0.85	0.35	0.5	79.41	0.14	15	
F-75	15	0.46	78	0.28	7.5	0.85	0.35	0.5	92.47	0.25	15	
F-75	15	0.75	21	0.28	7.5	0.85	0.35	0.5	77.14	0.12	15	
F-75	30	0.57	60	0.27	30.0	0.98	0.3	0.68	82.80	0.12	15	
F-75	30	0.45	78	0.27	30.0	0.98	0.3	0.68	89.66	0.28	15	
F-75	30	0.61	53	0.27	30.0	0.98	0.3	0.68	80.75	0.13	15	

Chapter-5

CONCLUSION

This work aims at predicting the cyclic resistance curve for silty sands by implementing the machine learning algorithms. For that purpose, data, which includes all the quantifiable influencing factors, is collected from the published work. The data includes results of cyclic triaxial test performed on the samples of silty sands prepared by moist tamping for confining pressure of 100KPa. The compiled data is then used in creating several machine learning models following the steps of feature selection and feature engineering. The created models are then tested and validated on the unseen data set. The following conclusions can be drawn from the results obtained:

- The compactness of the soil is the most influential factor in characterizing the mechanical behavior of soil under cyclic loading. The relative compaction proved to be a better density measure than relative density. It can account for fines content upto some extent unlike relative density. In most of the soils, relative compaction normalized the fines effect on cyclic resistance even better than equivalent void ratio.
- Feature selection procedures indicated e_{range} and D_{50} as equally importan following density measure (relative compaction/relative density). Thus any one of them (D_{50}/e_{range}) can be used along with Relative compaction as input parameter to generate cyclic resistance curve. When compared it is observed that Gaussian process regression algorithm outweighs ANN, Random Forest, XGBoost and Support Vector Machine for this problem. The error does not exceed 25% except one case in which error was around 50%. The error can be attributed to the combined effect of other influencing parameters including both quantifiable and non-quantifiable. Moreover, model guarantees to account the effect of fines but does not ensure the material specific effect. However, model was efficient enough to predict the variation of number of cycles with CSR.

Reference

Ahmadi, M. M., & Akbari Paydar, N. (2014). Requirements for soil-specific correlation between shear wave velocity and liquefaction resistance of sands. *Soil Dynamics and Earthquake Engineering*, *57*, 152–163. https://doi.org/10.1016/j.soildyn.2013.11.001

Akbari-Paydar, N., & Ahmadi, M. M. (2015). Correlation of shear wave velocity with liquefaction resistance for silty sand based on laboratory study. *15th Asian Regional Conference on Soil Mechanics and Geotechnical Engineering, ARC 2015: New Innovations and Sustainability*, 794–799. https://doi.org/10.3208/jgssp.IRN-01

Akhila, M., Rangaswamy, K., & Sankar, N. (2019). Undrained Response and Liquefaction Resistance of Sand–Silt Mixtures. *Geotechnical and Geological Engineering*, *37*(4), 2729–2745. https://doi.org/10.1007/s10706-018-00790-0

Akhila, V., & Adarsh, S. (2020). Application of artificial intelligence techniques in prediction of cyclic resistance ratio (CRR) of clean sands. *IOP Conference Series: Earth and Environmental Science*, *491*(1). https://doi.org/10.1088/1755-1315/491/1/012048

Amini, F., & Qi, G. Z. (2000). Liquefaction Testing of Stratified Silty Sands. *Journal of Geotechnical and Geoenvironmental Engineering*, *126*(3), 208–217. https://doi.org/10.1061/(asce)1090-0241(2000)126:3(208)

Andrus, R. D., Stokoe, K. H., & Juang, C. H. (2004). Guide for shear-wave-based liquefaction potential evaluation. *Earthquake Spectra*, *20*(2), 285–308. https://doi.org/10.1193/1.1715106

Ardakani, A., & Kohestani, V. R. (2015). Evaluation of liquefaction potential based on CPT results using C4.5 decision tree. *Journal of Artificial Intelligence and Data Mining*, *3*(1), 85–92. https://doi.org/10.5829/idosi.jaidm.2015.03.01.09

Askari, F., Dabiri, R., Shafiee, A., & Jafari, M. K. (2011). Liquefaction resistance of sand-silt mixtures using laboratory-based shear wave velocity. *International Journal of Civil Engineering*, *9*(2), 135–144.

Banko, M., & Brill, E. (2001). *Scaling to very very large corpora for natural language disambiguation*. 26–33. https://doi.org/10.3115/1073012.1073017

Baziar, M. H., Jafarian, Y., Shahnazari, H., Movahed, V., & Amin Tutunchian, M. (2011). Prediction of strain energy-based liquefaction resistance of sand-silt mixtures: An evolutionary approach. *Computers and Geosciences*, *37*(11), 1883–1893. https://doi.org/10.1016/j.cageo.2011.04.008

Baziar, M. H., & Sharafi, H. (2011). Assessment of silty sand liquefaction potential using hollow torsional tests — An energy approach. *Soil Dynamics and Earthquake Engineering*, *31*(7), 857–865. https://doi.org/10.1016/j.soildyn.2010.12.014

Belkhatir, M., Missoum, H., Arab, A., Della, N., & Schanz, T. (2011). Undrained shear strength of sand-silt mixture: Effect of intergranular void ratio and other parameters. *KSCE Journal of Civil Engineering*, *15*(8), 1335–1342. https://doi.org/10.1007/s12205-011-1051-x

Bemister-Buffington, J., Wolf, A. J., Raschka, S., & Kuhn, L. A. (2020). Machine learning to identify flexibility signatures of class a GPCR inhibition. *Biomolecules*, *10*(3). https://doi.org/10.3390/biom10030454

Boehmke, B., & Greenwell, B. (2019). Hands-On Machine Learning with R. *CRC Press*. https://doi.org/10.1201/9780367816377

Boulanger, RW and Idriss, I. M. (2014). CPT and SPT Based Liquefaction Triggering Procedures. *Center for Geotechnical Modeling*, *10–02*, 134.

Boulanger, I. (2010). *Spt-Based Liquefaction Triggering Procedures*. *December*, 136.

Boulanger, R. W., & Ziotopoulou, K. (2017). A Sand Plasticity Model for Earthquake Engineering Applications. *ProQuest Dissertations and Theses*, *2017*(March), 242.

Cappellaro, C. (2019). *The Influence of Fines Content, Fabric and Layered Structure on the Undrained Cyclic Behaviour of Christchurch Sandy Soils*.

Cetin, K. O., Asce, M., Seed, R. B., Armen, ;, Kiureghian, D., Tokimatsu, K., Leslie, ;, Harder, F., Robert, ;, Kayen, E., & Moss, R. E. S. (2004). Standard Penetration Test-Based Probabilistic and Deterministic Assessment of Seismic Soil Liquefaction Potential. *Journal of Geotechnical and Geoenvironmental Engineering*, *130*(12), 1314–1340. https://ascelibrary.org/doi/abs/10.1061/(ASCE)1090-0241(2004)130:12(1314)

Cubrinovski, M., & Rees, S. (2010). *Effects of Fines on Undrained Behaviour of Sands* (Issue May). https://doi.org/10.1061/40975(318)91

El, A., Sadrekarimi, A., & El, H. (2016). Cyclic resistance and liquefaction behavior of silt and sandy silt soils. *Soil Dynamics and Earthquake Engineering*, *83*, 98–109. https://doi.org/10.1016/j.soildyn.2016.01.004

Enomoto, T. (2019). Liquefaction and post-liquefaction properties of sand-silt mixtures and undisturbed silty sands. *Soils and Foundations*, *59*(6), 2311–2323. https://doi.org/10.1016/j.sandf.2019.09.005

Géron, A. (n.d.). Hands-on Machine Learning with Scikit-Learn, Keras, and TensorFlow. In *O'Reilly Media, Inc., 1005 Gravenstein Highway North, Sebastopol, CA 95472*.

Goh, A. T. C. (1996). Neural-Network Modeling of CPT Seismic Liquefaction Data. *Journal of Geotechnical Engineering*, *122*(1), 70–73. https://doi.org/10.1061/(asce)0733-9410(1996)122:1(70)

Goudarzy, M., Rahemi, N., Rahman, M. M., & Schanz, T. (2017). Predicting the Maximum Shear Modulus of Sands Containing Nonplastic Fines. *Journal of Geotechnical and Geoenvironmental Engineering*, *143*(9). https://doi.org/10.1061/(asce)gt.1943-5606.0001760

Goudarzy, M., Rahman, M. M., König, D., & Schanz, T. (2016). Influence of non-plastic fines content on maximum shear modulus of granular materials. *Soils and Foundations*, *56*(6), 973–983. https://doi.org/10.1016/j.sandf.2016.11.003

Green, R. A., & Mitchell, J. K. (2001). *Energy-Based Evaluation and Remediation of Liquefiable Soils*. https://doi.org/10.1061/40744(154)191

Halevy, A., Norvig, P., & Pereira, F. (2009). The unreasonable effectiveness of data. *IEEE Intelligent Systems*, *24*(2), 8–12. https://doi.org/10.1109/MIS.2009.36

Hsiao, D. H., & Phan, V. T. A. (2016). Evaluation of static and dynamic properties of sand-fines mixtures through the state and equivalent state parameters. *Soil Dynamics and Earthquake Engineering*, *84*, 134–144. https://doi.org/10.1016/j.soildyn.2016.02.006

Huang, Y. T., Huang, A. Bin, Kuo, Y. C., & Tsai, M. D. (2004). A laboratory study on the undrained strength of a silty sand from Central Western Taiwan. *Soil Dynamics and Earthquake Engineering*, *24*(9–10), 733–743. https://doi.org/10.1016/j.soildyn.2004.06.013

Idriss, I. M., & Boulanger, R. W. (2006). Semi-empirical procedures for evaluating liquefaction potential during earthquakes. *Soil Dynamics and Earthquake Engineering*, *26*(2-4 SPEC. ISS.), 115–130. https://doi.org/10.1016/j.soildyn.2004.11.023

Idriss, I. M., & Boulanger, R. W. (2008). Soil liquefaction during earthquakes. *Earthquake Engineering Research Institute*, *136*(6), 755.

Ishihara, K. (1993). Liquefaction and flow failure during earthquakes. *Geotechnique*, *43*(3), 351–451. https://doi.org/10.1680/geot.1993.43.3.351

Jefferies, M., & Been, K. (2006). *Soil Liquefaction: A Critical State Approach*. 1–677. https://doi.org/10.1201/b19114

Jefferies, M., Shuttle, D., & Been, K. (2015). *Principal stress rotation as cause of cyclic mobility*. *2*(2), 66–96. https://doi.org/10.1680/jgere.15.00002

Jiang, M. D., Yang, Z. X., Barreto, D., & Xie, Y. H. (2018). The influence of particle-size distribution on critical state behavior of spherical and non-spherical particle assemblies. *Granular Matter*, *20*(4). https://doi.org/10.1007/s10035-018-0850-x

Kayen, R., Moss, R. E. S., Thompson, E. M., Seed, R. B., Cetin, K. O., Kiureghian, A. Der, Tanaka, Y., & Tokimatsu, K. (2013). Shear-Wave Velocity–Based Probabilistic and Deterministic Assessment of Seismic Soil Liquefaction Potential. *Journal of Geotechnical and Geoenvironmental Engineering*, *139*(3), 407–419. https://doi.org/10.1061/(asce)gt.1943-5606.0000743

Kishida, T., & Tsai, C.-C. (2014). Seismic Demand of the Liquefaction Potential with Equivalent Number of Cycles for Probabilistic Seismic Hazard Analysis. *Journal of Geotechnical and Geoenvironmental Engineering*, *140*(3). https://doi.org/10.1061/(asce)gt.1943-5606.0001033

Kokusho, T. (2017). Innovative earthquake soil dynamics. *Innovative Earthquake Soil Dynamics*, 1–478. https://doi.org/10.1201/9781315645056

Kokusho, T., Ito, F., Nagao, Y., & Green, A. R. (2012). Influence of Non/Low-Plastic Fines and Associated Aging Effects on Liquefaction Resistance. *Journal of Geotechnical and Geoenvironmental Engineering*, *138*(6), 747–756. https://doi.org/10.1061/(asce)gt.1943-5606.0000632

Mandokhail, S. ullah J., Park, D., & Yoo, J. K. (2017). Development of normalized liquefaction resistance curve for clean sands. *Bulletin of Earthquake Engineering*, *15*(3), 907–929. https://doi.org/10.1007/s10518-016-0020-7

Marchetti, S. (2016). Incorporating the Stress History Parameter KD of DMT into the Liquefaction Correlations in Clean Uncemented Sands. *Journal of Geotechnical and Geoenvironmental Engineering*, *142*(2). https://doi.org/10.1061/(asce)gt.1943-5606.0001380

Michael H. Kutner, Christopher J. Nachtsheim, John Neter, W. L. (2013). Applied linear statistical models. *McGraw-Hill Education (India) Private Limited, New Delhi*.

Mohammadi, A., & Qadimi, A. (2015). Characterizing the process of liquefaction initiation in

Anzali shore sand through critical state soil mechanics. *Soil Dynamics and Earthquake Engineering*, *77*, 152–163. https://doi.org/10.1016/j.soildyn.2015.04.017

Moss, R. E., Seed, R. B., Kayen, R. E., Stewart, J. P., Der Kiureghian, A., & Cetin, K. O. (2006). CPT-Based Probabilistic and Deterministic Assessment of In Situ Seismic Soil Liquefaction Potential. *Journal of Geotechnical and Geoenvironmental Engineering*, *132*(8), 1032–1051. https://doi.org/10.1061/(asce)1090-0241(2006)132:8(1032)

Nong, Z., Park, S., & Lee, D. (2021). ScienceDirect Comparison of sand liquefaction in cyclic triaxial and simple shear tests. *Soils and Foundations*, *xxxx*. https://doi.org/10.1016/j.sandf.2021.05.002

Oka, L. G., Dewoolkar, M., & Olson, S. M. (2018). Comparing laboratory-based liquefaction resistance of a sand with non-plastic fines with shear wave velocity-based field case histories. *Soil Dynamics and Earthquake Engineering*, *113*, 162–173. https://doi.org/10.1016/j.soildyn.2018.05.028

Onder Cetin, K., & Tolga Bilge, H. (2012). Performance-Based Assessment of Magnitude (Duration) Scaling Factors. *Journal of Geotechnical and Geoenvironmental Engineering*, *138*(3), 324–334. https://doi.org/10.1061/(asce)gt.1943-5606.0000596

Papadopoulou, A. . (2008). *Laboratory investigation into the behavior of silty sands under monotonic and cyclic loading*. Ph.D. Thesis, Aristotle University of Thessaloniki, Thessaloniki, Greece.

Papadopoulou, A. I., & Tika, T. M. (2021). Laboratory-Based Correlation between Liquefaction Resistance and Shear Wave Velocity of Sand with Fines. *Geotechnics*, *1*(2), 219–242. https://doi.org/10.3390/geotechnics1020012

Papadopoulou, A., & Tika, T. (2008). The effect of fines on critical state and liquefaction resistance characteristics of non-plastic silty sands. *Soils and Foundations*, *48*(5), 713–725. https://doi.org/10.3208/sandf.48.713

Peacock, W. H., & Seed, H. B. (1968). Sand Liquefaction Under Cyclic Loading Simple Shear Conditions. *Journal of the Soil Mechanics and Foundations Division*, *94*(3), 689–708. https://doi.org/10.1061/jsfeaq.0001135

Pham, T. A. (2021). Application of Feedforward Neural Network and SPT Results in the Estimation of Seismic Soil Liquefaction Triggering. *Computational Intelligence and Neuroscience*, *2021*. https://doi.org/10.1155/2021/1058825

Qadimi, A., & Mohammadi, A. (2014). Evaluation of state indices in predicting the cyclic and monotonic strength of sands with different fi nes contents. *Soil Dynamics and Earthquake Engineering*, *66*, 443–458. https://doi.org/10.1016/j.soildyn.2014.08.002

Rahman, M. M., Lo, S. R., & Gnanendran, C. T. (2008). On equivalent granular void ratio and steady state behaviour of loose sand with fines. *Canadian Geotechnical Journal*, *45*(10), 1439–1456. https://doi.org/10.1139/T08-064

Rangaswamy, K., Boominathan, A., & Rajagopal, K. (2010). Influence of initial conditions on liquefaction resistance of silty sands. *Geomechanics and Geoengineering*, *5*(3), 199–211. https://doi.org/10.1080/17486021003706572

Robertson, P. K. (2009). Interpretation of cone penetration tests - A unified approach. *Canadian Geotechnical Journal*, *46*(11), 1337–1355. https://doi.org/10.1139/T09-065

Robertson, P. K., & Wride, C. E. (1998). Evaluating cyclic liquefaction potential using the cone penetration test. *Canadian Geotechnical Journal*, *35*(3), 442–459. https://doi.org/10.1139/t98-017

Roscoe, K. H., Schofield, A. N., & Wroth, C. P. (1958). On the yielding of soils. *Geotechnique*, *8*(1), 22–53. https://doi.org/10.1680/geot.1958.8.1.22

Sadrekarimi, A. (2016). Cyclic Shear Response of Fraser River Sand Using Cyclic Ring Shear. *American Society of Civil Engineersmerican Society of Civil Engineers*, *1971*, 167–176. https://doi.org/https://doi.org/10.1061/9780784480120.018

Seed, R. B., & Idriss, I. M. (1971). Simplified procedure for evaluating soil liquefaction potential. *ASCE J Soil Mech Found Div*, *26*(2), 115–130.

Sharafi, H., & Jalili, S. (2014). Assessment of Cyclic Resistance Ratio (CRR) in Silty Sands Using Artificial Neural Networks. *Open Journal of Civil Engineering*, *04*(03), 217–228. https://doi.org/10.4236/ojce.2014.43019

Sitharam, T. G., Dash, H. K., & Jakka, R. S. (2013). Postliquefaction Undrained Shear Behavior of Sand-Silt Mixtures at Constant Void Ratio. *International Journal of Geomechanics*, *13*(4), 421–429. https://doi.org/10.1061/(asce)gm.1943-5622.0000225

Tadist, K., Najah, S., Nikolov, N. S., Mrabti, F., & Zahi, A. (2019). Feature selection methods and genomic big data: a systematic review. *Journal of Big Data*, *6*(1). https://doi.org/10.1186/s40537-019-0241-0

Taylor, M. L., Cubrinovski, M., & Bradley, B. A. (2015). Earthquake-induced liquefaction triggering of Christchurch sandy soils. *New Zealand Society for Earthquake Engineering Conference*, *April*.

Thevanayagam, S., Shenthan, T., Mohan, S., & Liang, J. (2002). Undrained Fragility of Clean Sands, Silty Sands, and Sandy Silts. *Journal of Geotechnical and Geoenvironmental Engineering*, *128*(10), 849–859. https://doi.org/10.1061/(asce)1090-0241(2002)128:10(849)

Vaid, Y. P., & Sivathayalan, S. (1996). Static and cyclic liquefaction potential of Fraser Delta sand in simple shear and triaxial tests. *Canadian Geotechnical Journal*, *33*(2), 281–289. https://doi.org/10.1139/t96-007

Wang, J.-H., Moran, K., & Baxter, C. D. P. (2006). Correlation between Cyclic Resistance Ratios of Intact and Reconstituted Offshore Saturated Sands and Silts with the Same Shear Wave Velocity. *Journal of Geotechnical and Geoenvironmental Engineering*, *132*(12), 1574–1580. https://doi.org/10.1061/(asce)1090-0241(2006)132:12(1574)

Wei, X., & Yang, J. (2019a). Cyclic behavior and liquefaction resistance of silty sands with presence of initial static shear stress. *Soil Dynamics and Earthquake Engineering*, *122*(January), 274–289. https://doi.org/10.1016/j.soildyn.2018.11.029

Wei, X., & Yang, J. (2019b). ScienceDirect Characterizing the effects of fines on the liquefaction resistance of silty sands. *Soils and Foundations*, *59*(6), 1800–1812. https://doi.org/10.1016/j.sandf.2019.08.010

Wu, J., Kammerer, A. M., Riemer, M. F., Seed, R. B., & Pestana, J. M. (2004). Laboratory study of liquefaction triggering criteria. *13th World Conference on Earthquake Engineering*, 1–14.

Yang, J., & Luo, X. D. (2015). Author ' s Accepted Manuscript Exploring the relationship between critical state and particle shape for granular materials Reference : *Journal of the Mechanics and Physics of Solids*. https://doi.org/10.1016/j.jmps.2015.08.001

Yang, J., & Wei, L. M. (2012). Collapse of loose sand with the addition of fines: The role of particle shape. *Geotechnique*, *62*(12), 1111–1125. https://doi.org/10.1680/geot.11.P.062

Yang, S., Sandven, R., & Grande, L. (2004). Cyclic behavior of sand-silt mixtures. *Cyclic Behaviour of Soils and Liquefaction Phenomena*, 269–274. https://doi.org/10.1201/9781439833452.ch34

Youd, T. L., & Idriss, I. M. (2001). Liquefaction Resistance of Soils: Summary Report from the 1996 NCEER and 1998 NCEER/NSF Workshops on Evaluation of Liquefaction Resistance of Soils. *Journal of Geotechnical and Geoenvironmental Engineering*, *127*(4), 297–313. https://doi.org/10.1061/(asce)1090-0241(2001)127:4(297)

Young-Su, K., & Byung-Tak, K. (2006). Use of Artificial Neural Networks in the Prediction of Liquefaction Resistance of Sands. *Journal of Geotechnical and Geoenvironmental Engineering*, *132*(11), 1502–1504. https://doi.org/10.1061/(asce)1090-0241(2006)132:11(1502)

Zhang, P., Yu, Z., Yin, Y., & Jin, F. (2021). State - of - the - Art Review of Machine Learning Applications in Constitutive Modeling of Soils. *Archives of Computational Methods in Engineering*, *28*(5), 3661–3686. https://doi.org/10.1007/s11831-020-09524-z

Zhang, Y., Xie, Y., Zhang, Y., Qiu, J., & Wu, S. (2021). The adoption of deep neural network (DNN) to the prediction of soil liquefaction based on shear wave velocity. *Bulletin of Engineering Geology and the Environment*, *80*(6), 5053–5060. https://doi.org/10.1007/s10064-021-02250-1

Zhao, Z., Duan, W., & Cai, G. (2021). A novel PSO-KELM based soil liquefaction potential evaluation system using CPT and Vs measurements. *Soil Dynamics and Earthquake Engineering*, *150*. https://doi.org/10.1016/j.soildyn.2021.106930

Zhou, J., Li, E., Wang, M., Chen, X., Shi, X., & Jiang, L. (2019). Feasibility of Stochastic Gradient Boosting Approach for Evaluating Seismic Liquefaction Potential Based on SPT and CPT Case Histories. *Journal of Performance of Constructed Facilities*, *33*(3), 1–10. https://doi.org/10.1061/(asce)cf.1943-5509.0001292

Zhou, Y.-G., & Chen, Y.-M. (2007). Laboratory Investigation on Assessing Liquefaction Resistance of Sandy Soils by Shear Wave Velocity. *Journal of Geotechnical and Geoenvironmental Engineering*, *133*(8), 959–972. https://doi.org/10.1061/(asce)1090-0241(2007)133:8(959)

APPENDIX-A

Table-A Training Data Set

Sr.	Sand Type	Fines Content (%)	Void Ratio	Relative Density (%)	D_{50}	Cu	D_{10}/d_{50}	e*	e_{max}	e_{min}	e_{range}	Relative Compaction	Cyclic Stress Ratio	Cycles to Initial Liq'n	Reference
1	Ahmedabad sand	0	0.54	54	0.39	3.75	3.158	0.54	0.68	0.42	0.26	92.208	0.190	16	
2	Ahmedabad sand	0	0.54	54	0.39	3.75	3.158	0.54	0.68	0.42	0.26	92.208	0.130	100	
3	Ahmedabad sand	0	0.54	54	0.39	3.75	3.158	0.54	0.68	0.42	0.26	92.208	0.180	26	
4	Ahmedabad sand	0	0.54	54	0.39	3.75	3.158	0.54	0.68	0.42	0.26	92.208	0.205	12	
5	Ahmedabad sand	0	0.44	92	0.39	3.75	3.158	0.44	0.68	0.42	0.26	98.611	0.374	20	
6	Ahmedabad sand	0	0.54	54	0.39	3.75	3.158	0.54	0.68	0.42	0.26	92.208	0.184	20	
7	Ahmedabad sand	0	0.54	54	0.39	3.75	3.158	0.54	0.68	0.42	0.26	92.208	0.153	50	
8	Ahmedabad sand	5	0.54	32	0.38	3.75	3.158	0.62	0.64	0.32	0.32	85.714	0.158	20	
9	Ahmedabad sand	5	0.54	32	0.38	3.75	3.158	0.62	0.64	0.32	0.32	85.714	0.130	80	
10	Ahmedabad sand	5	0.44	63	0.37	3.75	3.158	0.51	0.64	0.32	0.32	91.667	0.230	20	
11	Ahmedabad sand	5	0.54	32	0.38	3.75	3.158	0.62	0.64	0.32	0.32	85.714	0.154	24	
12	Ahmedabad sand	5	0.54	32	0.38	3.75	3.158	0.62	0.64	0.32	0.32	85.714	0.180	7	(Sitharam et al., 2013)
13	Ahmedabad sand	10	0.54	27	0.36	3.75	3.158	0.68	0.64	0.28	0.36	83.117	0.130	12	
14	Ahmedabad sand	10	0.44	56	0.38	3.75	3.158	0.57	0.64	0.28	0.36	88.889	0.154	20	
15	Ahmedabad sand	10	0.54	27	0.36	3.75	3.158	0.68	0.64	0.28	0.36	83.117	0.100	165	
16	Ahmedabad sand	10	0.54	27	0.36	3.75	3.158	0.68	0.64	0.28	0.36	83.117	0.118	20	
17	Ahmedabad sand	10	0.54	27	0.36	3.75	3.158	0.68	0.64	0.28	0.36	83.117	0.115	25	
18	Ahmedabad sand	15	0.44	50	0.36	3.75	3.158	0.63	0.62	0.26	0.36	87.500	0.135	20	
19	Ahmedabad sand	15	0.54	22	0.34	3.75	3.158	0.74	0.62	0.26	0.36	81.818	0.109	20	
20	Ahmedabad sand	15	0.54	22	0.34	3.75	3.158	0.74	0.62	0.26	0.36	81.818	0.078	72	
21	Ahmedabad sand	15	0.54	22	0.34	3.75	3.158	0.74	0.62	0.26	0.36	81.818	0.124	7	
22	Ahmedabad sand	20	0.44	43	0.32	3.75	3.158	0.67	0.6	0.25	0.35	86.806	0.132	20	
23	Ahmedabad sand	25	0.54	16	0.31	3.75	3.158	0.82	0.7	0.26	0.44	81.818	0.105	20	
24	Anzali Sand	0	0.72	55	0.28	1.82	-	0.80	0.89	0.58	0.31	91.967	0.400	108	
25	Anzali Sand	0	0.75	44	0.28	1.82	-	0.84	0.89	0.58	0.31	90.131	0.450	11	

Sr.	Sand Type	Fines Content (%)	Void Ratio	Relative Density (%)	D_{50}	Cu	D_{10}/d_{50}	e*	e_{max}	e_{min}	e_{range}	Relative Compaction	Cyclic Stress Ratio	Cycles to Initial Liq'n	Reference
26	Anzali Sand	0	0.77	40	0.28	1.82	-	0.77	0.89	0.58	0.31	89.518	0.450	13	
27	Anzali Sand	0	0.79	33	0.28	1.82	-	0.79	0.89	0.58	0.31	88.367	0.350	51	
28	Anzali Sand	0	0.73	53	0.28	1.82	-	0.73	0.89	0.58	0.31	91.541	0.450	52	
29	Anzali Sand	0	0.74	48	0.28	1.82	-	0.74	0.89	0.58	0.31	90.805	0.500	6	
30	Anzali Sand	0	0.83	18	0.28	1.82	-	0.83	0.89	0.58	0.31	86.150	0.350	5	(Mohammadi & Qadimi, 2015)
31	Anzali Sand	0	0.78	35	0.28	1.82	-	0.78	0.89	0.58	0.31	88.664	0.350	80	
32	Anzali Sand	0	0.88	4	0.28	1.82	-	0.88	0.89	0.58	0.31	84.132	0.300	22	
33	Anzali Sand	0	0.85	13	0.28	1.82	-	0.85	0.89	0.58	0.31	85.359	0.300	29	
34	Anzali Sand	0	0.82	23	0.28	1.82	-	0.82	0.89	0.58	0.31	86.861	0.300	282	
35	Anzali Sand	0	0.75	47	0.28	1.82	-	0.75	0.89	0.58	0.31	90.544	0.500	7	
36	Cherthala Sand	0	0.71	50	0.28	2.36	3.111	0.71	0.858	0.578	0.28	92.173	0.127	79	
37	Cherthala Sand	0	0.71	50	0.28	2.36	3.111	0.71	0.858	0.578	0.28	92.173	0.178	28	
38	Cherthala Sand	0	0.71	50	0.28	2.36	3.111	0.71	0.858	0.578	0.28	92.173	0.152	55	
39	Cherthala Sand	10	0.69	50	0.26	4.00	3.111	0.87	0.847	0.554	0.293	91.736	0.152	42	
40	Cherthala Sand	10	0.69	50	0.26	4.00	3.111	0.87	0.847	0.554	0.293	91.736	0.127	66	(M. Akhila et al., 2019)
41	Cherthala Sand	10	0.69	50	0.26	4.00	3.111	0.87	0.847	0.554	0.293	91.736	0.178	20	
42	Cherthala Sand	30	0.62	50	0.20	6.25	3.111	0.96	0.789	0.462	0.327	90.303	0.152	29	
43	Cherthala Sand	30	0.62	50	0.20	6.25	3.111	0.96	0.789	0.462	0.327	90.303	0.127	51	
44	Cherthala Sand	30	0.62	50	0.20	6.25	3.111	0.96	0.789	0.462	0.327	90.303	0.178	8	
45	Chlef	0	0.70	50	0.68	3.36	13.600	0.70	0.854	0.535	0.319	90.560	0.350	5	
46	Chlef	0	0.70	50	0.68	3.36	13.600	0.70	0.854	0.535	0.319	90.560	0.250	12	
47	Chlef	0	0.70	50	0.68	3.36	13.600	0.70	0.854	0.535	0.319	90.560	0.150	158	
48	Chlef	5	0.68	45	0.59	5.55	13.600	0.76	0.815	0.51	0.305	89.881	0.250	5	
49	Chlef	5	0.68	45	0.59	5.55	13.600	0.76	0.815	0.51	0.305	89.881	0.350	3	(Belkhatir et al., 2011)
50	Chlef	5	0.63	60	0.59	5.55	13.600	0.71	0.815	0.51	0.305	92.496	0.150	167	
51	Chlef	5	0.79	12	0.59	5.55	13.600	0.87	0.815	0.51	0.305	84.499	0.150	24	
52	Chlef	5	0.79	12	0.59	5.55	13.600	0.87	0.815	0.51	0.305	84.499	0.350	2	
53	Chlef	5	0.79	12	0.59	5.55	13.600	0.87	0.815	0.51	0.305	84.499	0.250	3	

Sr.	Sand Type	Fines Content (%)	Void Ratio	Relative Density (%)	D_{50}	Cu	D_{10}/d_{50}	e*	e_{max}	e_{min}	e_{range}	Relative Compaction	Cyclic Stress Ratio	Cycles to Initial Liq'n	Reference
54	Chlef	5	0.68	45	0.59	5.55	13.600	0.76	0.815	0.51	0.305	89.881	0.150	71	
55	Chlef	5	0.63	60	0.59	5.55	13.600	0.71	0.815	0.51	0.305	92.496	0.350	5	
56	Chlef	5	0.63	60	0.59	5.55	13.600	0.71	0.815	0.51	0.305	92.496	0.250	13	
57	FBM	1	0.89	7	0.17	2.00	4.500	0.91	0.907	0.628	0.279	86.183	0.170	5	
58	FBM	1	0.74	60	0.17	2.00	4.500	0.76	0.907	0.628	0.279	93.563	0.475	5	
59	FBM	1	0.89	6	0.17	2.00	4.500	0.91	0.907	0.628	0.279	86.138	0.120	32	
60	FBM	1	0.89	6	0.17	2.00	4.500	0.91	0.907	0.628	0.279	86.138	0.209	2	
61	FBM	1	0.83	28	0.17	2.00	4.500	0.85	0.907	0.628	0.279	89.059	0.228	4	
62	FBM	1	0.82	31	0.17	2.00	4.500	0.84	0.907	0.628	0.279	89.401	0.370	2	
63	FBM	1	0.88	10	0.17	2.00	4.500	0.90	0.907	0.628	0.279	86.642	0.140	16	
64	FBM	1	0.74	62	0.17	2.00	4.500	0.75	0.907	0.628	0.279	93.833	0.334	7	
65	FBM	1	0.82	31	0.17	2.00	4.500	0.84	0.907	0.628	0.279	89.401	0.160	43	
66	FBM	1	0.74	59	0.17	2.00	4.500	0.76	0.907	0.628	0.279	93.402	0.206	126	
67	FBM	1	0.82	31	0.17	2.00	4.500	0.84	0.907	0.628	0.279	89.451	0.194	14	
68	FBM	1	0.73	62	0.17	2.00	4.500	0.75	0.907	0.628	0.279	93.887	0.566	4	
69	FBM	1	0.74	60	0.17	2.00	4.500	0.76	0.907	0.628	0.279	93.563	0.243	21	(Cubrinovski & Rees, 2010)
70	FBM	10	0.74	60	0.17	2.40	4.500	0.90	0.945	0.597	0.348	91.993	0.175	39	
71	FBM	10	0.74	58	0.17	2.40	4.500	0.91	0.945	0.597	0.348	91.571	0.279	5	
72	FBM	10	0.80	43	0.17	2.40	4.500	0.96	0.945	0.597	0.348	88.920	0.313	2.0	
73	FBM	10	0.74	59	0.17	2.40	4.500	0.90	0.945	0.597	0.348	91.782	0.316	3	
74	FBM	10	0.82	35	0.17	2.40	4.500	0.99	0.945	0.597	0.348	87.603	0.121	40	
75	FBM	10	0.74	59	0.17	2.40	4.500	0.90	0.945	0.597	0.348	91.782	0.200	22	
76	FBM	10	0.79	45	0.17	2.40	4.500	0.95	0.945	0.597	0.348	89.318	0.196	9	
77	FBM	10	0.82	37	0.17	2.40	4.500	0.98	0.945	0.597	0.348	87.989	0.192	5	
78	FBM	10	0.75	57	0.17	2.40	4.500	0.91	0.945	0.597	0.348	91.414	0.239	9	
79	FBM	10	0.71	67	0.17	2.40	4.500	0.87	0.945	0.597	0.348	93.337	0.218	21	
80	FBM	10	0.79	46	0.17	2.40	4.500	0.95	0.945	0.597	0.348	89.468	0.151	29	
81	FBM	10	0.71	68	0.17	2.40	4.500	0.87	0.945	0.597	0.348	93.392	0.284	8	

Sr.	Sand Type	Fines Content (%)	Void Ratio	Relative Density (%)	D_{50}	Cu	D_{10}/d_{50}	e*	e_{max}	e_{min}	e_{range}	Relative Compaction	Cyclic Stress Ratio	Cycles to Initial Liq'n	Reference
82	FBM	10	0.71	68	0.17	2.40	4.500	0.86	0.945	0.597	0.348	93.556	0.180	75	
83	FBM	10	0.75	57	0.17	2.40	4.500	0.91	0.945	0.597	0.348	91.466	0.436	3	
84	FBM	10	0.72	66	0.17	2.40	4.500	0.87	0.945	0.597	0.348	93.065	0.555	3	
85	FBM	10	0.71	67	0.17	2.40	4.500	0.87	0.945	0.597	0.348	93.337	0.349	4	
86	FBM	10	0.82	36	0.17	2.40	4.500	0.99	0.945	0.597	0.348	87.844	0.225	3	
87	FBM	10	0.79	46	0.17	2.40	4.500	0.95	0.945	0.597	0.348	89.418	0.233	4	
88	FBM	10	0.81	40	0.17	2.40	4.500	0.97	0.945	0.597	0.348	88.476	0.150	16	
89	FBM	10	0.79	44	0.17	2.40	4.500	0.96	0.945	0.597	0.348	89.168	0.257	3	
90	FBM	10	0.80	41	0.17	2.40	4.500	0.97	0.945	0.597	0.348	88.525	0.259	2.0	
91	FBM	20	0.61	75	0.17	11.00	4.500	0.86	0.895	0.511	0.384	94.085	0.429	7	
92	FBM	20	0.67	59	0.17	11.00	4.500	0.93	0.895	0.511	0.384	90.642	0.237	6	
93	FBM	20	0.67	59	0.17	11.00	4.500	0.93	0.895	0.511	0.384	90.588	0.357	3	
94	FBM	20	0.60	76	0.17	11.00	4.500	0.86	0.895	0.511	0.384	94.202	0.216	36	
95	FBM	20	0.60	76	0.17	11.00	4.500	0.86	0.895	0.511	0.384	94.261	0.288	14	(Cubrinovski & Rees, 2010)
96	FBM	20	0.67	59	0.17	11.00	4.500	0.94	0.895	0.511	0.384	90.479	0.159	40	
97	FBM	20	0.67	59	0.17	11.00	4.500	0.93	0.895	0.511	0.384	90.588	0.198	15	
98	FBM	30	0.70	47	0.17	12.20	4.500	1.04	0.86	0.527	0.333	89.718	0.148	5	
99	FBM	30	0.59	81	0.17	12.20	4.500	0.91	0.86	0.527	0.333	96.038	0.309	8	
100	FBM	30	0.69	50	0.17	12.20	4.500	1.03	0.86	0.527	0.333	90.195	0.195	5	
101	FBM	30	0.59	80	0.17	12.20	4.500	0.91	0.86	0.527	0.333	95.857	0.239	13	
102	FBM	30	0.59	81	0.17	12.20	4.500	0.91	0.86	0.527	0.333	95.917	0.199	33	
103	FBM	30	0.63	68	0.17	12.20	4.500	0.96	0.86	0.527	0.333	93.452	0.403	2	
104	FBM	30	0.69	51	0.17	12.20	4.500	1.03	0.86	0.527	0.333	90.248	0.253	2	
105	FBM	30	0.63	70	0.17	12.20	4.500	0.95	0.86	0.527	0.333	93.911	0.176	35	
106	FBM	30	0.69	50	0.17	12.20	4.500	1.03	0.86	0.527	0.333	90.195	0.150	14	
107	FBM	30	0.71	44	0.17	12.20	4.500	1.06	0.86	0.527	0.333	89.142	0.100	20	
108	FBM	30	0.69	50	0.17	12.20	4.500	1.03	0.86	0.527	0.333	90.195	0.121	27	
109	FBM	30	0.59	80	0.17	12.20	4.500	0.91	0.86	0.527	0.333	95.797	0.379	5	

Sr.	Sand Type	Fines Content (%)	Void Ratio	Relative Density (%)	D_{50}	Cu	D_{10}/d_{50}	e*	e_{max}	e_{min}	e_{range}	Relative Compaction	Cyclic Stress Ratio	Cycles to Initial Liq'n	Reference
110	FBM	30	0.63	69	0.17	12.20	4.500	0.96	0.86	0.527	0.333	93.624	0.199	25	
111	FBM	30	0.63	70	0.17	12.20	4.500	0.95	0.86	0.527	0.333	93.854	0.284	5	
112	Firozkooh Sand	0	0.69	60	0.25	1.65	10.000	0.69	0.84	0.58	0.26	93.491	0.250	15	
113	Firozkooh Sand	0	0.78	30	0.25	1.65	10.000	0.78	0.84	0.58	0.26	88.764	0.150	4	
114	Firozkooh Sand	0	0.69	60	0.25	1.65	10.000	0.69	0.84	0.58	0.26	93.491	0.310	2	
115	Firozkooh Sand	0	0.83	15	0.25	1.65	10.000	0.83	0.84	0.58	0.26	86.339	0.113	3	
116	Firozkooh Sand	0	0.69	60	0.25	1.65	10.000	0.69	0.84	0.58	0.26	93.491	0.210	68	
117	Firozkooh Sand	0	0.83	15	0.25	1.65	10.000	0.83	0.84	0.58	0.26	86.339	0.096	15	
118	Firozkooh Sand	0	0.69	60	0.25	1.65	10.000	0.69	0.84	0.58	0.26	93.491	0.240	24	
119	Firozkooh Sand	0	0.78	30	0.25	1.65	10.000	0.78	0.84	0.58	0.26	88.764	0.132	15	
120	Firozkooh Sand	0	0.78	30	0.25	1.65	10.000	0.78	0.84	0.58	0.26	88.764	0.130	16	
121	Firozkooh Sand	0	0.83	15	0.25	1.65	10.000	0.83	0.84	0.58	0.26	86.339	0.078	114	
122	Firozkooh Sand	0	0.78	30	0.25	1.65	10.000	0.78	0.84	0.58	0.26	88.764	0.120	44	
123	Firozkooh Sand	15	0.70	30	0.23	1.65	10.000	0.93	0.82	0.4	0.42	82.353	0.150	10	
124	Firozkooh Sand	15	0.70	30	0.23	1.65	10.000	0.93	0.82	0.4	0.42	82.353	0.140	17	(Askari et al., 2011)
125	Firozkooh Sand	15	0.69	60	0.23	1.65	10.000	0.92	0.82	0.4	0.42	82.840	0.220	17	
126	Firozkooh Sand	15	0.76	15	0.23	1.65	10.000	1.00	0.82	0.4	0.42	79.545	0.075	350	
127	Firozkooh Sand	15	0.70	30	0.23	1.65	10.000	0.93	0.82	0.4	0.42	82.353	0.142	15	
128	Firozkooh Sand	15	0.76	15	0.23	1.65	10.000	1.00	0.82	0.4	0.42	79.545	0.124	7	
129	Firozkooh Sand	15	0.76	15	0.23	1.65	10.000	1.00	0.82	0.4	0.42	79.545	0.110	20	
130	Firozkooh Sand	15	0.58	60	0.23	1.65	10.000	0.79	0.82	0.4	0.42	88.608	0.230	15	
131	Firozkooh Sand	15	0.69	60	0.23	1.65	10.000	0.92	0.82	0.4	0.42	82.840	0.210	24	
132	Firozkooh Sand	15	0.69	60	0.23	1.65	10.000	0.92	0.82	0.4	0.42	82.840	0.180	76	
133	Firozkooh Sand	15	0.76	15	0.23	1.65	10.000	1.00	0.82	0.4	0.42	79.545	0.112	15	
134	Firozkooh Sand	15	0.70	30	0.23	1.65	10.000	0.93	0.82	0.4	0.42	82.353	0.180	2	
135	Firozkooh Sand	30	0.53	60	0.21	1.65	10.000	0.88	0.84	0.35	0.49	88.235	0.230	15	
136	Firozkooh Sand	30	0.69	30	0.21	1.65	10.000	1.08	0.84	0.35	0.49	79.882	0.079	58	
137	Firozkooh Sand	30	0.69	30	0.21	1.65	10.000	1.08	0.84	0.35	0.49	79.882	0.110	7	

Sr.	Sand Type	Fines Content (%)	Void Ratio	Relative Density (%)	D_{50}	Cu	D_{10}/d_{50}	e*	e_{max}	e_{min}	e_{range}	Relative Compaction	Cyclic Stress Ratio	Cycles to Initial Liq'n	Reference
138	Firozkooh Sand	30	0.53	60	0.21	1.65	10.000	0.88	0.84	0.35	0.49	88.235	0.180	48	(Askari et al., 2011)
139	Firozkooh Sand	30	0.53	60	0.21	1.65	10.000	0.88	0.84	0.35	0.49	88.235	0.220	13	
140	Firozkooh Sand	30	0.69	30	0.21	1.65	10.000	1.08	0.84	0.35	0.49	79.882	0.085	34	
141	Firozkooh Sand	30	0.69	30	0.21	1.65	10.000	1.08	0.84	0.35	0.49	79.882	0.096	15	
142	Firozkooh Sand	30	0.53	60	0.21	1.65	10.000	0.88	0.84	0.35	0.49	88.235	0.240	8	
143	futtsu sand	0	0.88	51	0.18	1.90	2.000	0.88	1.083	0.68	0.403	89.482	0.146	34	(Kokusho et al., 2012)
144	futtsu sand	0	0.87	52	0.18	1.90	2.000	0.87	1.083	0.68	0.403	89.675	0.157	17	
145	futtsu sand	0	0.80	71	0.18	1.90	2.000	0.80	1.083	0.68	0.403	93.496	0.198	16	
146	futtsu sand	0	0.80	71	0.18	1.90	2.000	0.80	1.083	0.68	0.403	93.496	0.313	4.2	
147	futtsu sand	0	0.94	36	0.18	1.90	2.000	0.94	1.083	0.68	0.403	86.691	0.124	16	
148	futtsu sand	0	0.95	34	0.18	1.90	2.000	0.95	1.083	0.68	0.403	86.332	0.144	1.7	
149	futtsu sand	0	0.80	69	0.18	1.90	2.000	0.80	1.083	0.68	0.403	93.078	0.259	3.6	
150	futtsu sand	0	0.87	53	0.18	1.90	2.000	0.87	1.083	0.68	0.403	89.868	0.150	12	
151	futtsu sand	0	0.80	70	0.18	1.90	2.000	0.80	1.083	0.68	0.403	93.287	0.299	3.5	
152	futtsu sand	0	0.97	27	0.18	1.90	2.000	0.97	1.083	0.68	0.403	85.098	0.118	32	
153	futtsu sand	5	0.96	30	0.16	2.00	2.000	1.06	1.124	0.593	0.531	81.081	0.139	3.7	
154	futtsu sand	5	0.76	69	0.16	2.00	2.000	0.84	1.124	0.593	0.531	90.634	0.160	14	
155	futtsu sand	5	0.77	67	0.16	2.00	2.000	0.86	1.124	0.593	0.531	90.090	0.197	2.6	
156	futtsu sand	5	0.84	53	0.16	2.00	2.000	0.93	1.124	0.593	0.531	86.455	0.115	29	
157	futtsu sand	5	0.99	26	0.16	2.00	2.000	1.08	1.124	0.593	0.531	80.214	0.096	19	
158	futtsu sand	5	0.82	57	0.16	2.00	2.000	0.91	1.124	0.593	0.531	87.464	0.132	36	
159	futtsu sand	5	0.98	28	0.16	2.00	2.000	1.07	1.124	0.593	0.531	80.645	0.120	6.8	
160	futtsu sand	10	0.85	51	0.16	2.70	2.000	1.02	1.167	0.542	0.625	83.430	0.151	2.7	
161	futtsu sand	10	0.86	49	0.16	2.70	2.000	1.03	1.167	0.542	0.625	82.870	0.123	9.6	
162	futtsu sand	10	0.78	62	0.16	2.70	2.000	0.95	1.167	0.542	0.625	86.654	0.120	4.8	
163	futtsu sand	10	0.75	67	0.16	2.70	2.000	0.91	1.167	0.542	0.625	88.202	0.109	13	
164	futtsu sand	10	0.87	48	0.16	2.70	2.000	1.04	1.167	0.542	0.625	82.592	0.096	33	
165	futtsu sand	20	1.03	36	0.15	2.70	2.000	1.35	1.324	0.517	0.807	74.601	0.088	19	

Sr.	Sand Type	Fines Content (%)	Void Ratio	Relative Density (%)	D_{50}	Cu	D_{10}/d_{50}	e*	e_{max}	e_{min}	e_{range}	Relative Compaction	Cyclic Stress Ratio	Cycles to Initial Liq'n	Reference
166	futtsu sand	20	0.93	49	0.15	2.70	2.000	1.23	1.324	0.517	0.807	78.659	0.082	37	(Kokusho et al., 2012)
167	futtsu sand	20	0.76	70	0.15	2.70	2.000	1.03	1.324	0.517	0.807	86.237	0.111	5.7	
168	futtsu sand	20	0.89	54	0.15	2.70	2.000	1.18	1.324	0.517	0.807	80.340	0.103	7.6	
169	futtsu sand	20	1.03	37	0.15	2.70	2.000	1.34	1.324	0.517	0.807	74.898	0.118	2.7	
170	futtsu sand	20	0.99	41	0.15	2.70	2.000	1.30	1.324	0.517	0.807	76.111	0.070	120	
171	futtsu sand	20	0.71	76	0.15	2.70	2.000	0.98	1.324	0.517	0.807	88.678	0.094	29	
172	Hokksund sand	0	0.85	25	0.44	2.38	6.000	0.85	0.95	0.59	0.36	85.761	0.350	7.4	(S. Yang et al., 2004)
173	Hokksund sand	0	0.85	25	0.44	2.38	6.000	0.85	0.95	0.59	0.36	85.761	0.300	25.3	
174	Hokksund sand	0	0.85	26	0.44	2.38	6.000	0.85	0.95	0.59	0.36	85.853	0.250	50	
175	Hokksund sand	0	0.85	25	0.44	2.38	6.000	0.85	0.95	0.59	0.36	85.761	0.490	15	
176	Hokksund sand	5	0.78	26	0.43	3.43	6.000	0.87	0.87	0.58	0.29	88.714	0.250	31.5	
177	Hokksund sand	5	0.78	26	0.43	3.43	6.000	0.87	0.87	0.58	0.29	88.714	0.370	15	
178	Hokksund sand	5	0.78	25	0.43	3.43	6.000	0.87	0.87	0.58	0.29	88.615	0.300	14.3	
179	Hokksund sand	5	0.78	26	0.43	3.43	6.000	0.87	0.87	0.58	0.29	88.714	0.350	9.4	
180	Hokksund sand	10	0.71	34	0.42	6.59	6.000	0.87	0.8	0.52	0.28	88.941	0.200	85.3	
181	Hokksund sand	10	0.70	36	0.42	6.59	6.000	0.86	0.8	0.52	0.28	89.202	0.250	38.5	
182	Hokksund sand	10	0.71	35	0.42	6.59	6.000	0.86	0.8	0.52	0.28	89.097	0.350	15	
183	Hokksund sand	15	0.67	28	0.41	11.00	6.000	0.89	0.78	0.42	0.36	85.183	0.199	15	
184	Hokksund sand	15	0.67	28	0.41	11.00	6.000	0.89	0.78	0.42	0.36	85.183	0.200	12.5	
185	Hokksund sand	15	0.67	29	0.41	11.00	6.000	0.88	0.78	0.42	0.36	85.285	0.150	139.5	
186	Hokksund sand	20	0.64	32	0.34	13.03	6.000	0.90	0.73	0.4	0.33	85.627	0.200	4.4	
187	Hokksund sand	20	0.66	31	0.34	13.03	6.000	0.93	0.73	0.4	0.33	84.490	0.100	106.4	
188	Hokksund sand	20	0.64	31	0.34	13.03	6.000	0.91	0.73	0.4	0.33	85.418	0.125	62.4	
189	Hokksund sand	20	0.64	31	0.34	13.03	6.000	0.90	0.73	0.4	0.33	85.470	0.150	26.4	
190	Hokksund sand	20	0.66	31	0.34	13.03	6.000	0.93	0.73	0.4	0.33	84.490	0.176	15	
191	Hokksund sand	30	0.61	36	0.33	13.50	6.000	0.95	0.72	0.4	0.32	86.795	0.125	13.3	
192	Hokksund sand	30	0.62	35	0.33	13.50	6.000	0.95	0.72	0.4	0.32	86.634	0.150	7.3	
193	Hokksund sand	30	0.62	33	0.33	13.50	6.000	0.96	0.72	0.4	0.32	86.420	0.122	15	

Sr.	Sand Type	Fines Content (%)	Void Ratio	Relative Density (%)	D_{50}	Cu	D_{10}/d_{50}	e*	e_{max}	e_{min}	e_{range}	Relative Compaction	Cyclic Stress Ratio	Cycles to Initial Liq'n	Reference
194	Hokksund sand	30	0.62	33	0.33	13.50	6.000	0.96	0.72	0.4	0.32	86.420	0.100	28.5	(S. Yang et al., 2004)
195	Hokksund sand	30	0.61	35	0.33	13.50	6.000	0.95	0.72	0.4	0.32	86.741	0.200	3	
196	M31	0	0.67	66	0.30	1.30	11.111	0.67	0.841	0.582	0.259	94.727	0.240	10.2	
197	M31	0	0.69	60	0.30	1.30	11.111	0.69	0.841	0.582	0.259	93.854	0.370	3	
198	M31	0	0.67	66	0.30	1.30	11.111	0.67	0.841	0.582	0.259	94.731	0.240	15	
199	M31	0	0.68	61	0.30	1.30	11.111	0.68	0.841	0.582	0.259	93.998	0.190	61.7	
200	M31	0	0.77	28	0.30	1.30	11.111	0.77	0.841	0.582	0.259	89.455	0.150	14.4	
201	M31	0	0.66	69	0.30	1.30	11.111	0.66	0.841	0.582	0.259	95.170	0.420	3.4	
202	M31	0	0.68	63	0.30	1.30	11.111	0.68	0.841	0.582	0.259	94.223	0.228	15	
203	M31	0	0.66	71	0.30	1.30	11.111	0.66	0.841	0.582	0.259	95.416	0.257	15	
204	M31	0	0.77	26	0.30	1.30	11.111	0.77	0.841	0.582	0.259	89.194	0.190	7	
205	M31	0	0.77	26	0.30	1.30	11.111	0.77	0.841	0.582	0.259	89.194	0.100	63	
206	M31	0	0.65	72	0.30	1.30	11.111	0.65	0.841	0.582	0.259	95.617	0.330	4.8	
207	M31	0	0.61	90	0.30	1.30	11.111	0.61	0.841	0.582	0.259	98.389	0.460	4.2	
208	M31	5	0.68	37	0.30	1.60	11.111	0.76	0.762	0.544	0.218	91.832	0.250	11.4	A. . Papadopoulou, 2008; A. I. Papadopoulou & Tika, 2021)
209	M31	5	0.66	47	0.30	1.60	11.111	0.74	0.762	0.544	0.218	93.038	0.220	14	
210	M31	5	0.67	40	0.30	1.60	11.111	0.76	0.762	0.544	0.218	92.190	0.180	20.3	
211	M31	5	0.68	37	0.30	1.60	11.111	0.76	0.762	0.544	0.218	91.832	0.210	12.7	
212	M31	5	0.71	24	0.30	1.60	11.111	0.79	0.762	0.544	0.218	90.309	0.240	5.5	
213	M31	5	0.64	58	0.30	1.60	11.111	0.72	0.762	0.544	0.218	94.402	0.200	81.4	
214	M31	5	0.71	24	0.30	1.60	11.111	0.79	0.762	0.544	0.218	90.309	0.150	22.4	
215	M31	5	0.68	37	0.30	1.60	11.111	0.76	0.762	0.544	0.218	91.832	0.330	3.8	
216	M31	15	0.56	51	0.30	8.80	11.111	0.77	0.75	0.38	0.37	88.388	0.190	12	
217	M31	15	0.64	29	0.30	8.80	11.111	0.87	0.75	0.38	0.37	84.008	0.200	10.2	
218	M31	15	0.50	68	0.30	8.80	11.111	0.70	0.75	0.38	0.37	92.098	0.290	35.5	
219	M31	15	0.64	29	0.30	8.80	11.111	0.87	0.75	0.38	0.37	84.044	0.156	15	
220	M31	15	0.59	44	0.30	8.80	11.111	0.80	0.75	0.38	0.37	86.957	0.201	15	
221	M31	15	0.58	45	0.30	8.80	11.111	0.80	0.75	0.38	0.37	87.149	0.140	24.5	

Sr.	Sand Type	Fines Content (%)	Void Ratio	Relative Density (%)	D_{50}	Cu	D_{10}/d_{50}	e*	e_{max}	e_{min}	e_{range}	Relative Compaction	Cyclic Stress Ratio	Cycles to Initial Liq'n	Reference
222	M31	15	0.66	24	0.30	8.80	11.111	0.89	0.75	0.38	0.37	83.072	0.250	5.5	
223	M31	15	0.54	56	0.30	8.80	11.111	0.75	0.75	0.38	0.37	89.448	0.370	6.5	
224	M31	15	0.54	58	0.30	8.80	11.111	0.75	0.75	0.38	0.37	89.879	0.420	6	
225	M31	15	0.48	72	0.30	8.80	11.111	0.69	0.75	0.38	0.37	93.017	0.340	23.5	
226	M31	15	0.62	35	0.30	8.80	11.111	0.84	0.75	0.38	0.37	85.080	0.171	15	
227	M31	15	0.64	29	0.30	8.80	11.111	0.87	0.75	0.38	0.37	84.008	0.150	12.7	
228	M31	15	0.56	51	0.30	8.80	11.111	0.77	0.75	0.38	0.37	88.462	0.230	15	
229	M31	15	0.52	62	0.30	8.80	11.111	0.73	0.75	0.38	0.37	90.670	0.281	15	
230	M31	25	0.41	82	0.30	16.80	11.111	0.70	0.686	0.35	0.336	95.609	0.245	15	
231	M31	25	0.68	3	0.30	16.80	11.111	1.02	0.686	0.35	0.336	80.553	0.160	6.4	
232	M31	25	0.66	7	0.30	16.80	11.111	1.01	0.686	0.35	0.336	81.204	0.170	2.5	
233	M31	25	0.45	69	0.30	16.80	11.111	0.75	0.686	0.35	0.336	92.847	0.211	15	
234	M31	25	0.45	69	0.30	16.80	11.111	0.75	0.686	0.35	0.336	92.837	0.280	5	A. . Papadopoulou, 2008; A. I. Papadopoulou & Tika, 2021)
235	M31	25	0.65	10	0.30	16.80	11.111	0.99	0.686	0.35	0.336	81.699	0.090	28	
236	M31	25	0.66	7	0.30	16.80	11.111	1.01	0.686	0.35	0.336	81.204	0.120	10	
237	M31	25	0.66	9	0.30	16.80	11.111	1.00	0.686	0.35	0.336	81.534	0.130	8.2	
238	M31	25	0.48	62	0.30	16.80	11.111	0.78	0.686	0.35	0.336	91.278	0.194	15	
239	M31	25	0.52	49	0.30	16.80	11.111	0.84	0.686	0.35	0.336	88.736	0.170	36.4	
240	M31	25	0.46	67	0.30	16.80	11.111	0.76	0.686	0.35	0.336	92.410	0.190	13.4	
241	M31	35	0.62	37	0.27	24.60	11.111	1.03	0.777	0.345	0.432	83.170	0.170	6	
242	M31	35	0.39	90	0.27	24.60	11.111	0.74	0.777	0.345	0.432	96.972	0.177	15	
243	M31	35	0.46	75	0.27	24.60	11.111	0.83	0.777	0.345	0.432	92.440	0.149	15	
244	M31	35	0.47	72	0.27	24.60	11.111	0.84	0.777	0.345	0.432	91.749	0.230	4.6	
245	M31	35	0.44	79	0.27	24.60	11.111	0.81	0.777	0.345	0.432	93.681	0.150	7.3	
246	M31	35	0.46	74	0.27	24.60	11.111	0.83	0.777	0.345	0.432	92.376	0.149	15	
247	M31	35	0.63	34	0.27	24.60	11.111	1.05	0.777	0.345	0.432	82.509	0.080	40.4	
248	M31	35	0.48	69	0.27	24.60	11.111	0.86	0.777	0.345	0.432	90.940	0.141	15	
249	Mai Liao Silty Sand	0	0.97	32	0.13	1.88	2.667	0.97	1.125	0.646	0.479	83.553	0.180	20	

Sr.	Sand Type	Fines Content (%)	Void Ratio	Relative Density (%)	D_{50}	Cu	D_{10}/d_{50}	e*	e_{max}	e_{min}	e_{range}	Relative Compaction	Cyclic Stress Ratio	Cycles to Initial Liq'n	Reference
250	Mai Liao Silty Sand	0	0.73	82	0.13	1.88	2.667	0.73	1.125	0.646	0.479	95.145	0.460	45	
251	Mai Liao Silty Sand	0	0.93	41	0.13	1.88	2.667	0.93	1.125	0.646	0.479	85.285	0.210	20	
252	Mai Liao Silty Sand	0	0.73	82	0.13	1.88	2.667	0.73	1.125	0.646	0.479	95.145	0.570	9	
253	Mai Liao Silty Sand	0	0.73	82	0.13	1.88	2.667	0.73	1.125	0.646	0.479	95.145	0.520	20	
254	Mai Liao Silty Sand	0	0.73	82	0.13	1.88	2.667	0.73	1.125	0.646	0.479	95.145	0.535	16	
255	Mai Liao Silty Sand	0	0.80	68	0.13	1.88	2.667	0.80	1.125	0.646	0.479	91.444	0.440	20	
256	Mai Liao Silty Sand	0	0.85	57	0.13	1.88	2.667	0.85	1.125	0.646	0.479	88.973	0.340	20	
257	Mai Liao Silty Sand	0	0.85	57	0.13	1.88	2.667	0.85	1.125	0.646	0.479	88.973	0.375	9	
258	Mai Liao Silty Sand	0	0.73	82	0.13	1.88	2.667	0.73	1.125	0.646	0.479	95.145	0.500	28	
259	Mai Liao Silty Sand	15	0.73	70	0.12	2.30	2.667	0.95	1.058	0.589	0.469	91.850	0.490	8	
260	Mai Liao Silty Sand	15	0.80	55	0.12	2.30	2.667	1.03	1.058	0.589	0.469	88.278	0.320	20	
261	Mai Liao Silty Sand	15	0.73	70	0.12	2.30	2.667	0.95	1.058	0.589	0.469	91.850	0.440	20	
262	Mai Liao Silty Sand	15	0.76	64	0.12	2.30	2.667	0.99	1.058	0.589	0.469	90.284	0.380	7	
263	Mai Liao Silty Sand	15	0.76	64	0.12	2.30	2.667	0.99	1.058	0.589	0.469	90.284	0.360	20	(Huang et al., 2004)
264	Mai Liao Silty Sand	15	0.80	67	0.12	2.30	2.667	1.03	1.058	0.589	0.469	88.278	0.260	150	
265	Mai Liao Silty Sand	15	0.76	64	0.12	2.30	2.667	0.99	1.058	0.589	0.469	90.284	0.320	75	
266	Mai Liao Silty Sand	15	0.73	70	0.12	2.30	2.667	0.95	1.058	0.589	0.469	91.850	0.410	42	
267	Mai Liao Silty Sand	15	0.80	55	0.12	2.30	2.667	1.03	1.058	0.589	0.469	88.278	0.300	40	
268	Mai Liao Silty Sand	15	0.76	64	0.12	2.30	2.667	0.99	1.058	0.589	0.469	90.284	0.365	18	
269	Mai Liao Silty Sand	15	0.76	64	0.12	2.30	2.667	0.99	1.058	0.589	0.469	90.284	0.338	36	
270	Mai Liao Silty Sand	30	0.73	78	0.11	3.70	2.667	1.06	1.213	0.593	0.62	92.081	0.210	20	
271	Mai Liao Silty Sand	30	0.73	78	0.11	3.70	2.667	1.06	1.213	0.593	0.62	92.081	0.200	32	
272	Mai Liao Silty Sand	30	0.73	78	0.11	3.70	2.667	1.06	1.213	0.593	0.62	92.081	0.240	7	
273	Mai Liao Silty Sand	30	0.76	73	0.11	3.70	2.667	1.09	1.213	0.593	0.62	90.511	0.200	7	
274	Mai Liao Silty Sand	30	0.73	78	0.11	3.70	2.667	1.06	1.213	0.593	0.62	92.081	0.229	13	
275	Mai Liao Silty Sand	30	0.76	73	0.11	3.70	2.667	1.09	1.213	0.593	0.62	90.511	0.165	18	
276	Mai Liao Silty Sand	30	0.76	73	0.11	3.70	2.667	1.09	1.213	0.593	0.62	90.511	0.180	11	
277	Mai Liao Silty Sand	30	0.76	73	0.11	3.70	2.667	1.09	1.213	0.593	0.62	90.511	0.154	29	

Sr.	Sand Type	Fines Content (%)	Void Ratio	Relative Density (%)	D_{50}	Cu	D_{10}/d_{50}	e*	e_{max}	e_{min}	e_{range}	Relative Compaction	Cyclic Stress Ratio	Cycles to Initial Liq'n	Reference
278	Mai Liao Silty Sand	30	0.76	73	0.11	3.70	2.667	1.09	1.213	0.593	0.62	90.511	0.160	20	(Huang et al., 2004)
279	Mai Liao Silty Sand	30	0.73	78	0.11	3.70	2.667	1.06	1.213	0.593	0.62	92.081	0.160	215	
280	Mai Liao Silty Sand	30	0.81	65	0.11	3.70	2.667	1.15	1.213	0.593	0.62	88.011	0.140	25	
281	Monterey Sand	0	0.70	65	0.46	1.50	10.000	0.70	0.821	0.631	0.19	96.115	0.439	73.1	Green & Mitchell, 2001)
282	Monterey Sand	0	0.83	-5	0.46	1.50	10.000	0.83	0.821	0.631	0.19	89.129	0.179	3.9	
283	Monterey Sand	0	0.70	64	0.46	1.50	10.000	0.70	0.821	0.631	0.19	95.997	0.590	12.6	
284	Monterey Sand	0	0.83	-4	0.46	1.50	10.000	0.83	0.821	0.631	0.19	89.222	0.180	5.0	
285	Monterey Sand	0	0.70	64	0.46	1.50	10.000	0.70	0.821	0.631	0.19	95.997	0.505	58.1	
286	Monterey Sand	0	0.67	81	0.46	1.50	10.000	0.67	0.821	0.631	0.19	97.846	0.598	30.1	
287	Monterey Sand	0	0.73	46	0.46	1.50	10.000	0.73	0.821	0.631	0.19	94.113	0.362	108.1	
288	Monterey Sand	0	0.67	81	0.46	1.50	10.000	0.67	0.821	0.631	0.19	97.846	0.511	168.1	
289	Monterey Sand	0	0.74	43	0.46	1.50	10.000	0.74	0.821	0.631	0.19	93.732	0.343	87.0	
290	Monterey Sand	0	0.73	48	0.46	1.50	10.000	0.73	0.821	0.631	0.19	94.278	0.484	7.1	
291	Monterey Sand	0	0.74	43	0.46	1.50	10.000	0.74	0.821	0.631	0.19	93.732	0.395	36.0	
292	Monterey Sand	0	0.74	43	0.46	1.50	10.000	0.74	0.821	0.631	0.19	93.763	0.465	12.1	
293	Monterey Sand	0	0.73	47	0.46	1.50	10.000	0.73	0.821	0.631	0.19	94.164	0.522	6.1	
294	Monterey Sand	0	0.73	47	0.46	1.50	10.000	0.73	0.821	0.631	0.19	94.164	0.389	50.6	
295	Monterey Sand	0	0.71	57	0.46	1.50	10.000	0.71	0.821	0.631	0.19	95.272	0.399	351.0	
296	Monterey Sand	0	0.73	47	0.46	1.50	10.000	0.73	0.821	0.631	0.19	94.226	0.408	34.6	
297	Monterey Sand	0	0.71	58	0.46	1.50	10.000	0.71	0.821	0.631	0.19	95.378	0.525	15.1	
298	Monterey Sand	0	0.71	58	0.46	1.50	10.000	0.71	0.821	0.631	0.19	95.378	0.597	5.1	
299	Monterey Sand	5	0.65	55	0.44	1.70	10.000	0.73	0.755	0.566	0.189	94.794	0.408	25.0	
300	Monterey Sand	5	0.63	65	0.44	1.70	10.000	0.71	0.755	0.566	0.189	95.914	0.426	83.1	
301	Monterey Sand	5	0.60	80	0.44	1.70	10.000	0.68	0.755	0.566	0.189	97.632	0.591	28.1	
302	Monterey Sand	5	0.66	50	0.44	1.70	10.000	0.74	0.755	0.566	0.189	94.277	0.401	38.1	
303	Monterey Sand	5	0.63	64	0.44	1.70	10.000	0.71	0.755	0.566	0.189	95.880	0.488	22.6	
304	Monterey Sand	5	0.64	63	0.44	1.70	10.000	0.72	0.755	0.566	0.189	95.759	0.552	10.1	
305	Monterey Sand	5	0.60	82	0.44	1.70	10.000	0.68	0.755	0.566	0.189	97.885	0.525	46.1	

Sr.	Sand Type	Fines Content (%)	Void Ratio	Relative Density (%)	D_{50}	Cu	D_{10}/d_{50}	e*	e_{max}	e_{min}	e_{range}	Relative Compaction	Cyclic Stress Ratio	Cycles to Initial Liq'n	Reference
306	Monterey Sand	10	0.52	80	0.42	2.20	10.000	0.66	0.702	0.47	0.232	96.896	0.601	44.0	
307	Monterey Sand	10	0.58	52	0.42	2.20	10.000	0.73	0.702	0.47	0.232	92.917	0.495	8.0	
308	Monterey Sand	10	0.58	52	0.42	2.20	10.000	0.73	0.702	0.47	0.232	92.917	0.398	35.0	
309	Monterey Sand	10	0.56	63	0.42	2.20	10.000	0.70	0.702	0.47	0.232	94.469	0.595	9.1	
310	Monterey Sand	10	0.58	52	0.42	2.20	10.000	0.73	0.702	0.47	0.232	92.985	0.306	173.1	
311	Monterey Sand	10	0.56	63	0.42	2.20	10.000	0.70	0.702	0.47	0.232	94.469	0.403	112.1	
312	Monterey Sand	10	0.51	81	0.42	2.20	10.000	0.66	0.702	0.47	0.232	97.089	0.514	109.1	
313	Monterey Sand	15	0.51	63	0.40	11.50	10.000	0.72	0.67	0.419	0.251	93.779	0.358	45.1	
314	Monterey Sand	15	0.64	11	0.40	11.50	10.000	0.86	0.67	0.419	0.251	86.425	0.215	38.0	
315	Monterey Sand	15	0.46	82	0.40	11.50	10.000	0.66	0.67	0.419	0.251	96.864	0.673	20.1	
316	Monterey Sand	15	0.46	82	0.40	11.50	10.000	0.66	0.67	0.419	0.251	96.864	0.501	49.0	
317	Monterey Sand	15	0.46	82	0.40	11.50	10.000	0.66	0.67	0.419	0.251	96.931	0.579	23.1	
318	Monterey Sand	15	0.64	11	0.40	11.50	10.000	0.87	0.67	0.419	0.251	86.372	0.178	99.0	
319	Monterey Sand	15	0.51	63	0.40	11.50	10.000	0.72	0.67	0.419	0.251	93.842	0.469	10.1	Green & Mitchell, 2001)
320	Monterey Sand	15	0.64	11	0.40	11.50	10.000	0.87	0.67	0.419	0.251	86.372	0.306	8.0	
321	Monterey Sand	25	0.35	97	0.37	17.00	10.000	0.63	0.627	0.344	0.283	99.331	0.417	338.2	
322	Monterey Sand	25	0.35	98	0.37	17.00	10.000	0.63	0.627	0.344	0.283	99.476	0.614	56.0	
323	Monterey Sand	25	0.63	-1	0.37	17.00	10.000	0.96	0.627	0.344	0.283	82.448	0.247	8.0	
324	Monterey Sand	25	0.34	98	0.35	25.30	10.000	0.61	0.625	0.335	0.29	99.546	0.516	52.0	
325	Monterey Sand	25	0.40	76	0.35	25.30	10.000	0.69	0.625	0.335	0.29	95.025	0.305	124.1	
326	Monterey Sand	25	0.40	76	0.35	25.30	10.000	0.69	0.625	0.335	0.29	95.084	0.407	21.0	
327	Monterey Sand	25	0.41	76	0.35	25.30	10.000	0.69	0.625	0.335	0.29	94.947	0.470	14.1	
328	Monterey Sand	25	0.63	0	0.35	25.30	10.000	0.96	0.625	0.335	0.29	82.110	0.149	55.0	
329	Monterey Sand	25	0.45	61	0.35	25.30	10.000	0.74	0.625	0.335	0.29	92.134	0.251	60.0	
330	Monterey Sand	25	0.45	60	0.35	25.30	10.000	0.75	0.625	0.335	0.29	92.006	0.311	29.1	
331	Monterey Sand	25	0.45	61	0.35	25.30	10.000	0.74	0.625	0.335	0.29	92.264	0.450	6.1	
332	Monterey Sand	25	0.63	-2	0.35	25.30	10.000	0.96	0.625	0.335	0.29	81.905	0.226	8.0	
333	Monterey Sand	35	0.52	56	0.31	38.50	10.000	0.90	0.69	0.378	0.312	90.903	0.081	42.4	

Sr.	Sand Type	Fines Content (%)	Void Ratio	Relative Density (%)	D_{50}	Cu	D_{10}/d_{50}	e*	e_{max}	e_{min}	e_{range}	Relative Compaction	Cyclic Stress Ratio	Cycles to Initial Liq'n	Reference
334	PSM-1	0	0.81	41	0.21	2.20	5.556	0.81	0.927	0.642	0.285	90.718	0.368	4	
335	PSM-1	0	0.90	10	0.21	2.20	5.556	0.90	0.927	0.642	0.285	86.512	0.121	71	
336	PSM-1	0	0.91	5	0.21	2.20	5.556	0.91	0.927	0.642	0.285	85.834	0.150	17	
337	PSM-1	0	0.91	6	0.21	2.20	5.556	0.91	0.927	0.642	0.285	85.924	0.249	2.0	
338	PSM-1	0	0.81	43	0.21	2.20	5.556	0.81	0.927	0.642	0.285	90.919	0.243	13	
339	PSM-1	0	0.81	42	0.21	2.20	5.556	0.81	0.927	0.642	0.285	90.869	0.200	54	
340	PSM-1	10	0.78	23	0.21	2.90	5.556	0.94	0.861	0.505	0.356	84.551	0.198	13	
341	PSM-1	10	0.78	22	0.21	2.90	5.556	0.95	0.861	0.505	0.356	84.408	0.176	25	
342	PSM-1	10	0.81	14	0.21	2.90	5.556	0.98	0.861	0.505	0.356	83.012	0.178	12	
343	PSM-1	10	0.82	12	0.21	2.90	5.556	0.99	0.861	0.505	0.356	82.829	0.159	18	
344	PSM-1	20	0.75	23	0.21	12.20	5.556	1.03	0.834	0.449	0.385	82.942	0.161	12	
345	PSM-1	20	0.67	42	0.21	12.20	5.556	0.94	0.834	0.449	0.385	86.559	0.233	11	
346	PSM-1	20	0.73	26	0.21	12.20	5.556	1.01	0.834	0.449	0.385	83.564	0.141	28	
347	PSM-1	20	0.67	44	0.21	12.20	5.556	0.94	0.834	0.449	0.385	86.975	0.219	16	(Cubrinovski & Rees, 2010)
348	PSM-2	0	0.82	41	0.18	2.20	4.444	0.82	0.941	0.637	0.304	90.143	0.243	10	
349	PSM-2	0	0.81	44	0.18	2.20	4.444	0.81	0.941	0.637	0.304	90.642	0.265	4.0	
350	PSM-2	0	0.90	14	0.18	2.20	4.444	0.90	0.941	0.637	0.304	86.249	0.121	50	
351	PSM-2	0	0.90	14	0.18	2.20	4.444	0.90	0.941	0.637	0.304	86.158	0.214	2	
352	PSM-2	0	0.81	42	0.18	2.20	4.444	0.81	0.941	0.637	0.304	90.243	0.191	59	
353	PSM-2	0	0.90	14	0.18	2.20	4.444	0.90	0.941	0.637	0.304	86.249	0.150	12	
354	PSM-2	10	0.80	24	0.18	2.60	4.444	0.96	0.888	0.506	0.382	83.853	0.141	30	
355	PSM-2	10	0.72	45	0.18	2.60	4.444	0.88	0.888	0.506	0.382	87.660	0.284	8	
356	PSM-2	10	0.79	25	0.18	2.60	4.444	0.96	0.888	0.506	0.382	83.993	0.177	9	
357	PSM-2	10	0.72	45	0.18	2.60	4.444	0.87	0.888	0.506	0.382	87.813	0.246	50	
358	PSM-2	25	0.63	61	0.18	68.80	4.444	0.92	0.941	0.42	0.521	87.385	0.159	74	
359	PSM-2	25	0.58	70	0.18	68.80	4.444	0.87	0.941	0.42	0.521	89.987	0.288	12	
360	PSM-2	25	0.58	69	0.18	68.80	4.444	0.87	0.941	0.42	0.521	89.760	0.266	15	
361	PSM-2	25	0.62	61	0.18	68.80	4.444	0.92	0.941	0.42	0.521	87.546	0.239	9	

Sr.	Sand Type	Fines Content (%)	Void Ratio	Relative Density (%)	D_{50}	Cu	D_{10}/d_{50}	e*	e_{max}	e_{min}	e_{range}	Relative Compaction	Cyclic Stress Ratio	Cycles to Initial Liq'n	Reference
362	Silica Sand No.6	0	0.87	42	0.16	1.60	7.059	0.87	1.046	0.634	0.412	87.286	0.152	11	
363	Silica Sand No.6	0	0.87	42	0.16	1.60	7.059	0.87	1.046	0.634	0.412	87.193	0.169	12	
364	Silica Sand No.6	0	0.87	42	0.16	1.60	7.059	0.87	1.046	0.634	0.412	87.193	0.155	20	
365	Silica Sand No.6	0	0.86	45	0.16	1.60	7.059	0.86	1.046	0.634	0.412	87.802	0.133	184	
366	Silica Sand No.6	20	0.66	52	0.14	11.30	7.059	0.93	0.91	0.428	0.482	86.076	0.155	13	
367	Silica Sand No.6	20	0.67	51	0.14	11.30	7.059	0.94	0.91	0.428	0.482	85.766	0.129	29	
368	Silica Sand No.6	20	0.66	51	0.14	11.30	7.059	0.94	0.91	0.428	0.482	85.921	0.176	12	(Enomoto, 2019)
369	Silica Sand No.6	20	0.66	51	0.14	11.30	7.059	0.94	0.91	0.428	0.482	85.869	0.145	20	
370	Silica Sand No.6	30	0.63	50	0.13	12.90	7.059	0.98	0.885	0.383	0.502	84.639	0.118	20	
371	Silica Sand No.6	30	0.63	50	0.13	12.90	7.059	0.98	0.885	0.383	0.502	84.691	0.056	374	
372	Silica Sand No.6	30	0.64	49	0.13	12.90	7.059	0.99	0.885	0.383	0.502	84.484	0.154	4.5	
373	Silica Sand No.6	30	0.63	51	0.13	12.90	7.059	0.98	0.885	0.383	0.502	84.795	0.132	12	
374	Silica Sand No.6	30	0.64	49	0.13	12.90	7.059	0.99	0.885	0.383	0.502	84.484	0.092	46	
375	Toyoura sand	10	0.91	7	0.19	3.27	2.488	1.09	0.94	0.54	0.4	80.544	0.123	15	
376	Toyoura sand	10	0.80	36	0.19	3.27	2.488	0.96	0.94	0.54	0.4	85.794	0.248	15	
377	Toyoura sand	10	0.72	55	0.19	3.27	2.488	0.88	0.94	0.54	0.4	89.431	0.378	15	
378	Toyoura sand	10	0.72	55	0.19	3.27	2.488	0.88	0.94	0.54	0.4	89.431	0.422	10	
379	Toyoura sand	10	0.91	7	0.19	3.27	2.488	1.09	0.94	0.54	0.4	80.544	0.113	10	
380	Toyoura sand	10	0.91	8	0.19	3.27	2.488	1.08	0.94	0.54	0.4	80.797	0.141	15	
381	Toyoura sand	10	0.91	8	0.19	3.27	2.488	1.08	0.94	0.54	0.4	80.797	0.148	10	
382	Toyoura sand	10	0.80	36	0.19	3.27	2.488	0.96	0.94	0.54	0.4	85.794	0.269	10	(Wei & Yang, 2019a)
383	Toyoura sand	10	0.85	23	0.19	3.27	2.488	1.02	0.94	0.54	0.4	83.288	0.172	15	
384	Toyoura sand	10	0.85	23	0.19	3.27	2.488	1.02	0.94	0.54	0.4	83.288	0.179	10	
385	Toyoura sand	20	0.92	3	0.19	3.70	2.488	1.22	0.93	0.48	0.45	77.204	0.073	15	
386	Toyoura sand	20	0.91	5	0.19	3.70	2.488	1.21	0.93	0.48	0.45	77.650	0.104	15	
387	Toyoura sand	20	0.80	30	0.19	3.70	2.488	1.08	0.93	0.48	0.45	82.451	0.190	15	
388	Toyoura sand	20	0.72	47	0.19	3.70	2.488	0.99	0.93	0.48	0.45	86.097	0.311	10	
389	Toyoura sand	20	0.91	5	0.19	3.70	2.488	1.21	0.93	0.48	0.45	77.650	0.110	10	

Sr.	Sand Type	Fines Content (%)	Void Ratio	Relative Density (%)	D_{50}	Cu	D_{10}/d_{50}	e*	e_{max}	e_{min}	e_{range}	Relative Compaction	Cyclic Stress Ratio	Cycles to Initial Liq'n	Reference
390	Toyoura sand	20	0.92	3	0.19	3.70	2.488	1.22	0.93	0.48	0.45	77.204	0.080	10	
391	Toyoura sand	20	0.80	30	0.19	3.70	2.488	1.08	0.93	0.48	0.45	82.451	0.204	10	
392	Toyoura sand	20	0.72	47	0.19	3.70	2.488	0.99	0.93	0.48	0.45	86.097	0.284	15	
393	Yatserville	0	0.75	70	0.17	2.40	2.870	0.75	0.972	0.653	0.319	94.527	0.323	11.1	
394	Yatserville	0	0.89	26	0.17	2.40	2.870	0.89	0.972	0.653	0.319	87.445	0.224	5	
395	Yatserville	0	1.01	-11	0.17	2.40	2.870	1.01	0.972	0.653	0.319	82.410	0.076	31.4	
396	Yatserville	0	0.89	25	0.17	2.40	2.870	0.89	0.972	0.653	0.319	87.327	0.168	14	
397	Yatserville	0	1.01	-10	0.17	2.40	2.870	1.01	0.972	0.653	0.319	82.437	0.090	14.5	
398	Yatserville	0	0.75	68	0.17	2.40	2.870	0.75	0.972	0.653	0.319	94.235	0.342	11.1	
399	Yatserville	0	1.09	-37	0.17	2.40	2.870	1.09	0.972	0.653	0.319	79.066	0.067	60.4	
400	Yatserville	0	0.76	68	0.17	2.40	2.870	0.76	0.972	0.653	0.319	94.184	0.286	23.1	
401	Yatserville	0	1.08	-32	0.17	2.40	2.870	1.08	0.972	0.653	0.319	79.661	0.087	11.3	
402	Yatserville	0	1.07	-32	0.16	2.40	2.870	1.07	0.972	0.653	0.319	79.698	0.110	2.3	
403	Yatserville	0	0.88	27	0.17	2.40	2.870	0.88	0.972	0.653	0.319	87.696	0.137	36.1	
404	Yatserville	0	1.08	-33	0.17	2.40	2.870	1.08	0.972	0.653	0.319	79.612	0.066	43.3	
405	Yatserville	0	1.11	-45	0.17	2.40	2.870	1.11	0.972	0.653	0.319	78.195	0.063	78.5	(Green & Mitchell, 2001)
406	Yatserville	4	1.00	-30	0.16	2.60	2.870	1.08	0.911	0.609	0.302	80.361	0.111	6.3	
407	Yatserville	4	0.82	31	0.16	2.60	2.870	0.89	0.911	0.609	0.302	88.505	0.229	19.1	
408	Yatserville	4	0.83	28	0.16	2.60	2.870	0.90	0.911	0.609	0.302	88.022	0.136	8.6	
409	Yatserville	4	0.94	-10	0.16	2.60	2.870	1.02	0.911	0.609	0.302	82.938	0.127	7.2	
410	Yatserville	4	0.94	-9	0.16	2.60	2.870	1.01	0.911	0.609	0.302	83.016	0.113	12	
411	Yatserville	4	0.75	52	0.16	2.60	2.870	0.82	0.911	0.609	0.302	91.751	0.335	7.1	
412	Yatserville	4	0.85	20	0.16	2.60	2.870	0.93	0.911	0.609	0.302	86.888	0.211	15	
413	Yatserville	4	0.75	52	0.16	2.60	2.870	0.82	0.911	0.609	0.302	91.798	0.283	11.1	
414	Yatserville	4	0.83	28	0.16	2.60	2.870	0.90	0.911	0.609	0.302	88.124	0.163	3.2	
415	Yatserville	4	0.84	23	0.16	2.60	2.870	0.91	0.911	0.609	0.302	87.358	0.148	6.3	
416	Yatserville	4	0.94	-11	0.16	2.60	2.870	1.02	0.911	0.609	0.302	82.771	0.094	28.3	
417	Yatserville	4	1.02	-37	0.16	2.60	2.870	1.10	0.911	0.609	0.302	79.605	0.077	30.3	

Sr.	Sand Type	Fines Content (%)	Void Ratio	Relative Density (%)	D_{50}	Cu	D_{10}/d_{50}	e*	e_{max}	e_{min}	e_{range}	Relative Compaction	Cyclic Stress Ratio	Cycles to Initial Liq'n	Reference
418	Yatserville	4	1.02	-36	0.16	2.60	2.870	1.10	0.911	0.609	0.302	79.724	0.081	20.3	
419	Yatserville	4	0.82	30	0.16	2.60	2.870	0.89	0.911	0.609	0.302	88.314	0.243	11.1	
420	Yatserville	4	0.75	52	0.16	2.60	2.870	0.82	0.911	0.609	0.302	91.751	0.249	33.1	
421	Yatserville	4	0.82	30	0.16	2.60	2.870	0.89	0.911	0.609	0.302	88.314	0.188	54	
422	Yatserville	7	0.77	29	0.16	2.60	2.870	0.89	0.872	0.528	0.344	86.286	0.297	15.1	
423	Yatserville	7	0.96	-25	0.15	2.60	2.870	1.09	0.872	0.528	0.344	77.998	0.132	4.3	
424	Yatserville	7	0.78	27	0.16	2.60	2.870	0.90	0.872	0.528	0.344	85.935	0.225	58.1	
425	Yatserville	7	0.98	-32	0.16	2.60	2.870	1.11	0.872	0.528	0.344	77.131	0.088	29.6	
426	Yatserville	7	0.77	31	0.16	2.60	2.870	0.89	0.872	0.528	0.344	86.504	0.323	7.1	
427	Yatserville	7	0.89	-6	0.16	2.60	2.870	1.02	0.872	0.528	0.344	80.807	0.161	4.2	
428	Yatserville	7	0.90	-9	0.16	2.60	2.870	1.03	0.872	0.528	0.344	80.296	0.086	65	
429	Yatserville	7	0.90	-9	0.16	2.60	2.870	1.03	0.872	0.528	0.344	80.340	0.124	16.8	
430	Yatserville	7	0.76	34	0.16	2.60	2.870	0.87	0.872	0.528	0.344	87.012	0.307	6	
431	Yatserville	7	0.76	34	0.16	2.60	2.870	0.87	0.872	0.528	0.344	87.012	0.283	9.1	(Green & Mitchell, 2001)
432	Yatserville	7	0.96	-25	0.16	2.60	2.870	1.09	0.872	0.528	0.344	77.998	0.113	8.3	
433	Yatserville	7	0.94	-20	0.16	2.60	2.870	1.07	0.872	0.528	0.344	78.675	0.084	29.4	
434	Yatserville	7	0.76	34	0.16	2.60	2.870	0.87	0.872	0.528	0.344	87.064	0.241	20.1	
435	Yatserville	7	0.75	35	0.16	2.60	2.870	0.87	0.872	0.528	0.344	87.166	0.251	25.1	
436	Yatserville	12	0.66	55	0.15	3.50	2.870	0.84	0.84	0.517	0.323	91.274	0.284	11.1	
437	Yatserville	12	0.83	3	0.15	3.50	2.870	1.03	0.84	0.517	0.323	82.941	0.153	29	
438	Yatserville	12	0.87	-10	0.15	3.50	2.870	1.07	0.84	0.517	0.323	81.037	0.144	3.4	
439	Yatserville	12	0.75	28	0.15	3.50	2.870	0.94	0.84	0.517	0.323	86.628	0.267	7	
440	Yatserville	12	0.88	-12	0.15	3.50	2.870	1.08	0.84	0.517	0.323	80.773	0.097	31.4	
441	Yatserville	12	0.76	25	0.15	3.50	2.870	0.95	0.84	0.517	0.323	86.182	0.231	12.6	
442	Yatserville	12	0.87	-10	0.15	3.50	2.870	1.07	0.84	0.517	0.323	81.079	0.116	9.3	
443	Yatserville	12	0.70	44	0.15	3.50	2.870	0.88	0.84	0.517	0.323	89.330	0.386	12.1	
444	Yatserville	12	0.66	54	0.15	3.50	2.870	0.84	0.84	0.517	0.323	91.150	0.255	11.7	
445	Yatserville	12	0.83	3	0.15	3.50	2.870	1.03	0.84	0.517	0.323	82.853	0.188	10.9	

Sr.	Sand Type	Fines Content (%)	Void Ratio	Relative Density (%)	D_{50}	Cu	D_{10}/d_{50}	e*	e_{max}	e_{min}	e_{range}	Relative Compaction	Cyclic Stress Ratio	Cycles to Initial Liq'n	Reference
446	Yatserville	12	0.88	-11	0.15	3.50	2.870	1.08	0.84	0.517	0.323	80.870	0.090	28.3	
447	Yatserville	12	0.69	45	0.15	3.50	2.870	0.88	0.84	0.517	0.323	89.551	0.339	13.1	
448	Yatserville	12	0.66	57	0.15	3.50	2.870	0.84	0.84	0.517	0.323	91.594	0.312	7.1	
449	Yatserville	12	0.83	5	0.15	3.50	2.870	1.02	0.84	0.517	0.323	83.117	0.224	4	
450	Yatserville	12	0.70	42	0.15	3.50	2.870	0.89	0.84	0.517	0.323	89.076	0.370	15.1	
451	Yatserville	12	0.76	26	0.15	3.50	2.870	0.95	0.84	0.517	0.323	86.341	0.201	47.1	
452	Yatserville	17	0.57	78	0.15	4.50	2.870	0.79	0.802	0.502	0.3	95.754	0.376	16.7	
453	Yatserville	17	0.57	76	0.15	4.50	2.870	0.80	0.802	0.502	0.3	95.444	0.349	15.7	
454	Yatserville	17	0.82	-7	0.13	4.50	2.870	1.08	0.802	0.502	0.3	82.432	0.159	5.2	
455	Yatserville	17	0.75	17	0.15	4.50	2.870	1.00	0.802	0.502	0.3	85.780	0.263	6	
456	Yatserville	17	0.68	41	0.15	4.50	2.870	0.92	0.802	0.502	0.3	89.458	0.156	16.7	
457	Yatserville	17	0.83	-8	0.15	4.50	2.870	1.08	0.802	0.502	0.3	82.297	0.128	20.9	
458	Yatserville	17	0.72	28	0.15	4.50	2.870	0.96	0.802	0.502	0.3	87.381	0.248	7	
459	Yatserville	17	0.75	18	0.15	4.50	2.870	1.00	0.802	0.502	0.3	85.927	0.222	14	(Green & Mitchell, 2001)
460	Yatserville	17	0.72	26	0.15	4.50	2.870	0.97	0.802	0.502	0.3	87.123	0.212	25	
461	Yatserville	17	0.57	76	0.15	4.50	2.870	0.80	0.802	0.502	0.3	95.480	0.406	15.1	
462	Yatserville	17	0.83	-11	0.15	4.50	2.870	1.09	0.802	0.502	0.3	81.893	0.091	62.4	
463	Yatserville	17	0.69	38	0.15	4.50	2.870	0.93	0.802	0.502	0.3	88.934	0.102	118.8	
464	Yatserville	17	0.73	25	0.15	4.50	2.870	0.97	0.802	0.502	0.3	87.017	0.201	46.6	
465	Yatserville	17	0.69	38	0.15	4.50	2.870	0.93	0.802	0.502	0.3	89.029	0.245	2.5	
466	Yatserville	17	0.75	18	0.15	4.50	2.870	1.00	0.802	0.502	0.3	85.927	0.198	38	
467	Yatserville	26	0.66	27	0.13	6.60	2.870	0.96	0.728	0.483	0.245	89.225	0.190	69	
468	Yatserville	26	0.65	31	0.13	6.60	2.870	0.95	0.728	0.483	0.245	89.767	0.192	14.1	
469	Yatserville	26	0.66	29	0.13	6.60	2.870	0.96	0.728	0.483	0.245	89.436	0.273	5.1	
470	Yatserville	26	0.62	43	0.13	6.60	2.870	0.92	0.728	0.483	0.245	91.421	0.330	14.1	
471	Yatserville	26	0.75	-9	0.12	6.60	2.870	1.07	0.728	0.483	0.245	84.740	0.169	7.1	
472	Yatserville	26	0.66	28	0.13	6.60	2.870	0.96	0.728	0.483	0.245	89.330	0.219	9	
473	Yatserville	26	0.75	-10	0.13	6.60	2.870	1.07	0.728	0.483	0.245	84.598	0.126	30.1	

Sr.	Sand Type	Fines Content (%)	Void Ratio	Relative Density (%)	D_{50}	Cu	D_{10}/d_{50}	e*	e_{max}	e_{min}	e_{range}	Relative Compaction	Cyclic Stress Ratio	Cycles to Initial Liq'n	Reference
474	Yatserville	26	0.67	25	0.13	6.60	2.870	0.97	0.728	0.483	0.245	88.962	0.161	21	
475	Yatserville	26	0.66	28	0.13	6.60	2.870	0.96	0.728	0.483	0.245	89.383	0.249	13	
476	Yatserville	26	0.63	40	0.13	6.60	2.870	0.92	0.728	0.483	0.245	91.023	0.283	11.1	
477	Yatserville	26	0.62	43	0.13	6.60	2.870	0.92	0.728	0.483	0.245	91.366	0.301	14.1	
478	Yatserville	26	0.75	-9	0.13	6.60	2.870	1.07	0.728	0.483	0.245	84.740	0.151	9.4	
479	Yatserville	37	0.68	0	0.12	8.70	2.870	1.01	0.684	0.397	0.287	82.957	0.178	7	
480	Yatserville	37	0.61	24	0.12	8.70	2.870	0.93	0.684	0.397	0.287	86.557	0.285	4.1	
481	Yatserville	37	0.73	-16	0.10	8.70	2.870	1.07	0.684	0.397	0.287	80.702	0.118	7.7	(Green & Mitchell, 2001)
482	Yatserville	37	0.75	-25	0.12	8.70	2.870	1.10	0.684	0.397	0.287	79.606	0.078	46.3	
483	Yatserville	37	0.61	26	0.12	8.70	2.870	0.93	0.684	0.397	0.287	86.773	0.234	10	
484	Yatserville	37	0.66	8	0.12	8.70	2.870	0.99	0.684	0.397	0.287	84.060	0.141	9.1	
485	Yatserville	37	0.68	1	0.12	8.70	2.870	1.01	0.684	0.397	0.287	83.099	0.116	29	
486	Yatserville	37	0.67	5	0.12	8.70	2.870	1.00	0.684	0.397	0.287	83.598	0.112	35.7	
487	Yatserville	37	0.72	-11	0.12	8.70	2.870	1.05	0.684	0.397	0.287	81.417	0.092	19.3	
488	Yatserville	37	0.61	25	0.12	8.70	2.870	0.93	0.684	0.397	0.287	86.665	0.224	12.1	
489	Yatserville	37	0.67	4	0.12	8.70	2.870	1.00	0.684	0.397	0.287	83.498	0.194	3.4	